

AD-A130 515

LIDAR (LIGHT DETECTION AND RANGING) REMOTE MEASUREMENTS
OF STS-3 GROUND C... (U) COMPUTER GENETICS CORP WAKEFIELD
MASS B CAPUTO ET AL. APR 83 AFESC/ESL-TR-82-52

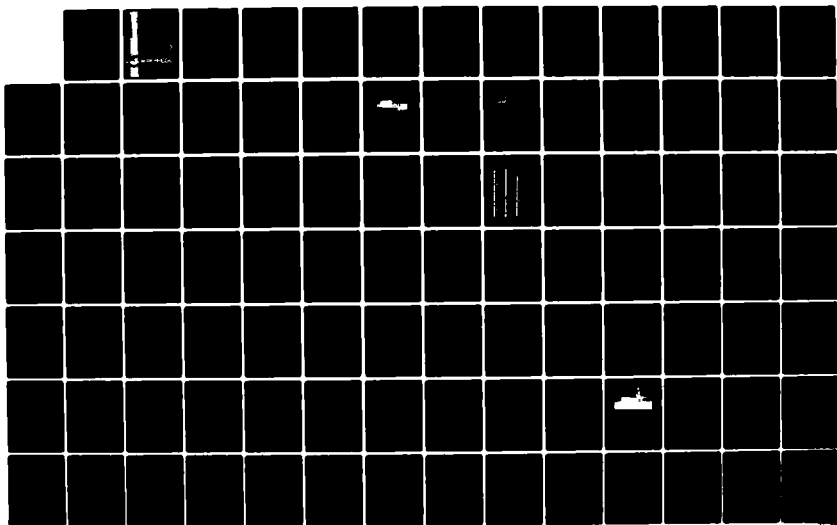
1/2

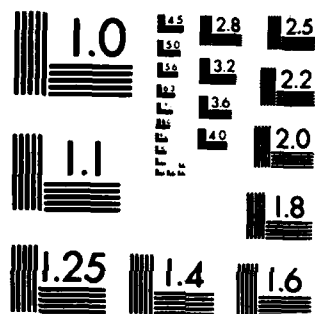
UNCLASSIFIED

NAS10-10299

F/G 17/8

NL





MICROCOPY RESOLUTION TEST CHART
NATIONAL BUREAU OF STANDARDS-1963-A

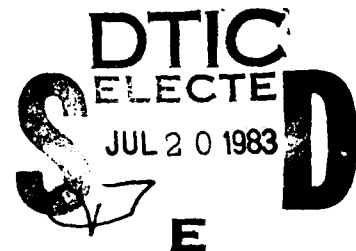
ADA130515

LIDAR REMOTE MEASUREMENTS OF STS-3 GROUND CLOUD EMISSIONS

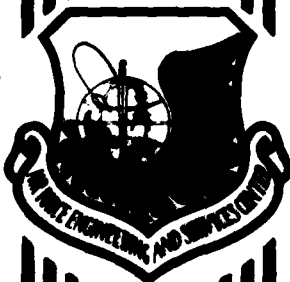
B. CAPUTO, R. JOHNSON, R. DOW
COMPUTER GENETICS CORP.
18 LAKESIDE OFFICE PARK
WAKEFIELD, MA 01880

APRIL 1983

FINAL REPORT
MARCH - APRIL 1982



APPROVED FOR PUBLIC RELEASE: DISTRIBUTION UNLIMITED



ENGINEERING & SERVICES LABORATORY
AIR FORCE ENGINEERING & SERVICES CENTER
TYNDALL AIR FORCE BASE, FLORIDA 32403

DTIC FILE COPY

83 07 20 002

NOTICE

PLEASE DO NOT REQUEST COPIES OF THIS REPORT FROM
HQ AFESC/RD (ENGINEERING AND SERVICES LABORATORY).

ADDITIONAL COPIES MAY BE PURCHASED FROM:

NATIONAL TECHNICAL INFORMATION SERVICE
5285 PORT ROYAL ROAD
SPRINGFIELD, VIRGINIA 22161

FEDERAL GOVERNMENT AGENCIES AND THEIR CONTRACTORS
REGISTERED WITH DEFENSE TECHNICAL INFORMATION CENTER
SHOULD DIRECT REQUESTS FOR COPIES OF THIS REPORT TO:

DEFENSE TECHNICAL INFORMATION CENTER
CAMERON STATION
ALEXANDRIA, VIRGINIA 22314

UNCLASSIFIED

SECURITY CLASSIFICATION OF THIS PAGE (When Data Entered)

REPORT DOCUMENTATION PAGE		READ INSTRUCTIONS BEFORE COMPLETING FORM
1. REPORT NUMBER ESL-TR-82-52	2. GOVT ACCESSION NO. AD A130 515	3. RECIPIENT'S CATALOG NUMBER
4. TITLE (and Subtitle) LIDAR REMOTE MEASUREMENTS OF STS-3 GROUND CLOUD EMISSIONS		5. TYPE OF REPORT & PERIOD COVERED Final Report March - April 1982
		6. PERFORMING ORG. REPORT NUMBER
7. AUTHOR(s) Bernard Caputo Richard Johnson Robert Dow		8. CONTRACT OR GRANT NUMBER(s) NAS10-10299
9. PERFORMING ORGANIZATION NAME AND ADDRESS Computer Genetics Corporation 18 Lakeside Office Park Wakefield MA 01880		10. PROGRAM ELEMENT, PROJECT, TASK AREA & WORK UNIT NUMBERS PE: 62601F JON: 19002023
11. CONTROLLING OFFICE NAME AND ADDRESS HQ AFESC/RDVS Tyndall AFB, Florida 32403		12. REPORT DATE April 1983
		13. NUMBER OF PAGES 98
14. MONITORING AGENCY NAME & ADDRESS (if different from Controlling Office) NASA/MD-C Kennedy Space Center, Florida 32899		15. SECURITY CLASS. (of this report) UNCLASSIFIED
		15a. DECLASSIFICATION/DOWNGRADING SCHEDULE
16. DISTRIBUTION STATEMENT (of this Report) Approved for public release; distribution unlimited.		
17. DISTRIBUTION STATEMENT (of the abstract entered in Block 20, if different from Report)		
18. SUPPLEMENTARY NOTES Availability of this report is specified on reverse of front cover.		
19. KEY WORDS (Continue on reverse side if necessary and identify by block number) Lidar Laser Radar Remote Sensing Space Shuttle		
20. ABSTRACT (Continue on reverse side if necessary and identify by block number) Under joint sponsorship by NASA and the USAF, Computer Genetics Corporation demonstrated the feasibility of lidar (Light Detection and Ranging) remote sensing techniques for the characterization of booster exhaust clouds produced by STS operations. Analysis of data performed shows that the mobile lidar test bed can successfully track ground clouds from an observation point greater than 7 kilometers distant and acquire cloud main body and fallout particulate backscatter data which can be correlated to geographical footprints. The STS-3 launch measurements demonstrated the practical feasibility of lidar to provide accurate		

DD FORM 1 JAN 73 1473 EDITION OF 1 NOV 65 IS OBSOLETE

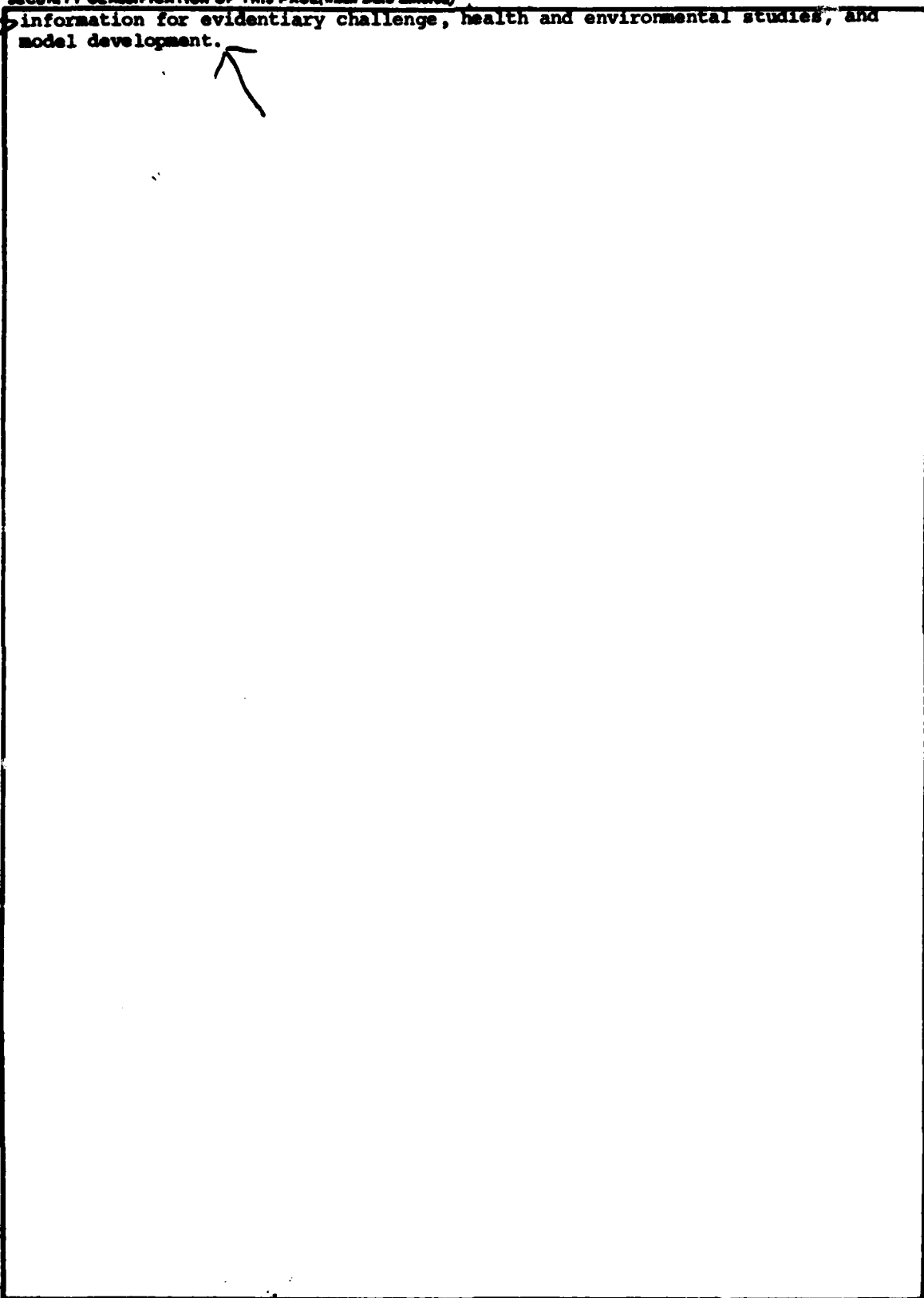
UNCLASSIFIED

SECURITY CLASSIFICATION OF THIS PAGE (When Data Entered)

UNCLASSIFIED

SECURITY CLASSIFICATION OF THIS PAGE (When Data Entered)

cont → information for evidentiary challenge, health and environmental studies, and model development.



UNCLASSIFIED

SECURITY CLASSIFICATION OF THIS PAGE (When Data Entered)

PREFACE

This report was prepared by the Computer Genetics Corporation, 18 Lakeside Office Park, Wakefield, MA 01880, under Contract No. NAS 10-10229 with the National Aeronautics and Space Administration, Kennedy Space Center, FL 32899. Funds were provided by the Air Force Engineering and Services Center (AFESC) and Space Division (SD).

Work under this contract was performed from March to April 1982. The Project Officers were Mr Hans Rudolph (NASA) and Capt Dan Berlinrut, AFESC/RDVS.

This report has been reviewed by the Public Affairs Office (PA) and is releasable to the National Technical Information Service (NTIS). At NTIS, it will be available to the general public, including foreign nationals.

This report has been reviewed and is approved for public release.

Daniel D. Berlinrut

DANIEL D. BERLINRUT, Capt, USAF, BSC
Air Quality Research Engineer

John T. Slankas

JOHN T. SLANKAS, Maj, USAF
Chief, Environmental Sciences
Branch

Michael J. Ryan

MICHAEL J. RYAN, Lt Col, USAF, BSC
Chief, Environics Division

Francis B. Crowley III

FRANCIS B. CROWLEY III, Col, USAF
Director, Engineering and Services
Laboratory

Accession For	
NTIS GRA&I	<input checked="" type="checkbox"/>
DTIC TAB	<input type="checkbox"/>
Unannounced	<input type="checkbox"/>
Justification	
By	
Distribution/	
Availability Codes	
Dist	Avail and/or Special
A	



TABLE OF CONTENTS

Section	Title	Page
I.	MANAGEMENT SUMMARY.....	1
	A. INTRODUCTION.....	1
	B. BACKGROUND.....	1
	C. SCOPE.....	2
	D. LIDAR REMOTE SENSING POTENTIAL FOR LAUNCH OPERATION MONITORING.....	3
	E. RECOMMENDED APPROACH TO LIDAR MONITORING OF STS GROUND CLOUD.....	4
II.	STS-3 OPERATIONAL CONSIDERATIONS.....	6
	A. REAL-TIME SOFTWARE FOR STS-3 DATA ACQUISITION...	7
	B. STS-3 BOOSTER EXHAUST CLOUD SCAN PATTERN.....	8
	C. LIDAR SCANNER RATES.....	12
	D. DETERMINATION OF SEED.....	12
	E. RESTRICTED LASER RADIATION REGIONS.....	14
	F. PRELAUNCH CALIBRATION.....	14
	G. POINTING AND TRACKING.....	16
III.	LIDAR MEASUREMENT OF STS-3 EXHAUST CLOUD.....	19
	A. STS-3 LAUNCH DATA ACQUISITION AND SCANNING SUMMARY.....	19
	B. LIDAR MEASUREMENT SPATIAL DISTRIBUTION FOR STS-3	20
	C. STS-3 LIDAR PERFORMANCE.....	23
	D. PRELIMINARY ANALYSIS OF STS-3 EXHAUST CLOUD LIDAR DATA.....	39
	1. Scattergraphs of Cloud Cross Sections.....	39
	2. Exhaust Cloud vs. Fallout Lidar Measurement.	39
	3. Lidar Track of STS-3 Exhaust Cloud.....	41
	4. Background as a Function of Azimuth.....	41

TABLE OF CONTENTS (CONTINUED)

Section	Title	Page
IV.	STS-5 LIDAR FIELD CALIBRATION AND TESTS.....	45
	A. BACKGROUND SCAN TESTS.....	45
	B. BORESIGHT AND TRIANGULATION CALIBRATIONS.....	45
	C. LASER CALIBRATION AND PERFORMANCE ASSESSMENT...	49
	D. ANTICIPATED GROUND CLOUD SIGNAL RETURN.....	49
	E. PRELAUNCH AND POSTLAUNCH TESTING.....	54
V.	CONCLUSIONS AND RECOMMENDATIONS.....	55
	A. GENERAL SUMMARY.....	55
	B. PRINCIPAL INVESTIGATOR LEVEL OF EFFORT.....	56
	C. SOFTWARE DEVELOPMENT AND DATA PROCESSING LEVEL OF EFFORT.....	56
	D. ADDITION OF LOG AMPLIFIER.....	56
	E. INCREASED DATA ACQUISITION RATE.....	57
	F. LIDAR LEGAL QUALIFICATION.....	57
	G. IMPROVED CLOUD TRACKING AND DATA ACQUISITION EFFICIENCY.....	58
	1. Track Ball Pointed Acquisition Video Camera	59
	2. Composite Video "Current" Telescope Point Display.....	59
	3. Range Height Indicator.....	59
	4. Telescope Boresighted Video Display and Recording System.....	60
	H. RADAR AIRCRAFT INTRUSION ALERT.....	60
	I. LIDAR MOBILITY.....	61
	J. DIRECT CALCULATION OF CLOUD ATTENUATION AND BACKSCATTER COEFFICIENTS.....	61
	K. SEED CHANGES.....	62

TABLE OF CONTENTS (CONCLUDED)

Section	Title	Page
APPENDIX		
A.	CGC MOBILE LIDAR SYSTEM DESCRIPTION.....	65
B.	STS-3 EXHAUST CLOUD CROSS SECTION SCATTERGRAPHS.....	78

LIST OF FIGURES

Figure	Title	Page
1	CGC Mobile Lidar at UCS-6.....	7
2	Lidar Scan Patterns for STS-3.....	9
3	Scan Pattern "F" Overlay with Azimuth and Elevation Scale Factors.....	10
4	T.V. Monitor Grid for Setting Exhaust Cloud Scan Pattern Reference.....	11
5	STS-3 Lidar Firing Regions Permitted vs. Restricted.....	15
6	Computer True Reference Input Scheme.....	17
7	Booster Exhaust Cloud Lidar Event Time Chart for STS-3.....	22
8	STS-3 Booster Exhaust Test Lidar Coverage Area..	24
9	STS-3 Booster Exhaust Test Lidar Scanning Distribution.....	25
10	Booster Exhaust Plume.....	26
11	Scan #137 - First Plume Contact.....	27
12	Scan #137 - Plume at 11:01:10.....	28
13	Scan #138 - Plume at 11:01:55.....	29
14	Scan #139 - Plume at 11:03:16.....	30
15	Scan #140 - Plume at 11:04:12.....	31
16	Scan #141 - Plume at 11:05:08.....	32
17	Scan #142 - Plume at 11:06:11.....	33
18	Scan #143 - Plume at 11:07:28.....	34
19	Scan #144 - Plume at 11:08:40.....	35
20	STS-3 Booster Exhaust Cloud Lidar Data T+1:33...	37
21	STS-3 Booster Exhaust Cloud Lidar Data T+2:03...	38

LIST OF FIGURES (CONTINUED)

Figure	Title	Page
22	Scan #139 Segment 3 11:03:21.....	40
	Scan #140 Segment 1 11:03:54.....	40
23	Lidar Observed Booster Exhaust Cloud Movement...	42
24	Lidar Observed Booster Exhaust Cloud Movement...	43
25	STS-3 Booster Exhaust Lidar Measurements Scan 141 Segment 1.....	44
26	Range and True Azimuth from UCS-6.....	48
27	Meteorological Tower Return.....	50
28	Pad 39B Return.....	51
29	Pad 39A Return.....	52
A-1	CGC Mobile Lidar.....	66
A-2	Cutaway Drawing of CGC Mobile Field Lidar.....	68
A-3	Mobile Lidar Van-Mounted Telescope Configuration.....	69
A-4	Existing CGC Mobile Lidar System.....	70
A-5	Parameter List.....	73
A-6	Typical Lidar Data Processing Flow Chart for Particulate Plume Measurement.....	74
A-7	Scattergraph of Typical Plume Cross Section....	76
A-8	Plume Scan #67.....	77
B-1	Scan #137-E2.....	81
B-2	Scan #138-F1.....	82
B-3	Scan #138-F3.....	83
B-4	Scan #138-F4.....	84
B-5	Scan #139-F1.....	85

LIST OF FIGURES (CONCLUDED)

Figure	Title	Page
B-6	Scan #139-F3.....	86
B-7	Scan #140-F1.....	87
B-8	Scan #140-F2.....	88
B-9	Scan #140-F3.....	89
B-10	Scan #141-F1.....	90
B-11	Scan #141-F3.....	91
B-12	Scan #142-F1.....	92
B-13	Scan #142-F3.....	93
B-14	Scan #143-F1.....	94
B-15	Scan #144-F1.....	95
B-16	Scan #145-F3.....	96

LIST OF TABLES

Table	Title	Page
1	LIDAR MEASUREMENT SUMMARY.....	21
2	PRELAUNCH BACKGROUND TEST.....	46
3	SUMMARY OF PRELAUNCH LIDAR TESTS.....	47
B-1	LIST OF SCATTERGRAPHS.....	80

SECTION I

MANAGEMENT SUMMARY

A. INTRODUCTION

Following is a report of the work performed in conjunction with the STS-3 launch by Computer Genetics Corporation (CGC) under joint NASA/USAF support through NASA/KSC contract NAS10-10229 to assess the feasibility of lidar (light detection and ranging) remote sensing techniques for the characterization of booster exhaust clouds produced by STS launch operations. The existing CGC mobile lidar facility tracks the development of emissions clouds and provides high density, three-dimensional maps of particulate concentrations and fallout unobtainable with traditional measurement techniques.

The objectives of this effort are to:

1. Provide quantitative assessment of lidar particulate mapping in support of typical launch operations.
2. Provide a data base for performance extrapolation through the "phase in" of additional lidar techniques to determine particle size and water vapor distribution and HCl concentration cross sections.
3. Develop optimal lidar cloud scanning software and operational procedures.
4. Develop software algorithms utilizing real-time lidar data which tracks cloud centroid and predicts plume trajectory.
5. Expand upon existing postlaunch lidar data processing techniques.
6. Develop and demonstrate specifications for lidar equipment and techniques optimized to launch monitoring applications.

B. BACKGROUND

During the first two shuttle launches, in situ sampling equipment measured considerable particulate fallout distribution from the booster exhaust cloud which was at variance with theoretical predictions. Subsequent analysis showed the deposition to contain high concentrations of acid resulting from the presence of HCl in the combustion process. The major portion of ground cloud emissions is composed of a complex distribution of H₂O, HCL, Al₂O₃ and Al Cl₃. Aging of the cloud is subject to particle settling, chemical recombination, growth, evaporative

processes and meteorological conditions. A ground level matrix of instrumentation vans and airborne instrumentation is used to sample acid deposition and cloud constituents. High resolution, three-dimensional, empirical measurements of constituent concentrations and spatial distribution as a function of time are needed to analyze the size, nature and behavior of the cloud, document deposition locations and to serve as input to theoretical models and model development. Fully developed and optimized remote sensing techniques can complement or replace many of the currently used sampling instruments providing permanent, three-dimensional, spatially resolved records of exhaust content location and behavior.

C. SCOPE

This report describes the operational considerations governing the application of the lidar to STS booster ground cloud measurements. These considerations, which include data acquisition rates, cloud coverage, safety operating restrictions, and scanning techniques developed to support STS measurements, are discussed in Section II. Based upon the experience gained during STS-2, simplified scan patterns resulted in improved scanning control and monitoring of scanning activity with greater cloud coverage.

A complete description and summary of quality and quantity of the lidar data acquired during the STS-3 launch are presented in Section III. Budget availability does not permit reduction and analysis of all available STS-3 data; however, a significant sampling of selected data is presented.

Section IV describes the calibration and system performance efforts employed before and immediately after the STS-3 launch. These include hard target range calibrations, background assessment to establish optimum system sensitivity, measurement of laser power output and alignment, etc.

Required laser eye safety restrictions during the STS-3 launch did not impede lidar data coverage, since westerly winds carried the exhaust cloud offshore to increasing range from the lidar at UCS-6. Nevertheless, software modifications to the lidar facility and procedural changes to the Operational Instructions KPB-01-2001, Lidar Operations for STS Exhaust Cloud Measurements, are recommended which will decrease the Safe Eye Exposure Distance (SEED), substantially increasing the lidar data acquisition potential for future STS launches.

STS-2 and STS-3 participation and experience have identified a number of procedural and system modifications recommended for implementation. These are documented under the Conclusions and Recommendations in Section V of this report.

Appendix A describes the existing CGC mobile lidar facility made available for the assessment. The CGC mobile lidar is a flexible configuration test bed used in conjunction with experimental programs, and which is capable of operating in Rayleigh, Mie, and Raman backscatter modes. With modest modifications, the system can be operated in the DIAL (Differential Absorption Lidar) mode. The lidar facility and supporting software library is also routinely used in power plant plume studies and plume model validation programs to measure particles, plume dimensions and dispersion, plume rise, and movement.

A representative cross section of the lidar data acquired by the CGC lidar during the STS-3 launch is presented as Appendix B. These data are presented in scattergraph form where, although the data have been decoded and labeled with azimuth, elevation, and range, they represent essentially raw data as recorded in real time. As stated above, a complete description of these data and a preliminary analysis comprise Section III.

D. LIDAR REMOTE SENSING POTENTIAL FOR LAUNCH OPERATION MONITORING

Highly spatially resolved, three-dimensional records of cloud composition and deposition location are not possible using in situ or airborne sampling equipment. Extensive progress has been reported over the past 8 to 10 years in the development of various lidar remote sensing techniques which can quantitatively analyze, monitor, and document transport and dispersion of the complex character of launch ground clouds. These include Mie scattering measurements of total particulate dispersion, multi-wavelength backscatter or depolarization techniques for particle sizing and distribution, DIAL to measure gas phase HCL, and Raman techniques to discriminate water in vapor from liquid states. These techniques are at various stages of investigation.

Mie scatter measurement of plume or cloud particles is the most advanced technique requiring mainly applications research and development. This is shown by the recent promulgation of Federal Code Regulation 40 CFR Part 60, October 28, 1981 (Reference 1). The regulation legally establishes the reliability and validity of the technique and assures the admissibility of lidar data as evidence in suits brought under the Clean Air Act. Lidar is now routinely used by EPA to measure plume opacity of power plants and heavy industrial operations.

A search of diverse literature reveals a substantial quantity (see References) of theoretical and experimental work to further develop particle sizing using polarization and multiwavelength techniques. Sizing algorithms have been shown to work by Kerker, Ariessohn, and Shimizu. A relatively new and promising technique is proposed by Caputo and Leonard (Reference 2) which

utilizes combined Raman and on-line techniques at multiple wavelengths to measure attenuation (α) separate from backscatter (β) for use in sizing algorithms. Sizing by use of lidar currently lacks field demonstration, and additional laboratory calibration tests would be prudent.

Successful measurements of HCl concentrations under field conditions are reported by Herrmann, Heinrich, Michaelis, and Weitkamp (Reference 3) in a German experiment. Despite problems encountered with the laser, data were successfully obtained with a sensitivity of 500 ppb by 100 meters. Numerous profiles at the plume peripherals were obtained in the 5 ppm - 15 ppm range. The literature describes other DIAL techniques which can be incorporated into the existing CGC test bed for STS evaluation.

Raman measurements of water vapor in the marine boundary layer showing good agreement with ground truth are reported by Caputo and Leonard (Reference 4). Operation as a daylight Raman water vapor instrument with ranges sufficient to support typical STS operations remains undemonstrated.

Each of the various parameters that can be measured with lidar techniques has different sensitivity levels, equipment and optimal data acquisition scanning scenarios. For example, in the Mie scatter particulate mode, as employed for STS launch monitoring, the laser has a maximum pulse repetition rate of 15. Backscatter from one pulse is sufficient to acquire good signal-to-noise (S/N) particulate cross-section data from 2048 individual 25-100 foot range cells. When substituting a DF laser and operating in the DIAL mode, DF lasers operating in the .5 to 3Hz range, require more than one shot to integrate the data to suitable S/N, and, in general, work for shorter ranges than the particulate lidar mode. For particle sizing, data is acquired at multiple wavelengths along the same line of sight.

Data acquired in the particulate mode of the existing CGC lidar are limited only by the slewing rate of the scanning telescope, resulting in scan rates and area coverage well matched to the natural cloud growth and transport, providing good physical plume size characterization. This would be sacrificed if the scanner were slowed to accommodate the slower measurement techniques.

E. RECOMMENDED APPROACH TO LIDAR MONITORING OF STS GROUND CLOUD

Because of the wide range of optimal scanning patterns and rates between the modes, it is envisioned that a comprehensive lidar plume characterization system will be composed of more than one receiver/transmitter, possibly located at different sites. The overall philosophy of monitoring is to always use a particulate lidar as the primary data acquisition device to provide

maximum temporally resolved plume documentation and to use the slower mode lidars to systematically sample various regions of the plume to obtain data on the other parameters. The rapidly acquired particulate data can be considered surrogates for the other parameters which, when coupled with their respective samples, can be used in software models to provide a more nearly complete characterization record.

Field measurements to evaluate each of the lidar remote sensing modes can be largely and economically supported with the existing CGC mobile lidar test bed design through modest, phased-in modifications. Ancillary electronics, computer software, and scanner are common to all of the modes. The increasing frequency of planned STS launches will provide evaluation data base acquisition opportunities as the various modes can be brought on-line. The data base acquired using the mobile test bed will determine feasibility and can be used, where applicable, to specify and develop parameter-optimized, dedicated, permanently installed instruments.

SECTION II

STS-3 OPERATIONAL CONSIDERATIONS

Preliminary prediction of wind conditions indicated that formation and movement of the booster exhaust cloud for STS-3 should be similar to that of STS-1. Video tapes, meteorological characteristics, and in situ measurement data obtained during STS-1 launch operations were reviewed. This information, coupled with the lidar tracking experience gained during the launch of STS-2, enabled the development of a more efficient lidar tracking/data acquisition technique. For STS-3, a single-scan pattern was developed to scan the booster exhaust cloud. By applying separate scale factors in real time to the vertical and horizontal dimensions of this scan pattern, the computer operator can configure the scan pattern to the approximate size and shape of the booster exhaust cloud.

A 28° field-of-view video camera and T.V. monitor with a 10 by 10 overlay grid would be used by the lidar field operating team to maintain cloud centroid track in a feedback loop closed through the computer console operator.

To eliminate any possibility of exposing the sensitive lidar optical detector to the booster flame, a scanning scenario was developed in conjunction with NASA/USAF personnel to initially point the scanner at Pad 39B. At T-00:10 the lidar would begin laser firing and acquiring hard target data from Pad B. At T+00:00, the computer would be commanded to start scanning toward Pad 39A, intercepting the expanding booster exhaust cloud, and then continue automatic scanning as described below. It was calculated that the scanner would not point at Pad 39A before T+00:15. By this time the STS-3 launch vehicle would be well above the scanner field of view and pose no optical hazard to the lidar detection system photomultiplier tube.

During the STS-3 planning phase, it was decided to decrease the sampling interval size to 50 ns to obtain higher measurement volume resolution. A total sampling window of 12,000 feet; however, would require real-time operator control to move the window in or out to track the cloud. The necessary software modifications were made to achieve this additional real-time flexibility for STS-3 support.

The lidar would be positioned on Camera Pad USC-6 (Figure 1) due West of and at an approximate range of 20,500 feet from Pad 39A. Sun angle and position at the scheduled STS-3 launch date and time were considered to be sufficiently to the South so as not to produce excessive signal-to-noise interference. A series of tests was scheduled for L-1 day to determine typical solar background levels for selection of system operational settings to provide optimum signal-to-noise ratio. A summary of these tests is presented in Section IV.

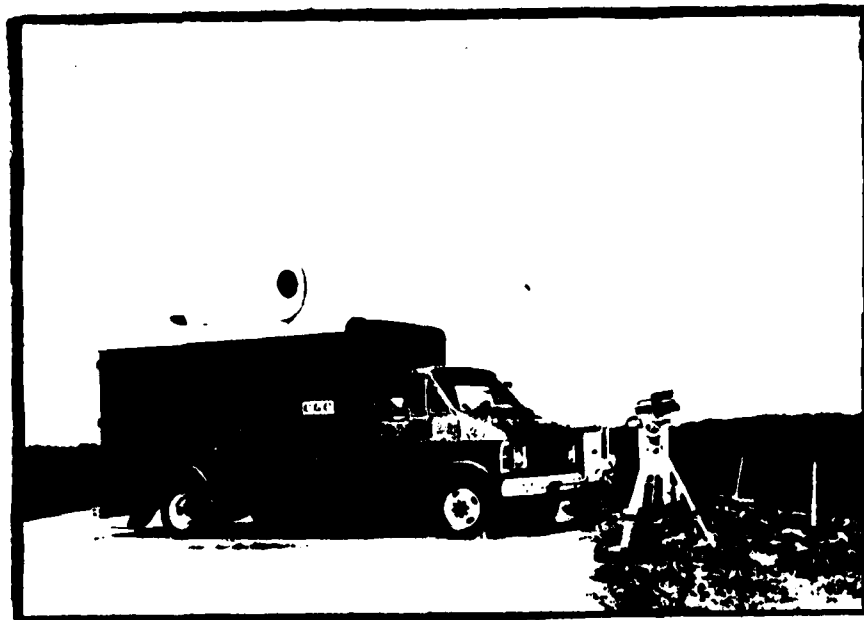


Figure 1. CGC Mobile Lidar at UCS-6

A. REAL-TIME SOFTWARE FOR STS-3 DATA ACQUISITION

Lidar cross sections are constructed from a series of discrete range resolved, line-of-sight (LOS) measurements positioned along a path (scan segment) across the measurement volume of interest. Each scan segment requires a finite execution time which is a function of telescope slew rates, segment length, and laser pulse repetition rate. Further improvements were made to the lidar real-time software to support STS-3. These improvements, based in part on the STS-2 experience, were designed to increase the measurement efficiency of the lidar system and to maximize the number of LOS through the booster exhaust cloud.

Maximum data acquisition rates are achieved by disabling all nonessential software features from the existing operating system which create computer overhead. This includes most of the real-time data processing and printing of results as printer operation incurs significant operational overhead. Some compromise in operational efficiency remains; however, since overall system tracking and scanning control is closed through the computer console operator.

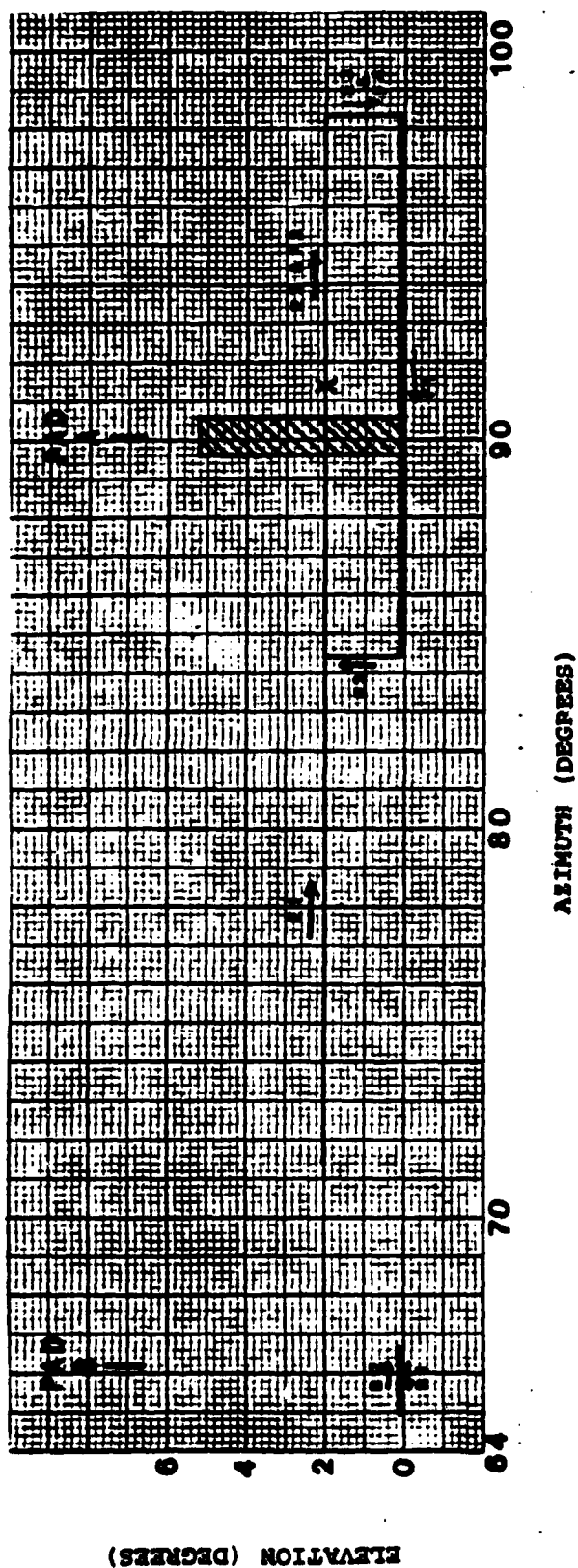
The most significant software improvements made as part of the STS-3 exhaust cloud measurement effort include a modification to increase TV tracking resolution from 1° to 0.1° , as well as

modifications in the real-time output. Although the standard real-time output is disabled during the STS launch measurement period to reduce computer system overhead, it was determined that some minimal real-time output was required. This real-time output is needed by the test director and the computer operator to monitor the lidar scanning activity. At each LOS, the true azimuth and elevation, as well as elapsed time since launch, are updated on the display terminal screen. This real-time display output is essentially the same as that used during STS-2. It was modified primarily in format to reduce the operator's task in interpreting the scanning parameters rapidly in real time. In addition, the STS-2 experience demonstrated the need to log selected scanning parameters at the end of each scan segment on the line printer. These records enable the test director to evaluate system operational performance in real time.

As discussed in the preceding section, the STS-3 measurement scenario included reducing the measurement range resolution from 50 feet to 25 feet. At this resolution, with a total range window of 12,000 feet, it can be expected that the exhaust cloud could move toward or away from the lidar by an amount sufficient to be outside the initially positioned window. The scanning control software was modified to permit real-time operator control of the range to the first measurement volume. Thus, the operator could now track the exhaust cloud in range by moving the measurement window in real time, while acquiring highly range resolved lidar data.

B. STS-3 BOOSTER EXHAUST CLOUD SCAN PATTERN

One of the most significant modifications to the lidar software operating system as the result of the STS-2 experience was in the scan pattern specification and in operator real-time control of the scan pattern. The scan pattern is a sequence of scanning segments through which the automatic scanning control software moves or scans the lidar laser beam over the measurement volume of interest. Three scan patterns were employed during the STS-3 mission (see Figure 2). Scan pattern "B" was designed to acquire hard target calibration data from Pad 39B at the initial phase of the STS-3 measurement period. Scan pattern "E", initiated at T+00:00, was designed to scan the lidar from Pad 39B to Pad 39A. At the completion of scan pattern "E", automatic scanning using scan pattern "F" is initiated and continues until a command is received to terminate lidar operations. During automatic scanning the console operator, using a transparent overlay of scan pattern "F" (see Figure 3), positions the scan pattern over the exhaust cloud by referencing TV monitor screen coordinates as in Figure 4. In addition, the aspect ratio of the scan pattern is closely matched to the exhaust cloud aspect ratio by the operator by setting appropriate independent scale factors for the azimuth and elevation legs of the scan pattern. The



NOTE: Scan pattern "B" is a 2 segment scan pattern defined so as to acquire hard target data from Pad 39B. Initiated at T-00:10.

Scan pattern "E" is a 3 segment scan pattern designed to move the lidar scanner to the initial booster exhaust cloud measurement area at Pad 39A. Initiated at T+00:00.

Scan pattern "F" is a 4 segment scan pattern designed as the primary control for lidar scanning of the booster exhaust cloud. Segments E2 and F3 and E3 and F4 are coincident. Scan pattern "F" automatically repeats.

Azimuth and elevation values indicated are for the start of the STS-3 measurement period and with both scale factors equal to 1.0.

Figure 2. Lidar Scan Patterns for STS-3

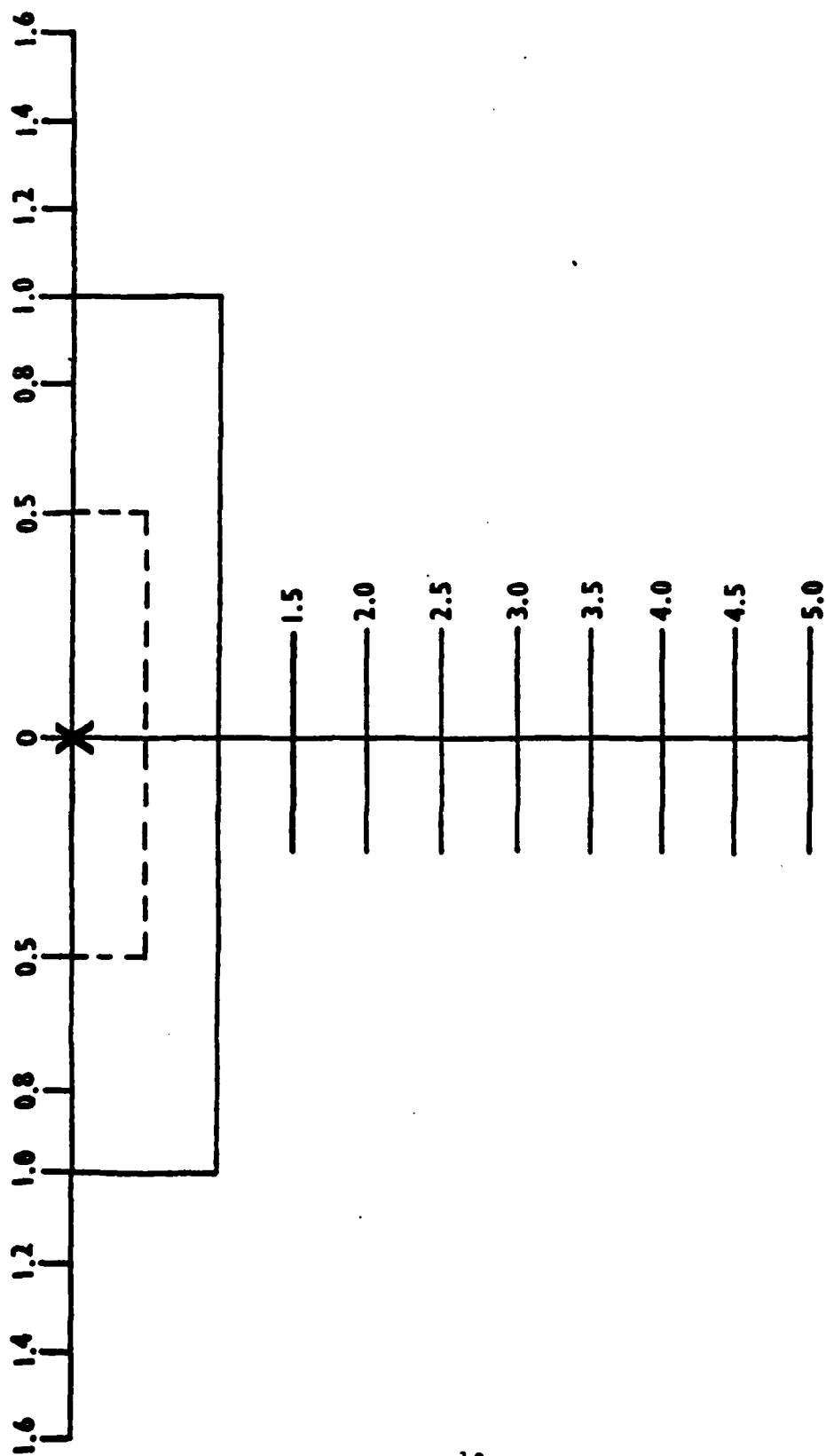
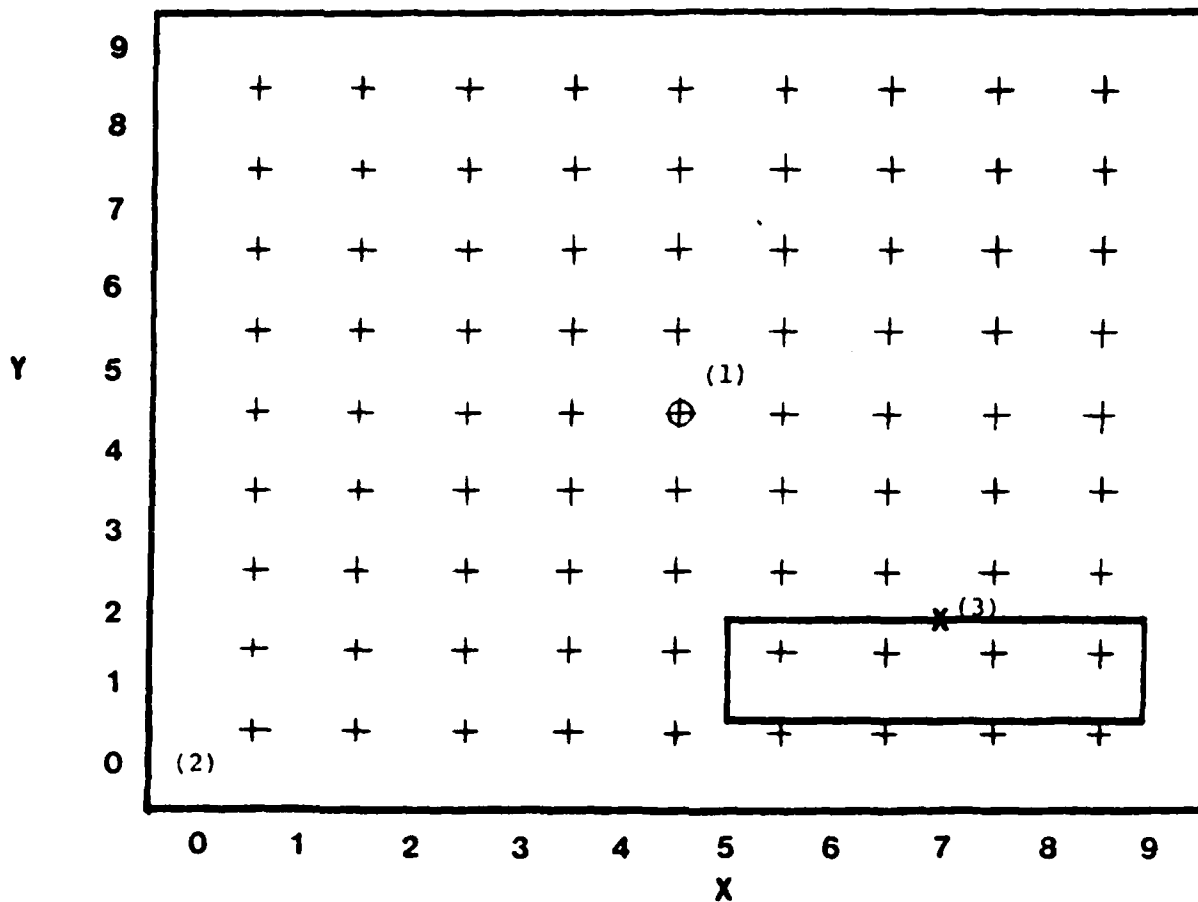


Figure 3. Scan Pattern "F" Overlay with Azimuth and Elevation Scale Factors.
The "X" Corresponds to TV Monitor Screen Reference.



- (1) Grid center true azimuth and elevation determined from command "V3" parameters.
- (2) Grid coordinates (0,0) are calculated knowing grid center position and camera field of view.
- (3) Grid coordinates (x,y) for scan pattern reference enables calculation of true azimuth and elevation for scan pattern segments.

Figure 4. T.V. Monitor Grid for Setting Exhaust Cloud Scan Pattern Reference.

illustration of the scan pattern "F" overlay in Figure 3 shows reference tick marks for the effect of azimuth and elevation scale factors on the size of the scan pattern dimensions.

C. LIDAR SCANNER RATES

Two factors in the existing configuration control the optimum firing rate and, therefore, the maximum accumulation of data during a mission. They are as follows:

1. The dye laser system deviates very substantially from its power output specification as the firing rate is increased beyond 3 pps. CGC and the manufacturer have investigated the phenomenon and determined that the flow rate of dye through the flashlamp at properly maintained temperatures is inadequate. A modification to the dye and cooling water circulator pumps and plumbing will substantially increase laser fire repetition rate at maintained power levels.

2. The greater volume of data per unit time which must be processed and recorded by the computer while it is controlling the balance of the subsystems requires modification to the software to reduce overhead. Additional core capacity is also required.

The effective laser firing rate achieved for the STS-3 scenario was 2.72 Hz. The relationship of computer system overhead to maximum laser pulse rate, along with important recommendations are discussed in Section V.

D. DETERMINATION OF SEED

Safe operation of a laser requires proper precautions to protect personnel from accidental eye exposure. Procedures used to assure safe laser operation at KSC are found in KHB-1860.2. A calculation can be made for each laser system depending upon its specification, mode of operation and ancillary equipment to determine a safe eye exposure distance (SEED). The standard used for the calculation is found in ANSI Z136.1, 1980 edition, page 57, i.e.,

$$H = \frac{1.27Qe^{-\mu r}}{(a + r\phi)^2}$$

where H is the radiant exposure in -Jcm^{-2} , Q is the total pulsed energy output of the laser in -joules, μ is the atmospheric attenuation coefficient, r is the range from laser to viewer in cm, a is the output beam diameter in cm, and ϕ is the beam divergence in radians.

Results of the calculation can vary, depending upon certain assumed values, operational modes and equipment failure mode assumptions. The CGC calculation of SEED for the current lidar configuration is 11,000 feet. A more conservative calculation, using a higher assumed value for total pulsed energy output, was provided by Pan Am Health Physics which established a 19,000 foot SEED. Other conclusions from the latter calculation are (a) at UCS-5, UCS-16, UCS-18, UCS-4, and the VAB there is an intrabeam viewing hazard to the unaided eye, and (b) at all other sites there could be a hazard when viewing with optical devices. It was further concluded that no hazard existed from diffuse reflection.

Recommendations based upon the Pan Am conclusions were:

a. Because of the large number of visitors in and around the VAB (9,025 feet from UCS-6) and other accessible areas outside of the impact limit line, the lidar should be restricted to operating within the impact limit line (ILL). This would preclude the need for goggles for observer personnel atop the VAB, as well as eliminate any possibility of injury to the general public gathered in that area.

b. An operational restriction should be placed on all observer personnel within the ILL to keep them from looking toward UCS-6 during laser data acquisition. Observer personnel inside the 19,000-foot laser exclusion area (USC-4, UCS-5, and UCS-16) should be supplied with goggles of proper O.D. for the specified observer site. Ground rescue personnel and UCS-6 personnel should be provided with goggles of minimum O.D. of 5.4. Any other personnel within a 19,000-foot radius of the lidar and inside the ILL should be equipped with goggles of O.D. corresponding to their position.

c. If the operational restriction is deemed impractical, then all observer personnel should be equipped with goggles of proper minimum O.D. Ground rescue personnel, UCS-6 personnel and all other personnel within a 19,000-foot radius around UCS-6 and inside the ILL should be equipped with goggles of minimum 5.4 O.D.

d. If it is thought desirable to operate the lidar in a 360° area, goggles should be provided to all personnel atop structures sufficiently high for intrabeam viewing to occur and consideration should be given to protection of the general viewing public within 19,000 feet of UCS-6 and outside the ILL.

e. If an emergency ground abort situation occurs, the lidar should cease transmission immediately to prevent interference with operations of ground rescue personnel and rescue aircraft.

The laser radiation operational window resulting from the recommendations is described in Section II E. The recommendations were further interpreted to restrict laser beam transmission outside the ILL (azimuth 131° to 330°) to +5° elevation or above.

E. RESTRICTED LASER RADIATION REGIONS

Geographic areas of laser radiation during launch are subject to the safety requirements as discussed in Section II D and administrative restrictions based upon SEED (Safe Eye Exposure Distance), deployment of personnel and other support operations. All laser radiation operations are coordinated with launch control and KSC range safety personnel. Figure 5 illustrates the regions authorized for laser radiation from UCS-6 during STS-3 launch operations. Restricted regions are shown in cross hatch. Azimuth angles are shown in true degrees. Lidar software was developed to prohibit laser triggers (firing) when the scanner is pointed within a restricted region. The ability of the computer to inhibit laser radiation in restricted zones was demonstrated to Pan Am Health Physics personnel as required in the approved laser radiation authorization document.

The restricted region from azimuth 131° to azimuth 330° applied to elevation angles below 5°. However, an additional restriction was imposed during the launch of STS-3; that the lidar would not fire the laser at any elevation within this azimuth range before T+20 minutes.

During the launch of STS-3, the booster exhaust cloud moved slowly to the East-Northeast. Consequently, the only laser firing restriction implemented was for the region which blocked Pad 39A.

F. PRELAUNCH CALIBRATION

System performance and measurement geometry accuracy are established through a series of triangulation and boresight tests conducted before and after the launch. Two or more "hard targets" of known azimuth and progressively greater range relative to the lidar placement are required. "Soft targets" such as overhead clouds are highly desirable. The objectives of the prelaunch tests are to:

- a. Verify optical system alignment after mobile lidar over the road transport.
- b. Maximize (peak) system sensitivity.
- c. Verify range calibration.
- d. Establish a reference point for the data reduction geometry of all lidar-acquired launch data.

The laser radiation operational window resulting from the recommendations is described in Section II E. The recommendations were further interpreted to restrict laser beam transmission outside the ILL (azimuth 131° to 330°) to +5° elevation or above.

E. RESTRICTED LASER RADIATION REGIONS

Geographic areas of laser radiation during launch are subject to the safety requirements as discussed in Section II D and administrative restrictions based upon SEED (Safe Eye Exposure Distance), deployment of personnel and other support operations. All laser radiation operations are coordinated with launch control and KSC range safety personnel. Figure 5 illustrates the regions authorized for laser radiation from UCS-6 during STS-3 launch operations. Restricted regions are shown in cross hatch. Azimuth angles are shown in true degrees. Lidar software was developed to prohibit laser triggers (firing) when the scanner is pointed within a restricted region. The ability of the computer to inhibit laser radiation in restricted zones was demonstrated to Pan Am Health Physics personnel as required in the approved laser radiation authorization document.

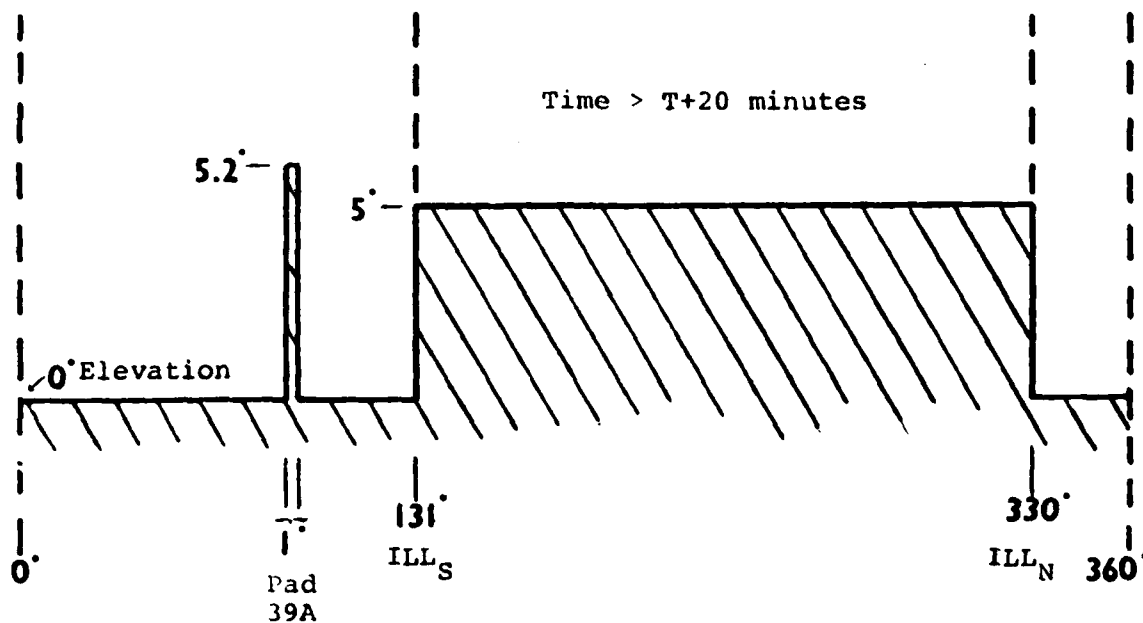
The restricted region from azimuth 131° to azimuth 330° applied to elevation angles below 5°. However, an additional restriction was imposed during the launch of STS-3; that the lidar would not fire the laser at any elevation within this azimuth range before T+20 minutes.

During the launch of STS-3, the booster exhaust cloud moved slowly to the East-Northeast. Consequently, the only laser firing restriction implemented was for the region which blocked Pad 39A.

F. PRELAUNCH CALIBRATION

System performance and measurement geometry accuracy are established through a series of triangulation and boresight tests conducted before and after the launch. Two or more "hard targets" of known azimuth and progressively greater range relative to the lidar placement are required. "Soft targets" such as overhead clouds are highly desirable. The objectives of the prelaunch tests are to:

- a. Verify optical system alignment after mobile lidar over the road transport.
- b. Maximize (peak) system sensitivity.
- c. Verify range calibration.
- d. Establish a reference point for the data reduction geometry of all lidar-acquired launch data.



STS-3 Restricted Regions for Lidar Firing at UCS-6.

- 1) Azimuth 89.5° thru 90.5° for Elevation $\leq 5.2^{\circ}$
 - 2) Azimuth 131° thru 330° for Elevation $\leq 5^{\circ}$
 - 3) Azimuth 0° thru 360° for Elevation $\leq 0^{\circ}$
 - 4) Azimuth 131° thru 330° for Elevation $\leq 90^{\circ}$
- & Time < T+20 minutes

Figure 5. STS-3 Lidar Firing Regions Permitted vs. Restricted.

- e. Initiate site-specific computer parameters.
- f. Establish ambient background levels.
- g. Test signal-to-noise ratios.
- h. Provide quality assurance data base.

A number of suitable hard targets specific to a UCS-6 lidar deployment have been authorized:

- a. 150 M weather tower located at UCS-16 at a range of 7400 feet.
- b. Lightning mast atop Pad 39A at a range of 20,500 feet.
- c. Lightning mast atop Pad 39B at a range of 16,600 feet.
- d. Water tanks at both Pads 39A and 39B.

Under current authorized lidar operation procedures, radiation of any of the targets requires extensive coordination with launch control and range safety and, in the case of Pad B, additional coordination with Air Force operations personnel. Substantial periods of time must be allocated for the conduct of calibration tests. Lidar triangulation, boresight, and scanning tests have been incorporated into the 72-hour STS countdown sequence.

G. POINTING AND TRACKING

A lidar system has a very narrow field of view specified to complement laser beam divergence and reject excess ambient background light. Scanning of the ground cloud with nominal dimensions of 4000 feet by 4000 feet requires a wider field (capable of 360° sky coverage) support subsystem which can aid the test conductor in the real-time lidar pointing and optimization of scanning. A basic system, utilizing a TV camera and lidar operator's monitor, was implemented to support STS-3 measurements. A 28° field-of-view video camera capable of accurately tracking and displaying the cloud is mounted on a surveyor's transit tripod with high-resolution graduated azimuth and elevation scales. Azimuth and elevation readings are relayed to the test conductor over a voice link to be entered in the lidar computer. This method for STS measurement is somewhat labor-intensive but proved to be an excellent concept which can be easily automated in the future as recommended in Section V.

Since the computer system controls the scanning of the lidar receiver/transmitter (R/T), a capability to input the current location of the cloud as presented on the TV monitor is required

in the absence of a direct reading of TV camera position by the computer. The scheme adopted consisted of several steps:

a. Relate R/T Azimuth to the True Azimuth. Command "V1" is incorporated into the software to provide this function (Figure 6). The operator drives the R/T to a known target and types "V1" on the operator console. The system responds with the current definition of "TRUE REFERENCE AZIMUTH." The operator either retains or alters the current definition, at which point the computer system equates the "TRUE REFERENCE AZIMUTH" to the current R/T pointing parameters. The system is now able to determine the true azimuth of the R/T during scanning. The R/T true elevation is set by leveling the R/T as described in Section IV B.

```
COMMAND = V1
PARAMETER # = 175 TRUE REFERENCE AZIMUTH = 901
COMMAND = V2
PARAMETER # = 176 TRUE TV AZIMUTH = 901
PARAMETER # = 177 TRUE AZIMUTH POSITON = 1800
COMMAND = V3
PARAMETER # = 178 TV CURRENT AZIMUTH = 1738
PARAMETER 3 = 179 TV CURRENT ELEVATION = 100
```

Figure 6. Computer True Reference Input Scheme

b. Relate the TV camera (and, consequently, the TV monitor) to the true azimuth. Command "V2" was incorporated for this purpose. The TV camera is pointed at a known target and the azimuth position is accurately noted. Via command V2 the operator is prompted to input "TRUE TV AZIMUTH" and the actual "TV AZIMUTH POSITION." The system now contains the reference data needed to calculate the true azimuth which corresponds to a given TV camera azimuth. The TV camera true elevation is established by leveling the azimuth plane of the tripod TV camera mount; the value is read directly.

c. Identify to the computer system the current azimuth and elevation of the TV camera. Command "V3" was incorporated to provide the operator with this capability. The operator is prompted to input "TV CURRENT AZIMUTH" and "TV CURRENT ELEVATION." Using these parameters the system can calculate the true azimuth and elevation reference for the scanning reference grid which overlays the TV monitor (illustrated in Figure 4). By entering the scanning reference grid coordinates, the operator can direct the system to scan a particular azimuth and elevation window as defined by the selected scan pattern. Section II B describes the scan pattern available to the operator to control the actual scanning scenario to be executed by the system.

Steps a and b described above are performed before the measurement period and are carried out as part of the lidar system setup procedure. Step c is performed initially prior to the measurement period and then in real time as required whenever the TV camera line of sight is changed to track the ground cloud. Changes in current TV position and TV monitor grid reference must be entered manually by the operator in a manner mutually exclusive with data acquisition resulting in a loss of data and reduced measurement efficiency.

SECTION III

LIDAR MEASUREMENT OF STS-3 EXHAUST CLOUD

The CGC mobile lidar was positioned at UCS-6 four days prior to the launch of STS-3. A number of checks and calibrations were conducted to establish system performance and to provide a data base of calibration data. The primary calibration activities included hard target triangulation tests and solar background sensitivity tests. These tests and calibration procedures are discussed in detail in Section IV.

The results of the solar background sensitivity tests were used to set the lidar detection system parameters for maximum S/N. These tests were made at L-1 day under conditions similar to those anticipated at the time of STS-3 launch.

As part of the subject assessment program, the CGC mobile lidar facility successfully tracked the STS-3 ground cloud from an observation point (UCS-6), 6 kilometers due West of Pad 39A and acquired particulate backscatter data to a lidar range of 7+ kilometers as the cloud was carried offshore by westerly winds. Signal-to-noise ratios of 12:1 were obtained by the lidar during the STS-3 launch, demonstrating the practical feasibility of lidar, operating in particulate mode, to track and document cloud behavior and fallout for challenge of evidence and model development. Solar background levels measured were, as expected, based upon sensitivity settings determined by the prelaunch background sensitivity tests.

Scattergraphs of STS-3 lidar data for 16 scan segments are presented in Appendix B.

A. STS-3 LAUNCH DATA ACQUISITION AND SCANNING SUMMARY

Preparatory to the STS-3 exhaust cloud measurements, the CGC lidar scanner was pointed toward Pad 39B. At T-00:10, the computer scanning program was initiated acquiring hard target data. At T+00:00, the command was given to begin automatic scanning. This command was received as the first segment of scan pattern "B" was nearing completion. An error in the scanning software resulted in a delay in beginning the execution of scan pattern "E" of approximately 40 seconds. The booster exhaust cloud, which was expanding toward Pad 39B, was first measured at T+00:54 at an azimuth of 86.5° or 3.6° North of the pad as viewed from UCS-6. Figure 11 illustrates the size and shape of the booster exhaust cloud at T+00:54 as reconstructed from the video recording of the launch. At this time the main body of the expanding cloud was beneath the lidar scan and the first lidar measurement was of an upper cloud structure approximately 1300 feet north of the launch site. This first measurement of the

cloud was made 3 seconds into the second segment of scan pattern "E". At the completion of scan pattern "E", the system automatically initiated scan pattern "F". As set up for STS-3, segments 2 and 3 of scan pattern "E" coincide with segments 3 and 4 of scan pattern "F". Automatic lidar scanning using scan pattern "F" continued until T+29:48, at which time scanning was terminated by the console operator. A summary of the 30 complete scans made during the measurement period is presented in Table 1.

Of the total 1798 seconds that lidar scanning was active, measurements were made for 1636 seconds (see Figure 7). Gaps in the measurement period totaling 162 seconds were the result of required operator interaction to manually input updated scanning parameters.

During the STS-3 launch, meteorological conditions were such that it was not necessary to manually track the booster exhaust cloud by movement of the tripod-mounted TV camera. The cloud remained within the field of view of the camera and tracking was accomplished entirely by the computer console operator by changing the TV monitor screen reference coordinates for the scanning pattern overlay. For this particular launch, the only other control input required of the operator were changes in the azimuth and elevation scale factors to size the scan pattern to the actual booster exhaust cloud dimensions. The time line chart presented in Figure 7 indicates the periods during which the lidar system was actively scanning and acquiring data and the periods during which scanning was halted by the console operator to input tracking information. Modifications to the scanning control software, based upon the STS-2 exhaust cloud tracking experience, enabled more rapid input of tracking parameters and, hence, a higher ratio of measurement time to total operational time. For STS-3 this ratio was 91.0 percent as compared to 68.9 percent for STS-2. Modifications are recommended in Section V to reduce or eliminate loss of measurement time from operator interaction during automatic scanning.

A total of 3560 laser pulses were fired into the exhaust cloud measurement volume during the STS-3 measurement period. Since each laser pulse generates 480 volumetric data values, a total of 1,708,800 range-resolved lidar measurements were made.

B. LIDAR MEASUREMENT SPATIAL DISTRIBUTION FOR STS-3

During the STS-3 lidar measurement period the atmospheric conditions were such that the exhaust cloud remained within the field of view of the TV camera as it was initially set up. Consequently, all tracking of the STS-3 exhaust cloud was done by updating the scan pattern reference coordinates on the TV monitor. The changes of the apparent size and shape of the cloud as viewed from UCS-6 were tracked by resetting the azimuth and elevation scale factors as appropriate.

TABLE 1. LIDAR MEASUREMENT SUMMARY, STS-3, 22 March 1982

SCAN #	SCAN PATTERN	TIME	MAGNETIC TAPE LD0116 RECORD NUMBERS
135	B	T-00:10	1 - 16
136	B	T+00:15	17 - 32
137	E	T+00:42	33 - 51
138	F	T+01:26	52 - 81
139	F	T+02:36	82 - 112
140	F	T+03:44	113 - 142
141	F	T+04:40	143 - 172
142	F	T+05:41	173 - 206
143	F	T+06:42	207 - 240
144	F	T+08:03	241 - 274
145	F	T+09:10	275 - 308
146	F	T+10:17	309 - 342
147	F	T+11:25	343 - 376
148	F	T+12:24	377 - 410
149	F	T+13:22	411 - 444
150	F	T+14:46	445 - 478
151	F	T+15:50	479 - 512
152	F	T+16:51	513 - 546
153	F	T+17:53	547 - 580
154	F	T+18:54	581 - 614
155	F	T+20:01	615 - 648
156	F	T+21:02	649 - 682
157	F	T+22:04	683 - 716
158	F	T+23:15	717 - 750
159	F	T+24:28	751 - 784
160	F	T+25:34	785 - 818
161	F	T+26:40	819 - 852
162	F	T+27:40	853 - 886
163	F	T+28:48	887 - 920
164	F	T+29:48	Scanning Terminated

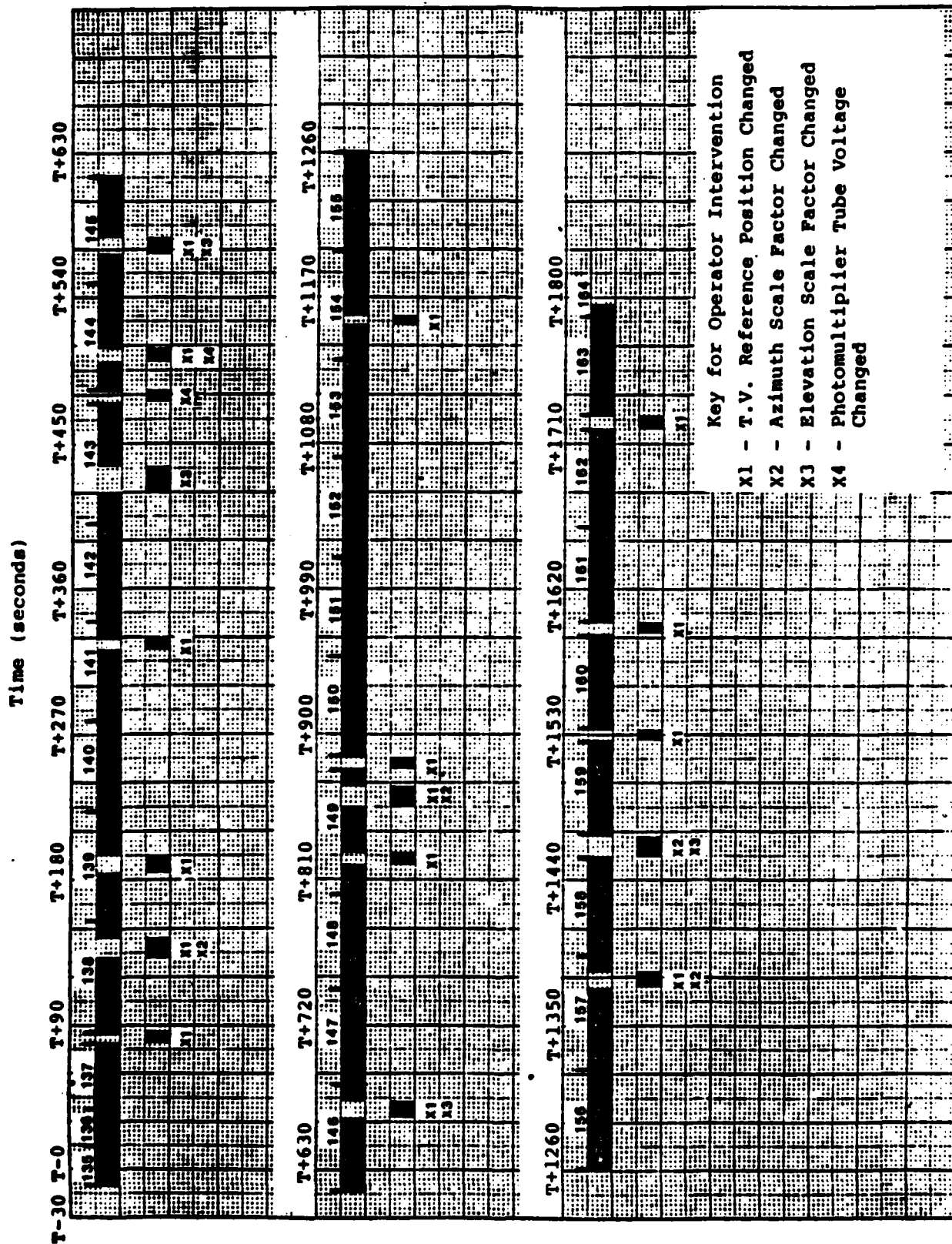


Figure 7. Booster Exhaust Cloud Lidar Event Time Chart for STS-3

Applying this procedure, the lidar successfully tracked the movement and growth of the STS-3 booster exhaust cloud through a total geographic sector shown in Figure 8. The shaded area of this figure indicates the lidar measurement zone as it was operated during the STS-3 cloud dispersion.

The azimuth and elevation coverage of the eight best-fit scan configurations executed during the STS-3 measurement period is shown in Figure 9. The dashed area indicated the Pad 39A laser firing exclusion area.

The scan pattern configurations selected by the operator and their relation to actual cloud movement are shown in Figures 10-19. The scan patterns are superimposed over reconstructed cloud dispersion at the times indicated. Two clouds are indicated here, (A) and (B). Cloud (A) represents the booster exhaust cloud and (B) the meteorological cloud present throughout the measurement period.

Figure 10 shows the initial stages of cloud development at an early time into the flight. Figure 11 indicates the point at which the first lidar return was received as the system scanned from Pad A toward Pad B. The entire scan pattern (Scan #137) associated with this initial return is shown in Figure 12. An associated scattergraph of this scan segment can be found in Appendix B. The cloud outlines were derived from the pointing system video recording made during the STS-3 measurement period.

Scanning scenarios for the booster exhaust cloud are determined in real time from cloud shape and movement characteristics as depicted on the video TV monitor (Figure 4). Orientation of the desired scanning scenario on the cloud is accomplished through operator/computer interaction based on video monitor observations. An indication that an offset occurred in the pointing of the TV camera/monitor subsystem comes from inconsistencies observed when relating the scan pattern to the corresponding cloud shape. This effect is exclusively related to the TV camera and monitor tracking system and manifests itself only in that the scan pattern overlay may not be exactly related to the cloud as viewed on the TV monitor. Initial indications; however, are that this problem appears to be more elevation-oriented than azimuth. The determination of the exact nature and magnitude of this misalignment of the TV camera/TV monitor tracking system requires more processing of data. The position of the scan pattern as drawn over the cloud shapes in Figures 11 through 19 is approximate and may shift slightly as a result of further processing.

C. STS-3 LIDAR PERFORMANCE

Prelaunch and postlaunch lidar subsystem evaluation, coupled with preliminary analysis of the STS-3 lidar data indicates that

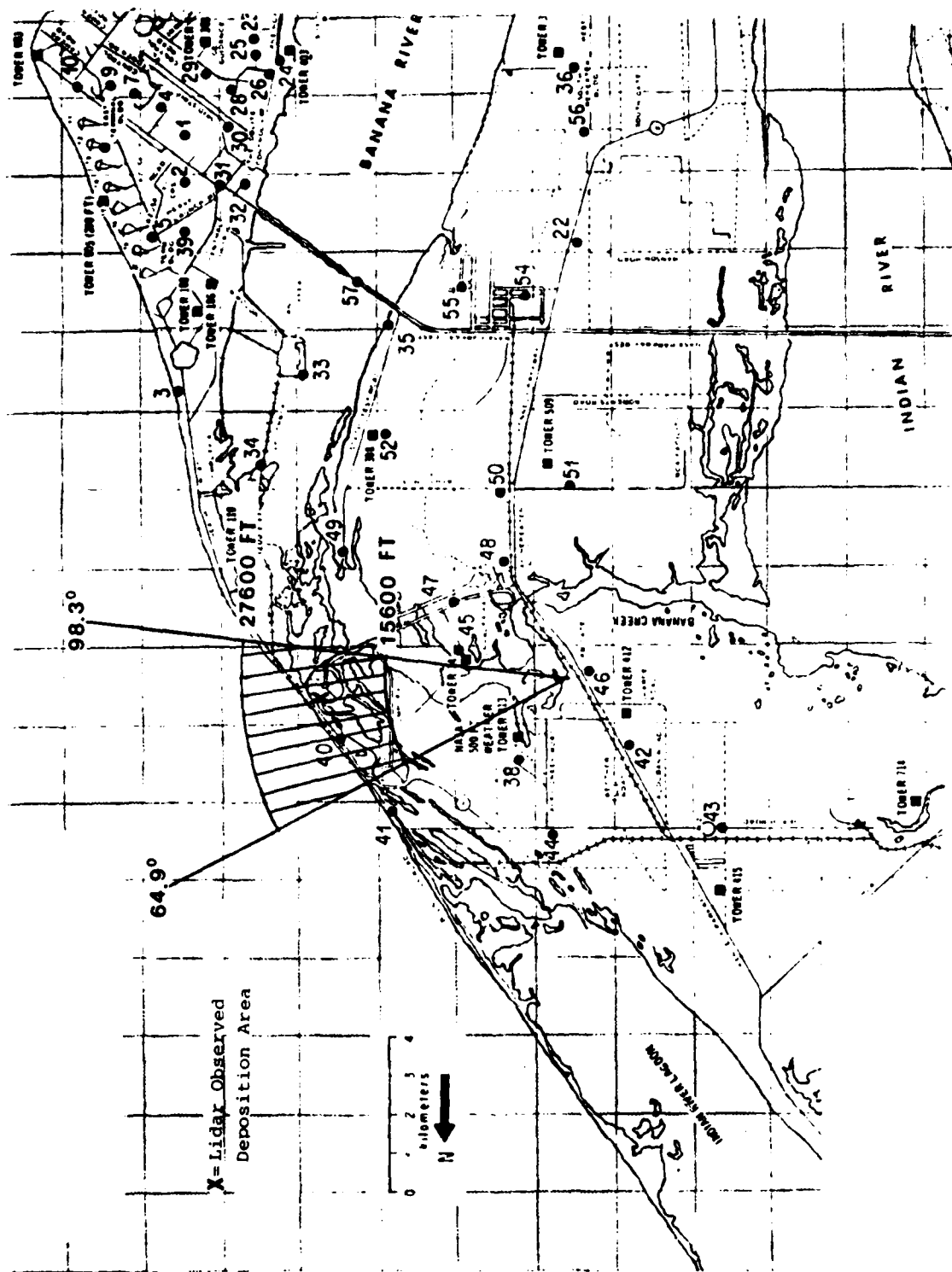


Figure 8. Booster Exhaust Test Lidar Coverage Area

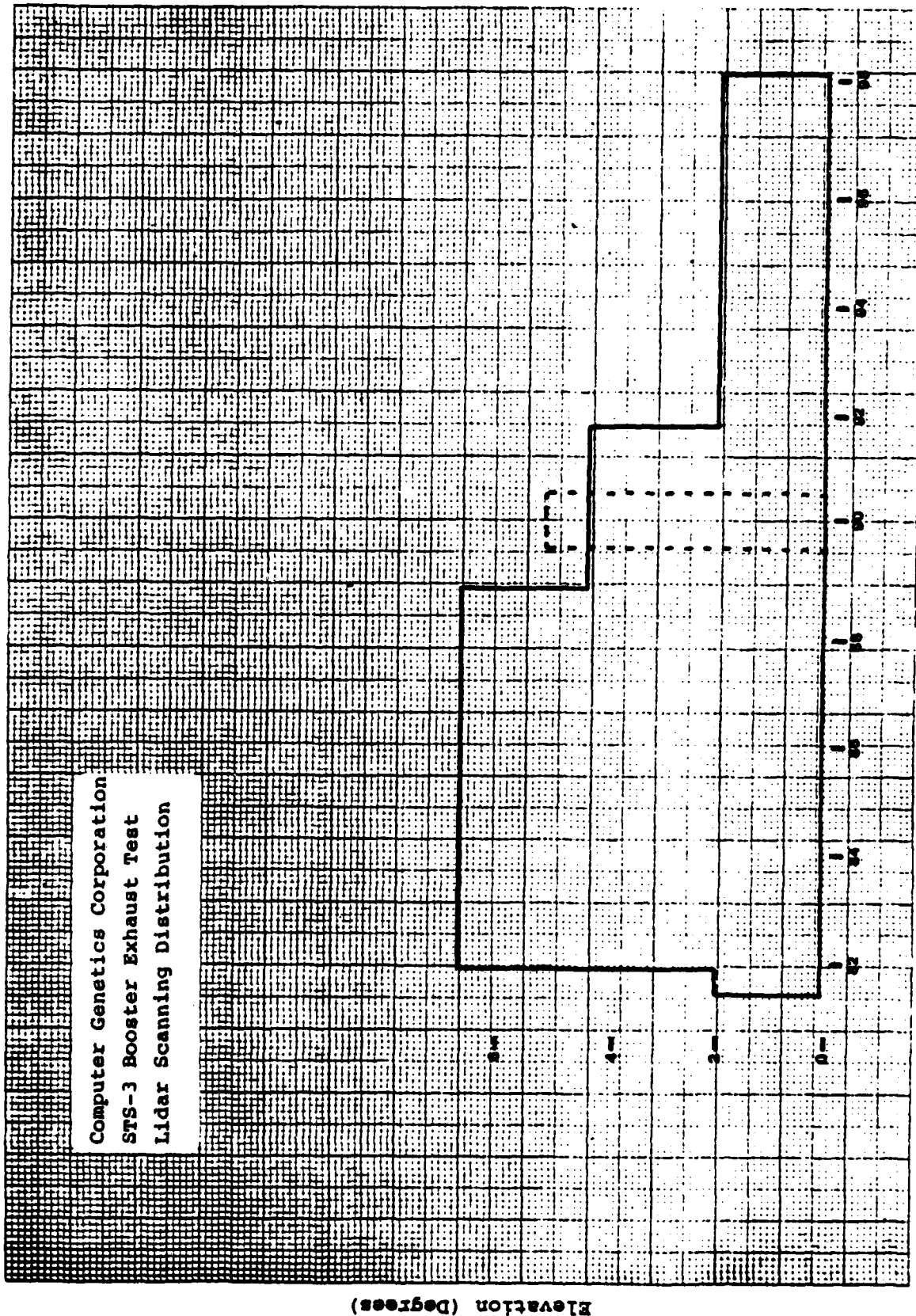


Figure 9. STS-3 Booster Exhaust Test Lidar Scanning Distribution

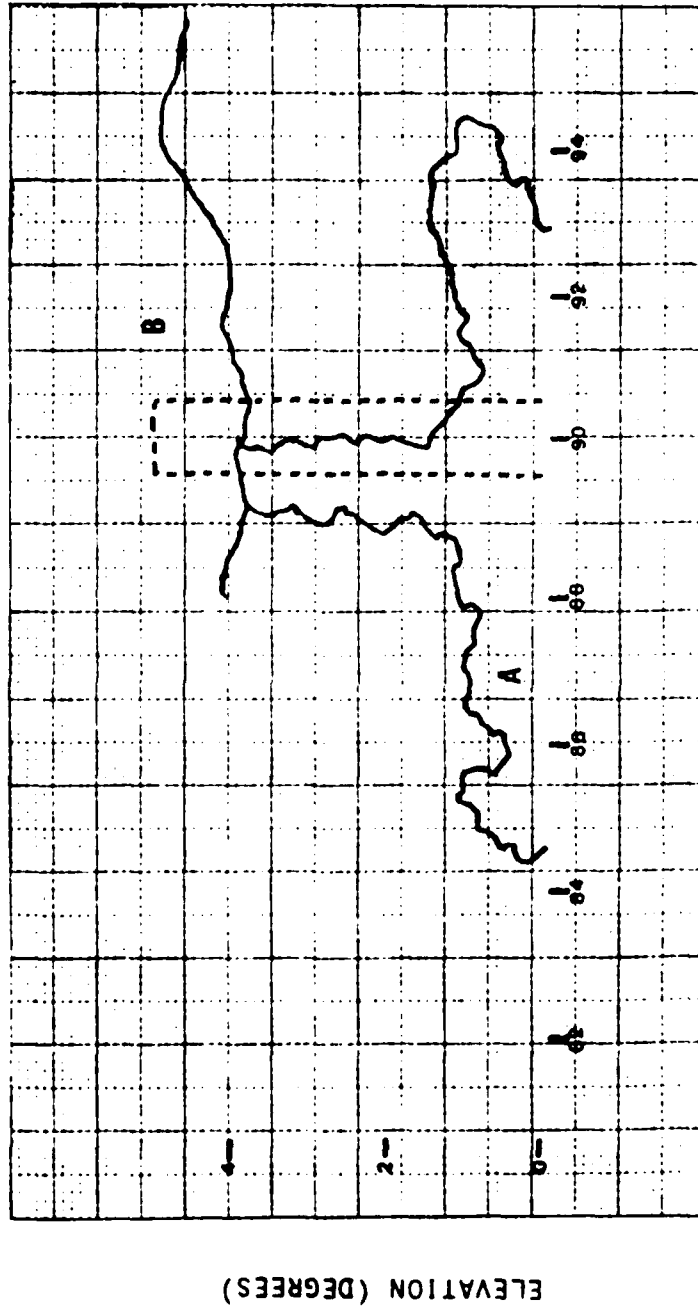
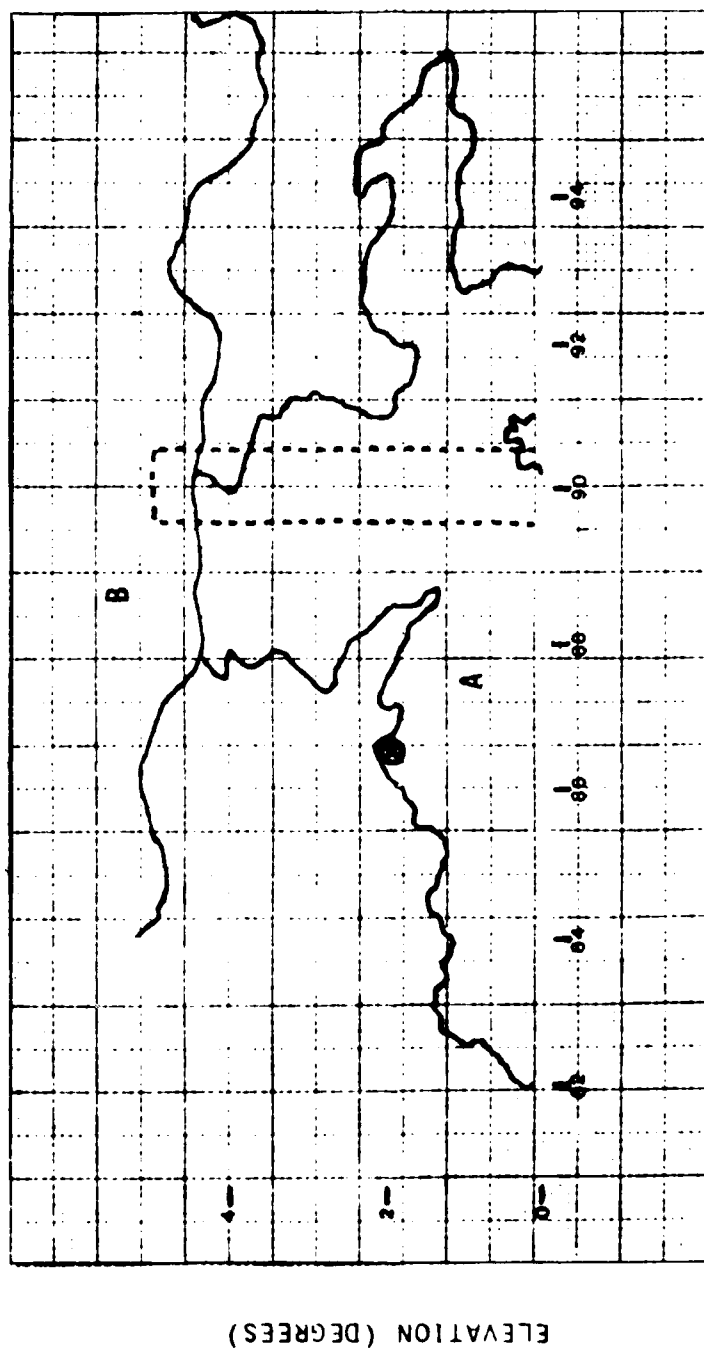
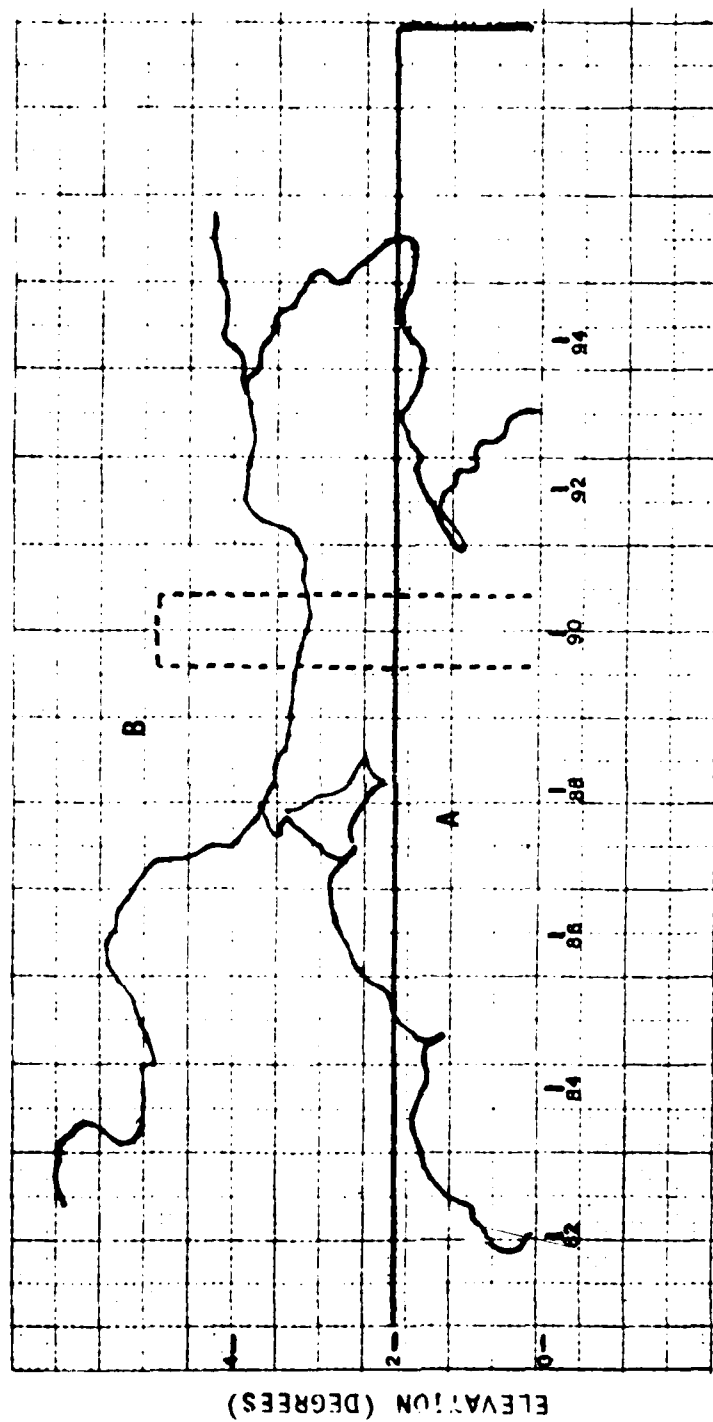


Figure 10. Booster Exhaust Plume T + 20 Seconds 11:00:20



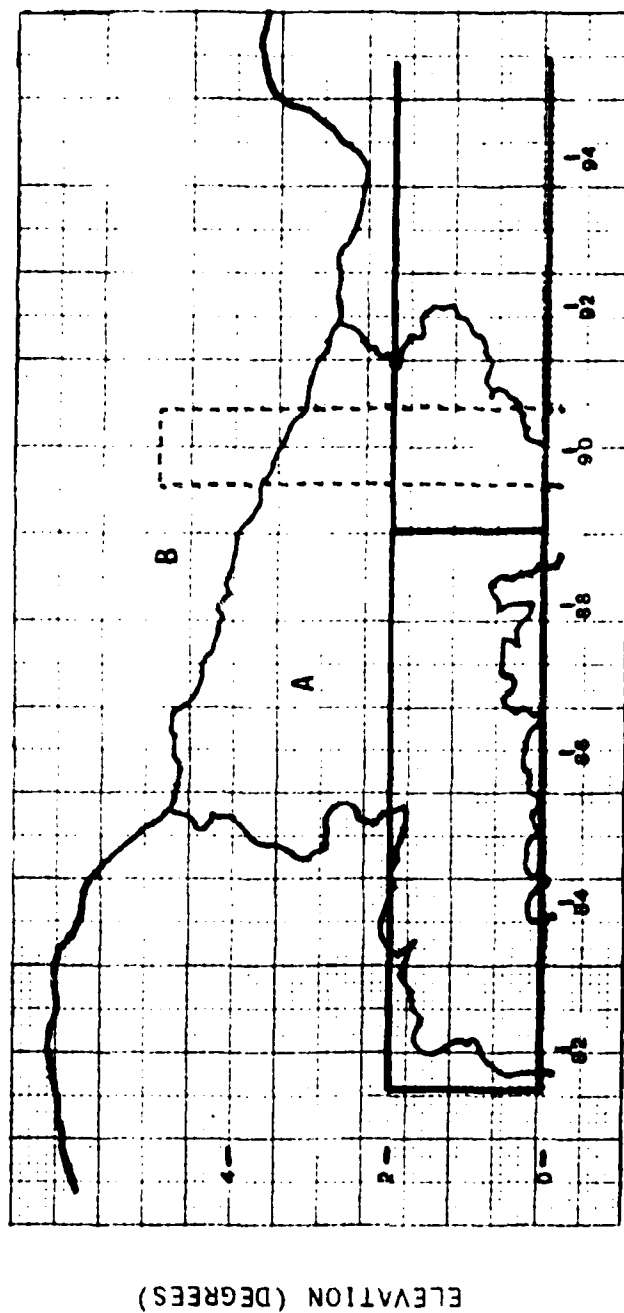
TRUE AZIMUTH (DEGREES)

Figure 11. Booster Exhaust Plume, T + 54 Seconds 11:00:54



TRUE AZIMUTH (DEGREES)

Figure 12. Scan #137, 11:00:42 - 11:01:19, Plume at 11:01:10



TRUE AZIMUTH (DEGREES)

Figure 13. Scan #138, 11:01:26 - 11:02:35, Plume at 11:01:55

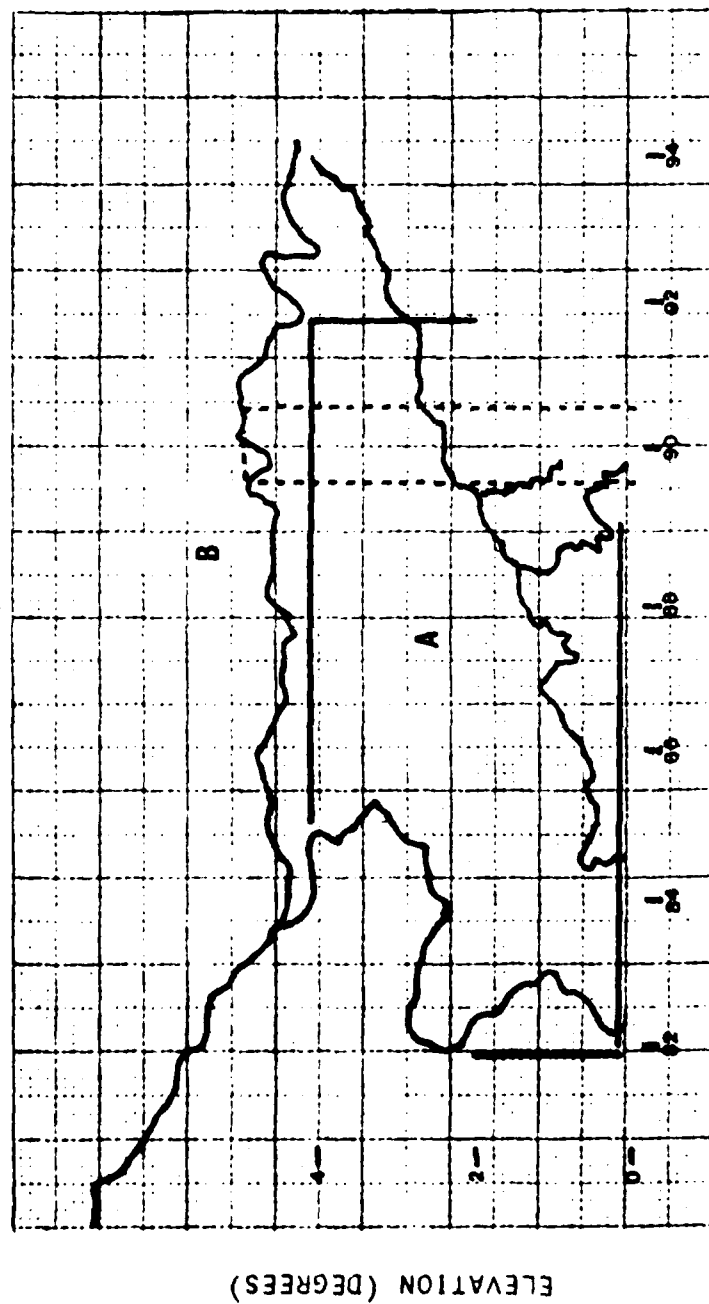
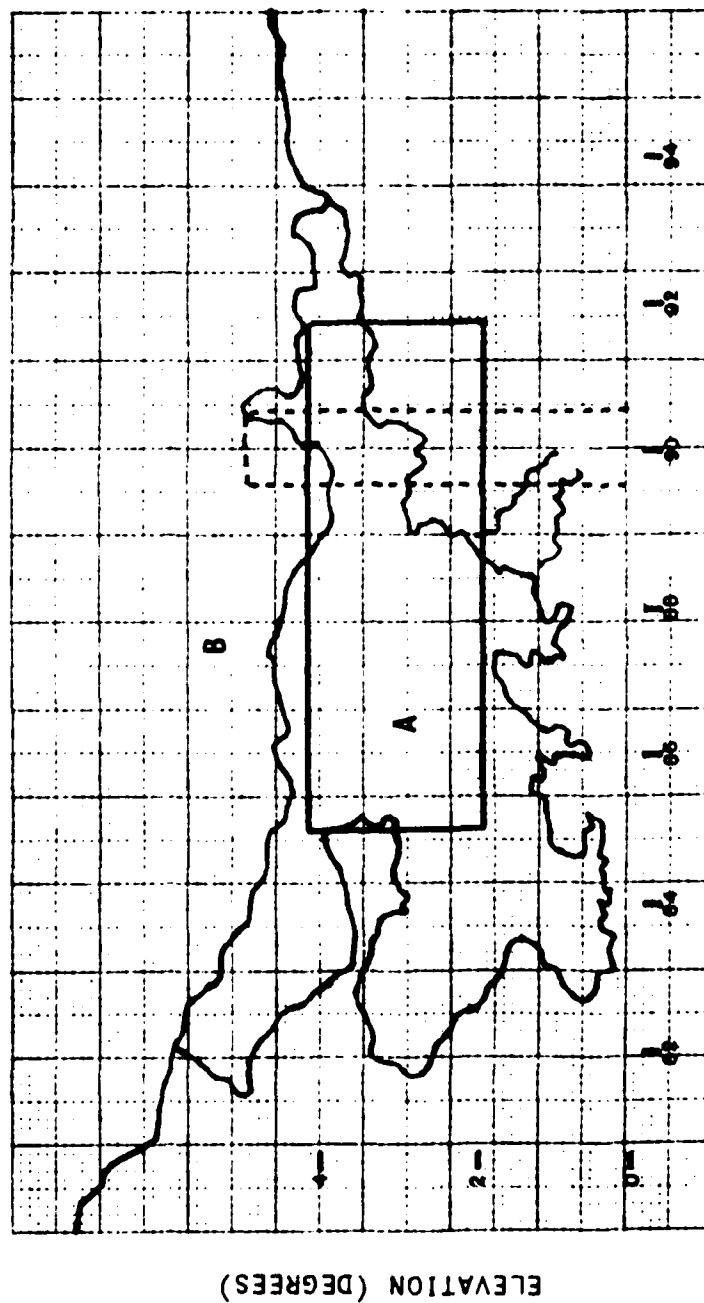
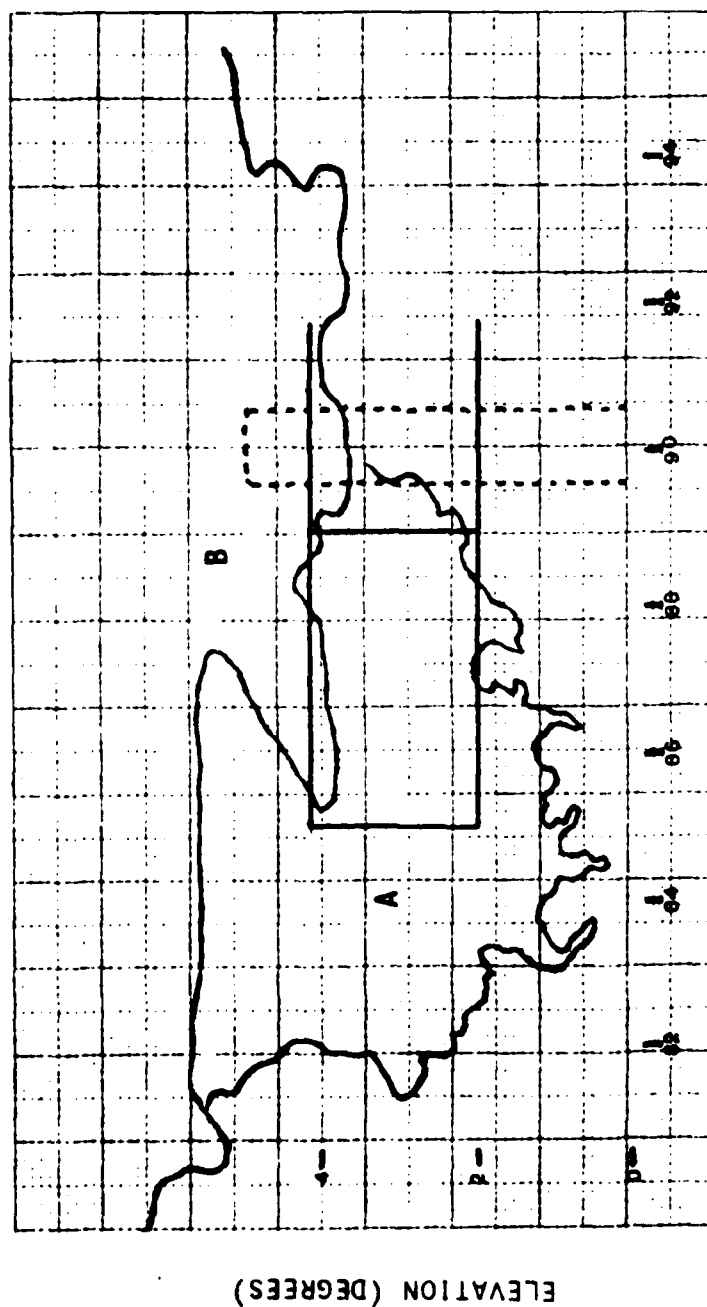


Figure 14. Scan #139, 11:02:36 - 11:03:43, Plume at 11:03:16



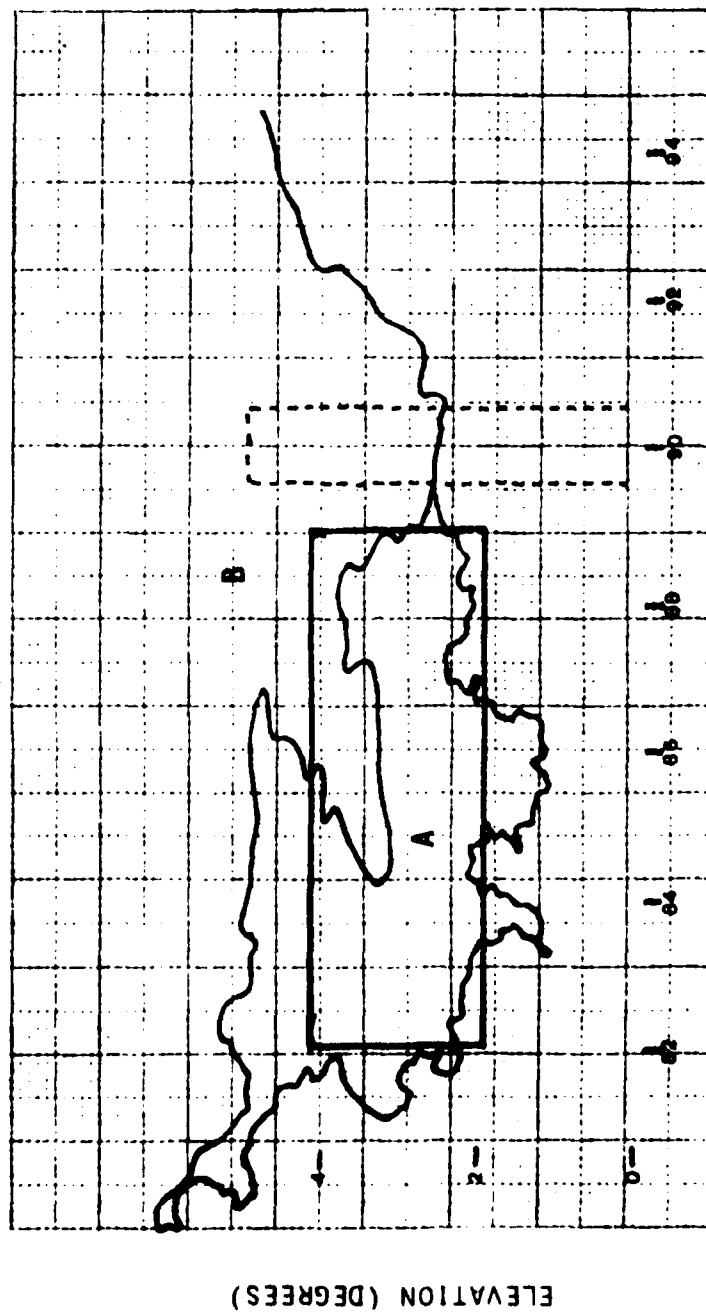
TRUE AZIMUTH (DEGREES)

Figure 15. Scan #140, 11:03:44 - 11:04:39, Plume at 11:04:12



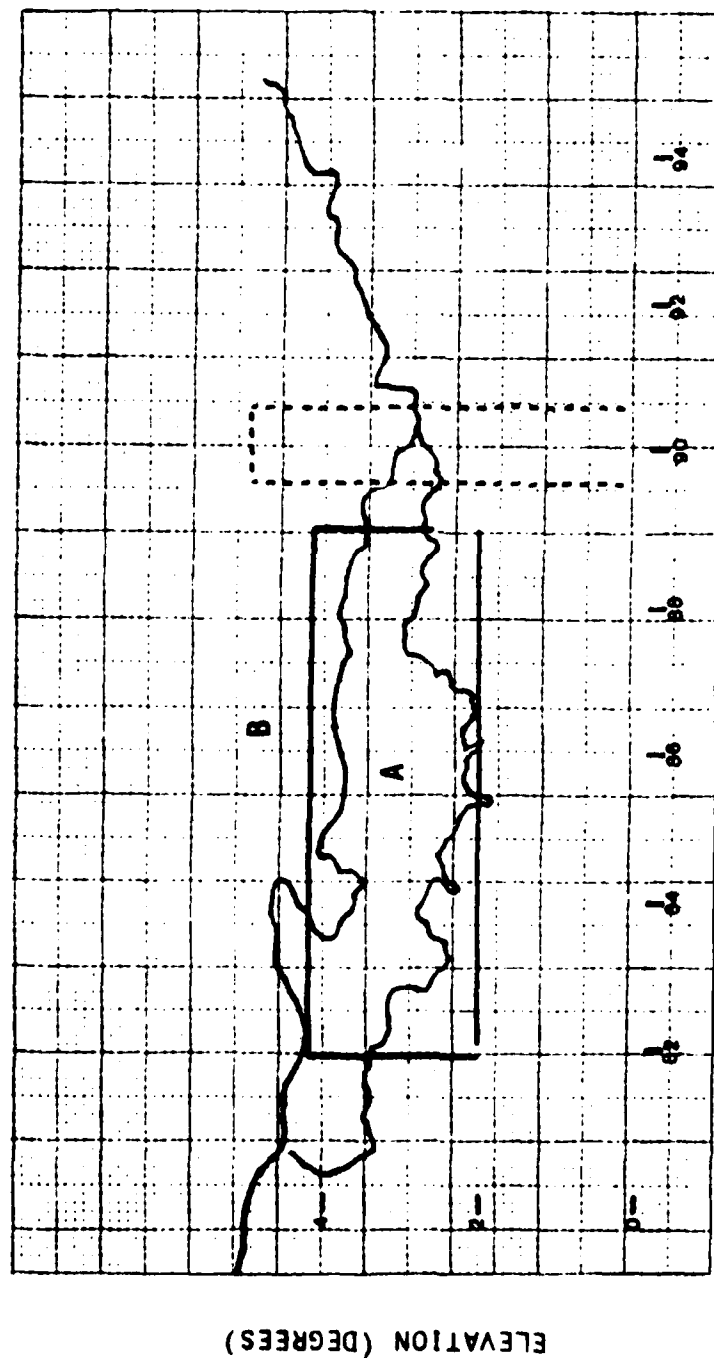
TRUE AZIMUTH (DEGREES)

Figure 16. Scan #141, 11:04:40 - 11:05:40, Plume at 11:05:08



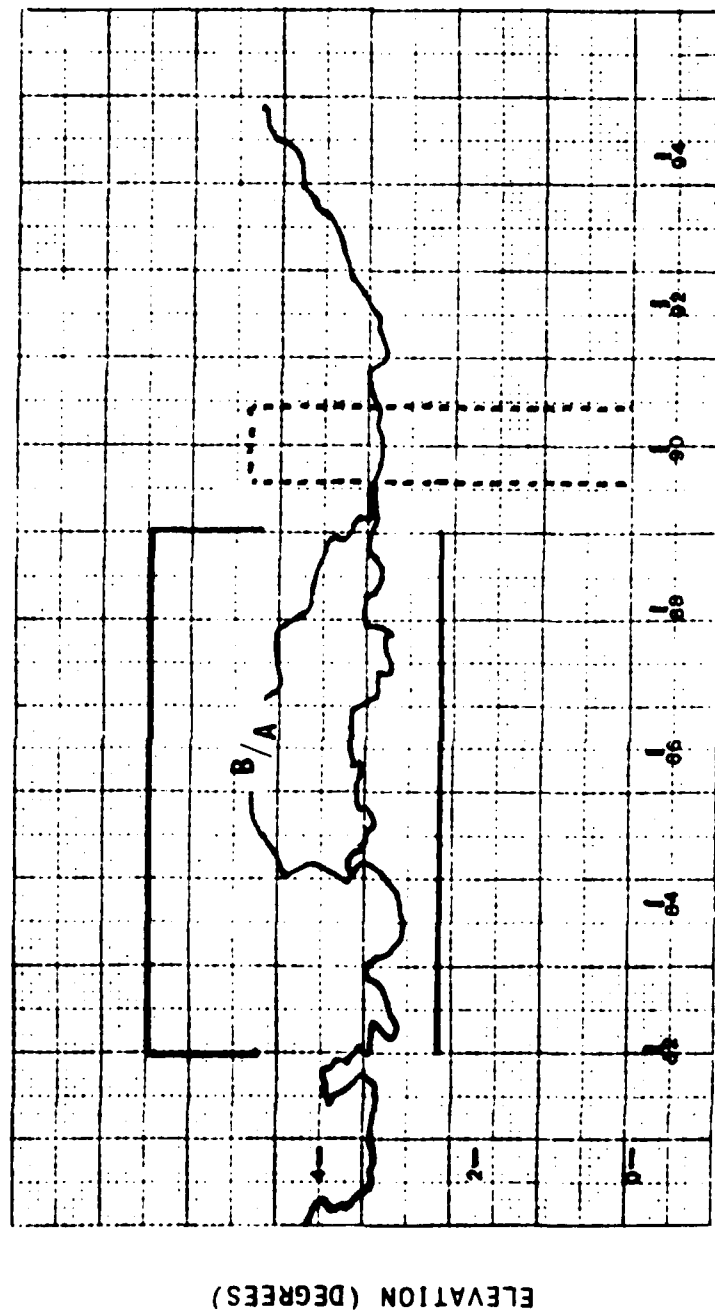
TRUE AZIMUTH (DEGREES)

Figure 17. Scan #142, 11:05:41 - 11:06:41, Plume at 11:06:11



TRUE AZIMUTH (DEGREES)

Figure 18. Scan #143, 11:06:42 - 11:07:56, Plume at 11:07:28



TRUE AZIMUTH (DEGREES)

Figure 19. Scan #144, 11:08:03 - 11:09:09, Plume at 11:08:40

the lidar performed as expected throughout the measurement period. Figures 20 and 21 illustrate typical lidar measurements obtained during the STS-3 mission. The only malfunction experienced was a software effort which resulted in a delay of 40 seconds at the start of the measurement period. This effort had no other impact on the overall lidar performance.

The operating characteristics of the several lidar subsystems were evaluated prior to launch, under conditions similar to those expected during STS-3 operations. These operating characteristics were modified as needed to enable acquisition of the best quality data. The lidar subsystems involved were the photomultiplier (PM) tube, transmitter/ receiver optics, computer/digitizer/magnetic tape recorder, tracker, and laser.

Evaluation of PM tube performance characteristics under expected launch conditions was made. Calibration of influencing parameters such as ambient background levels and signal-to-noise ratios was conducted as described in Section IVB. In addition, steps were taken to protect the sensitive optics damaged in the STS-2 experiment. These included software modifications to restrict scanning of Pad A for a predetermined elapsed time and the construction of a telescope baffle to reduce ambient background levels. STS-3 postlaunch background tests revealed no decrease in PM tube performance as was experienced in STS-2.

Consistent with pretest alignment procedures, transmitter/ receiver alignment integrity after travel was measured. These tests determined that some minor misalignment was in evidence. Utilizing the boresighting and triangulation testing (Section IV B), the system was "peaked" to achieve the highest signal-to-noise ratio. Postlaunch testing determined that alignment integrity was maintained throughout the mission.

Analysis of the data acquisition subsystem (computer, digitizer, magnetic tape recording) utilizing prelaunch, real-time, and postlaunch recorded data has shown that all measurements were made with a high degree of reliability. Except for the computer software error identified in Section IIIA, all data acquisition subsystem operations functioned properly.

Tracking of the booster exhaust cloud for a total of 30 minutes has been found to be fairly efficient. As seen in Figure 7, this efficiency has been determined to be 91 percent. As discussed in Section IIIB, Figures 11 through 13 depict the exhaust cloud's position in relation to the scan pattern used. This type of representation has been used for the first 8 minutes only. As can be seen, booster exhaust cloud (A) and meteorological cloud (B) became increasingly difficult to discern, both in real time and from the system video record of the event.

TIME: T+1:33
AZIMUTH: 89.5°
ELEVATION: 0.1°

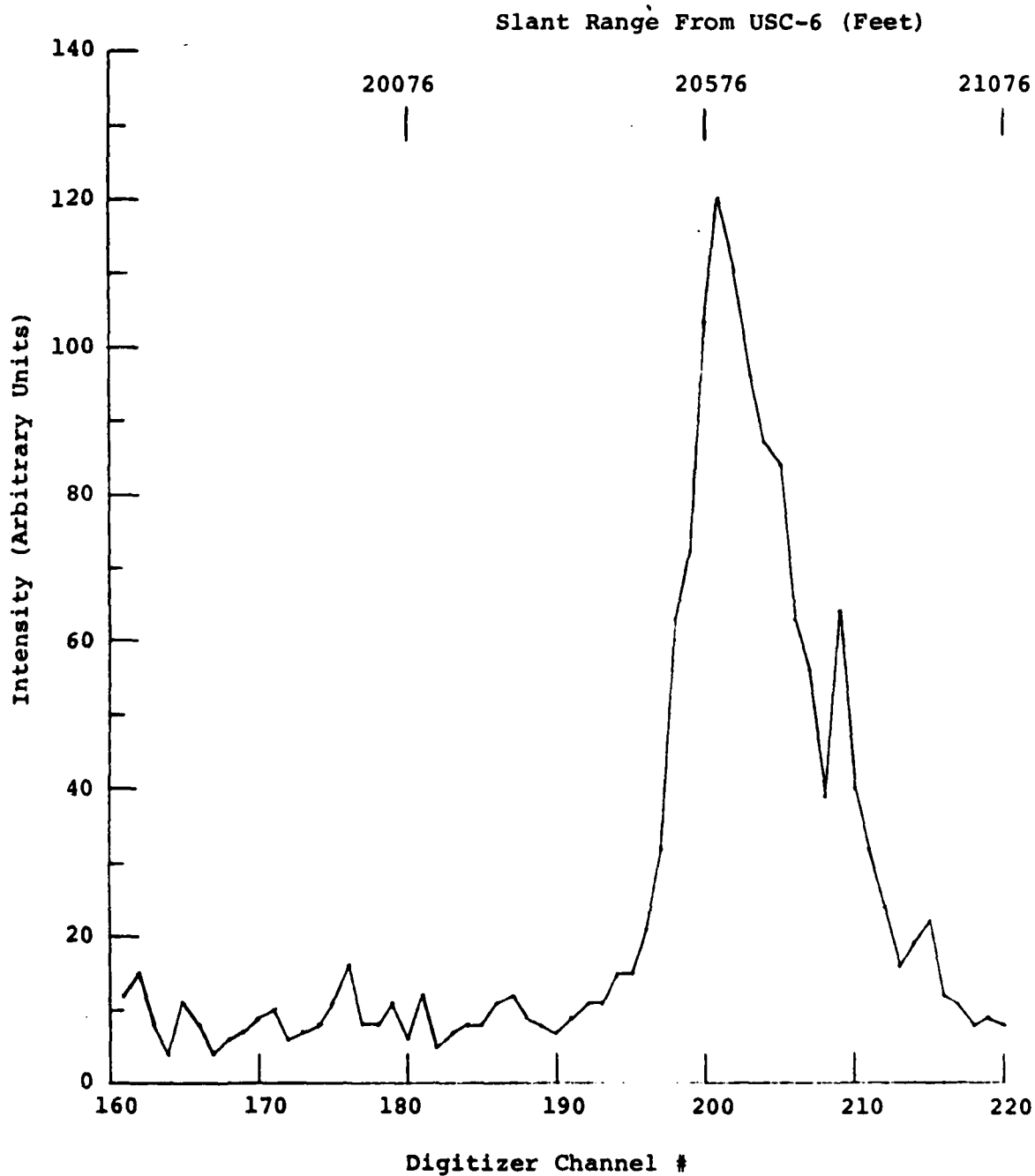


Figure 20. STS-3 Booster Exhaust Cloud Lidar Data,
22 March 1982

TIME: T+2:03
AZIMUTH: 87.4°
ELEVATION: 2.0°

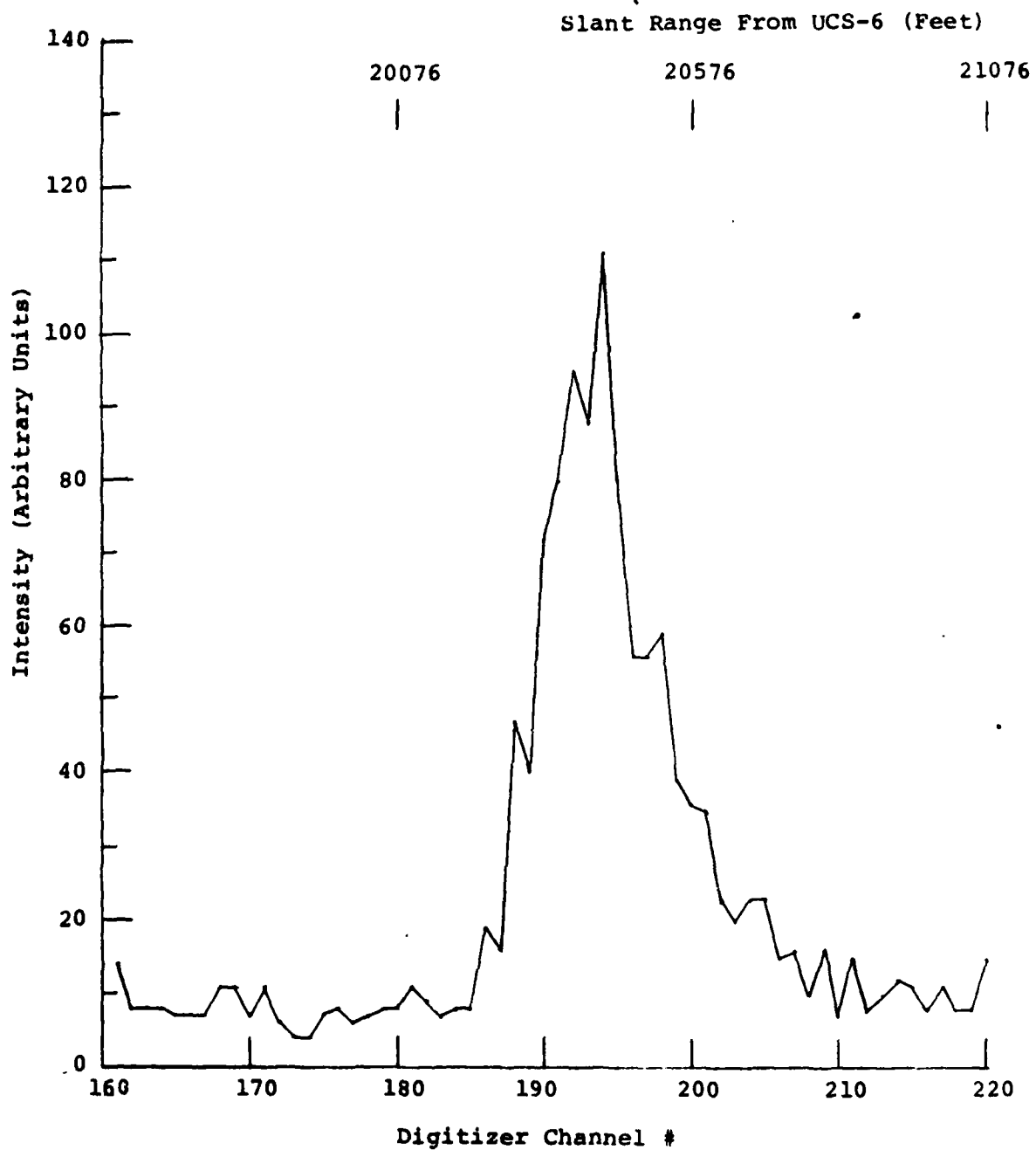


Figure 21. STS-3 Booster Exhaust Cloud Lidar Data, 22 March 1982

Laser subsystem performance tests prior to STS-3 determined that real-time adjustment of laser operating parameters were necessary to maintain constant output power and beam quality. Real-time adjustment procedures which can be automated at a later date were then initiated and used during the test. Measurement of prelaunch and postlaunch output power and beam quality revealed no changes in laser performance.

D. PRELIMINARY ANALYSIS OF STS-3 EXHAUST CLOUD LIDAR DATA

1. Scattergraphs of Cloud Cross Sections

Representative lidar data from the STS-3 mission are presented in Appendix B as computer-generated, two-dimensional cloud cross sections in scattergraph form. Although the data are not in true perspective because of the coordinate system used in a scattergraph presentation, they locate lidar cloud return in the vast field of values for a given field of view. Consecutive lines of sight for a given scan segment are placed together, resulting in a plot of the cloud returns position as a function of azimuth or elevation and range. Correlation of the scattergraphs with the appropriate scan patterns and approximate cloud shape can be accomplished with the use of Figures 11 - 13. After returns have been isolated in this manner they can be processed, using a variety of data reduction and presentation techniques.

It appears that where the lidar return is from the dense part of the cloud the signal exhibits the characteristics of a hard target return (see Scan #137-E2). However, where the cloud density is much lower, the laser beam penetrates well into the measurement volume (see Scan #141-F3). While it is beyond the level of effort proposed for STS-3, this data could be processed to generate attenuation coefficient and backscatter coefficient profiles for each line-of-sight through the cloud.

2. Exhaust Cloud vs. Fallout Lidar Measurement

An examination of the scattergraphs for Scan Segments 139-F3 and 140-F1 shows somewhat different characteristics in the lidar backscatter between them. The data from 139-F3 exhibits the characteristics of a hard target indicating that this scan is through a dense area of the cloud, whereas the data from 140-F1 are quite different, indicating a much less dense medium. The data for two LOS, one from each scan segment at the same azimuth (87°), are plotted in Figure 20. The top plot in the figure shows the lidar return from the dense cloud at an elevation of 4.3 degrees and a range from UCS-6 of 20,350 feet. The bottom plot shows the lidar return from the much less dense materials as seen at a lower elevation of 2.0 and appears to be associated with fallout beneath the cloud. The strongest return corresponds to a range of 21,200 feet from UCS-6.

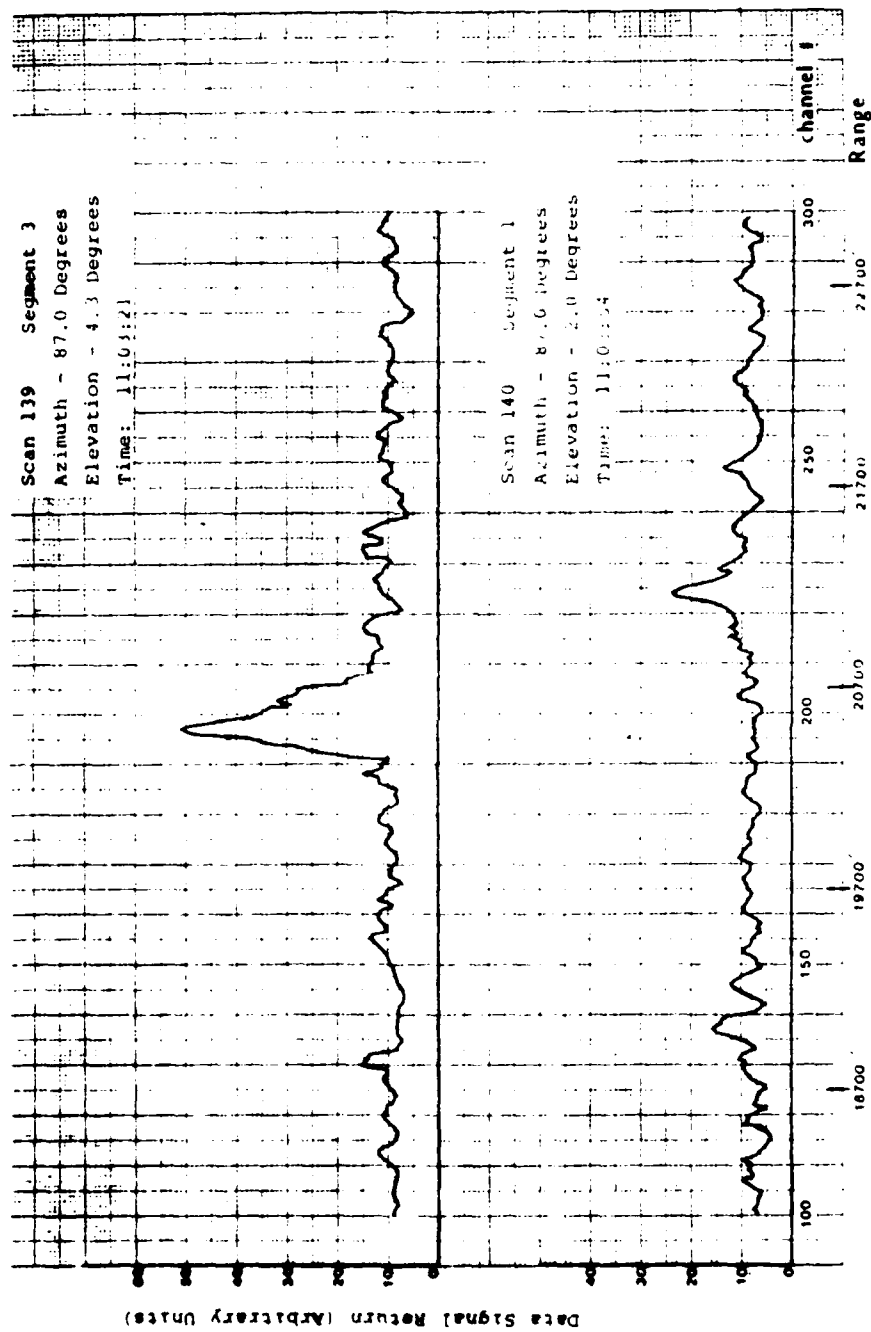


Figure 22. Scans #139 and #140

Figure 22. Scans #139 and #140

These two LOS were made 33 seconds apart under relatively stable atmospheric conditions. The difference in range between these lidar returns is 850 feet. This separation is consistent with the dimensions of the cloud which would be 2000 - 3000 feet at 4 minutes after launch.

3. Lidar Track of STS-3 Exhaust Cloud

Using data from the scattergraphs of scans through the dense part of the exhaust cloud, the position of the near face of the cloud can be determined. Figure 23 provides a plot of the exhaust cloud face as determined for each of four consecutive scan segments through the dense part of the STS-3 exhaust cloud. Figure 24 provides a plot of these same four cloud face measurements on a Pad 39A map. The movement of the cloud for this 3-minute period is clearly illustrated.

As described in Section 2, Figure 22 provides data plots of the lidar measurement for two lines of sight, both at an azimuth of 87.0 degrees. The location of the apparent fallout (footprint) measured by the lidar as plotted in Figure 22 is marked by an "X" in Figure 23. Additional fallout locations could be plotted with further processing of the STS-3 lidar data base. The locus of these locations would provide a time sequence track of the deposition area for the STS-3 exhaust cloud.

The data and results presented in these two figures are representative of the lidar measurements made of the STS-3 booster exhaust cloud. They clearly demonstrate the feasibility of using a lidar to make parametric measurements of STS launch exhaust clouds.

4. Background as a Function of Azimuth

When producing the preliminary scattergraphs for this report, background levels appeared to increase to the right of each scattergraph. It was concluded that, although the field of view of the lidar scans was narrow (≈ 7 degrees), the position of the sun caused a significant increase in the ambient background level as the lidar scanned to the South.

Figure 25 illustrates the ambient background levels for one of the horizontal segments of Scan #141. This segment extends from 84.9 degrees to 91.8 degrees azimuth at a constant elevation of 2 degrees. It can be seen that the ambient background level increases as the azimuth increases. Although this background effect was noted, it was decided to generate the preliminary scattergraphs using a constant background level for all lines of sight for each scattergraph. The background level used was the average background level for the extent of the scattergraph (see Introduction to Appendix B).

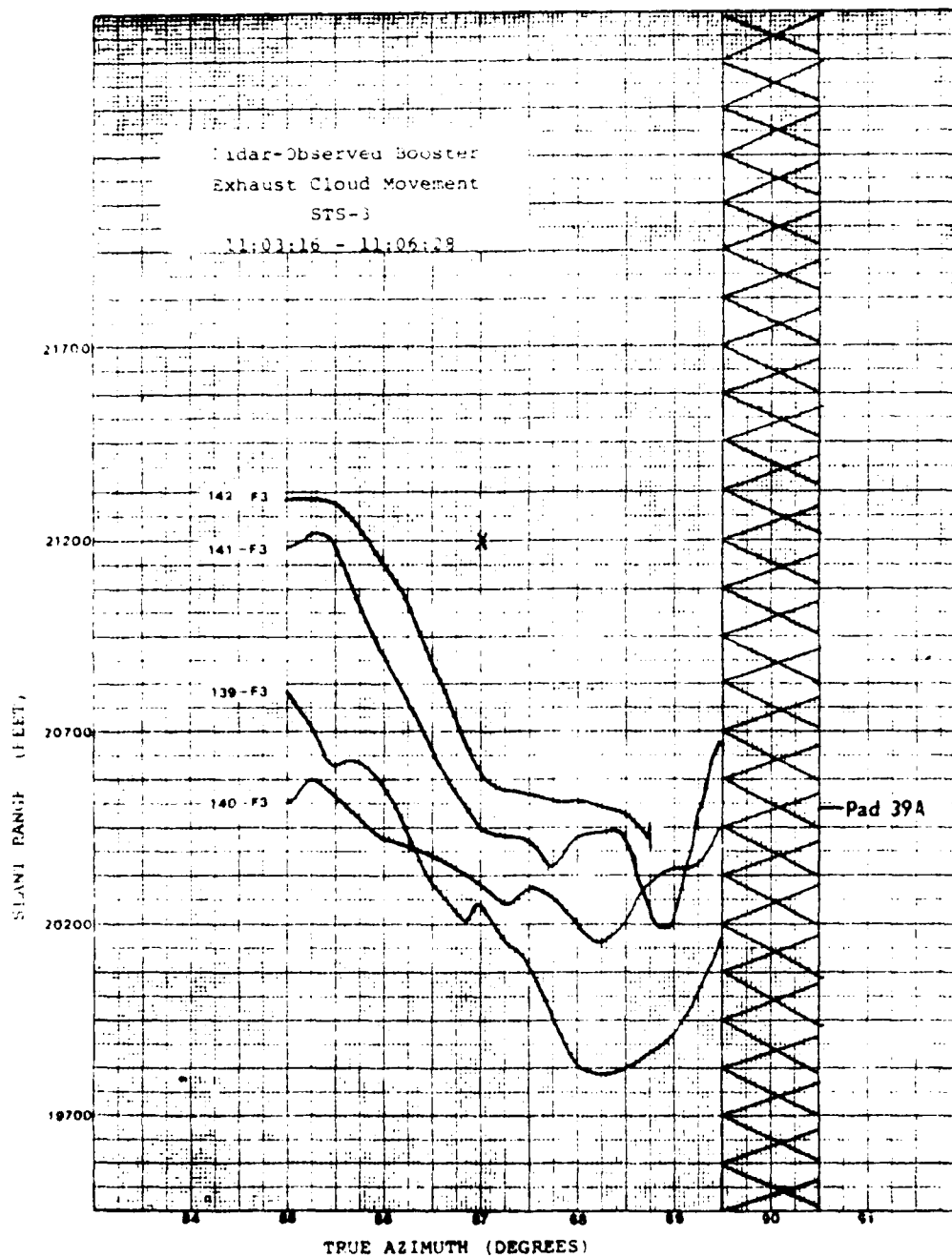


Figure 23. Lidar-Observed Booster Exhaust Cloud Movement, STS-3, 11:03:16 - 11:06:28

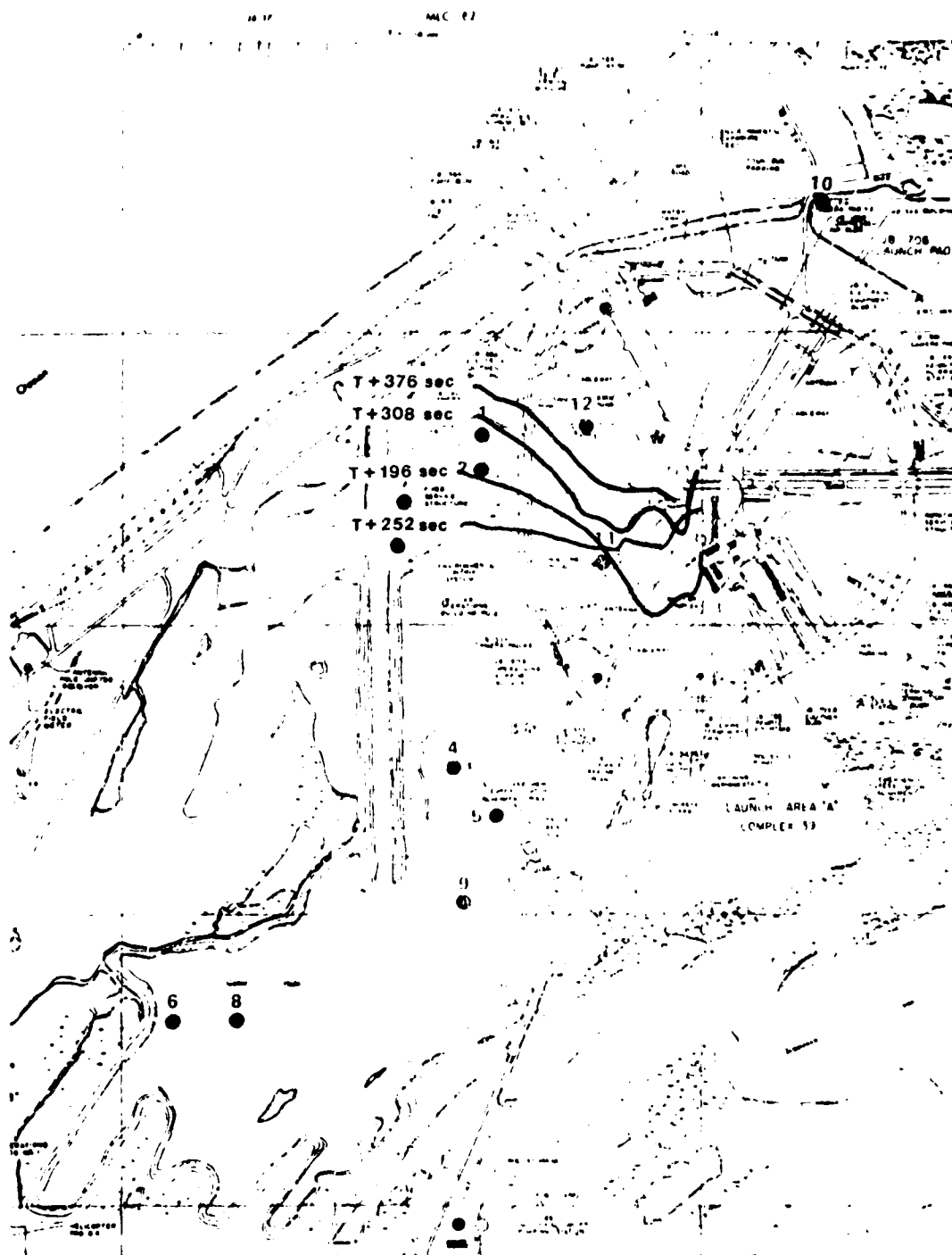


Figure 24. Lidar-Observed Booster Exhaust Cloud Movement.
STS-3, 11:03:16 - 11:06:28

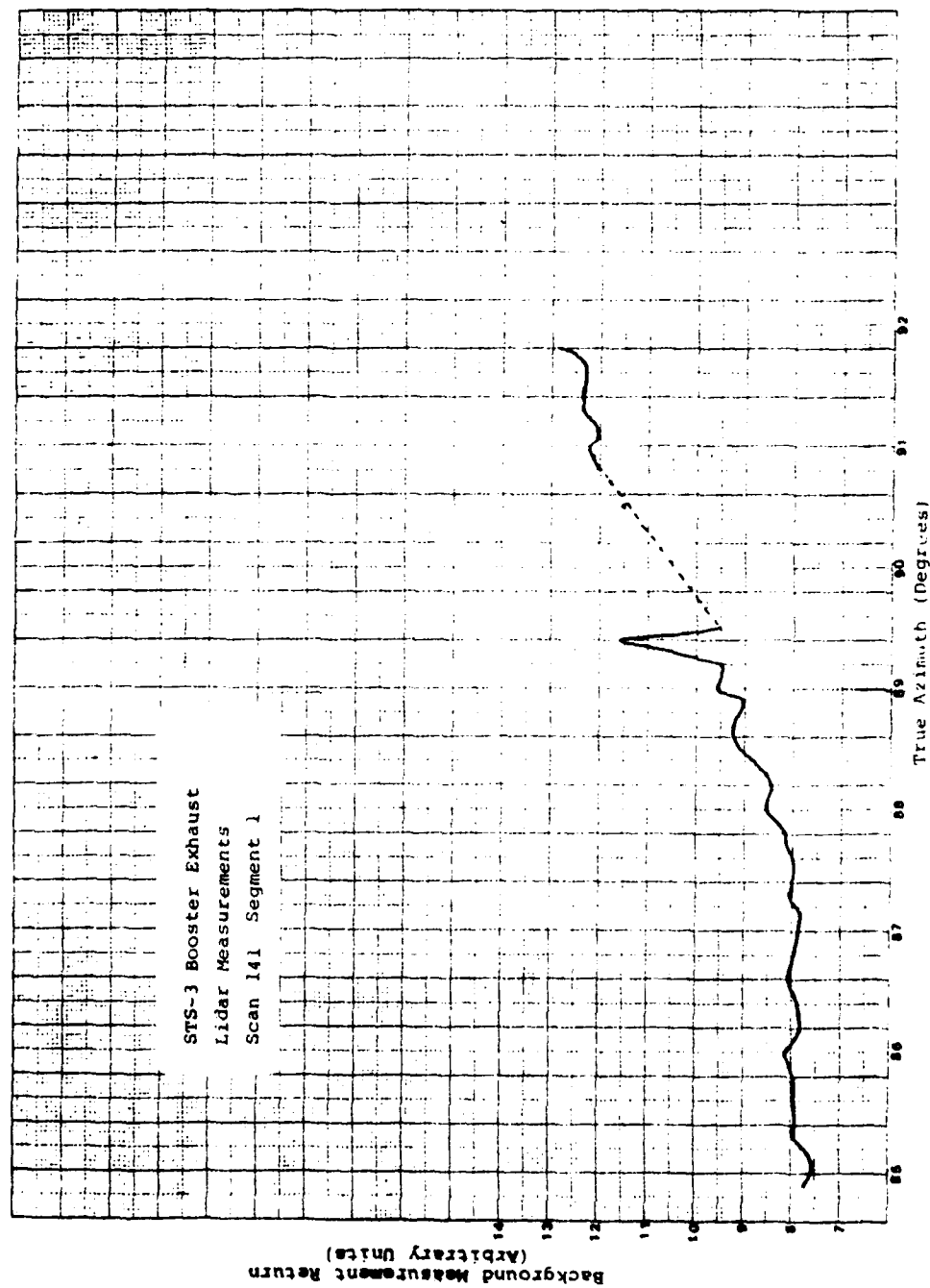


Figure 25. STS-3 Booster Exhaust Lidar Measurements, Scan #141, Segment 1

SECTION IV

STS-3 LIDAR FIELD CALIBRATION AND TESTS

A. BACKGROUND SCAN TESTS

As described in Section IIF, background scanning tests prior to launch are needed to determine the optimum photomultiplier tube operating voltage under typical launch conditions. Results of ambient background tests prior to STS-3 are shown in Table 1. In this table the number of ambient background counts for various combinations of PM tube voltages and receiver filters are shown.

B. BORESIGHT AND TRIANGULATION CALIBRATIONS

The requirement for hard target prelaunch tests as standard lidar operational procedure is discussed in Section IIF. An additional procedure required for accurate topographically related cloud data is precise leveling of the lidar system in azimuth and elevation from a site of known or surveyed UTM coordinates. Camera Pad UCS6, used as the STS-3 lidar observation station is a presurveyed monumented site with excellent viewing characteristics. The procedure to level the lidar onsite is easily and accurately accomplished with the CGC mobile system through use of its four permanently mounted and aligned remote controlled leveling jacks. Initial course leveling is done using permanently installed bubble level readouts. Residual errors in true level are measured in two planes to an accuracy of 10^{-3} degrees by inclinometers mounted and aligned with the telescope housing.

Prior to external radiation calibration tests conducted during the 72-hour countdown sequence, an internal laser subsystem alignment is performed with the beam blocked to external viewing by retaining the telescope in the "stowed" position. Using an internal alignment fixture and coaxial Helium neon alignment laser, beam position is verified to within a few tens of milliradians. Dye laser beam quality and peak power is adjusted and an internal scattering target in the telescope shroud is used to tune transmitter wavelength to the optimal value for the dye and filter combination selected.

A series of far-field boresight and triangulation tests was conducted as part of the 72-hour countdown sequence for the scheduled STS-3 launch date. Table 2 summarized the boresighting and triangulation tests, giving date, time, and associated parameters for each test. Data for these hard target and alignment tests were recorded on magnetic tape. The azimuth angles and map-measured distances to targets of use are shown in Figure 26. Prelaunch scanning tests simulating actual launch conditions, conducted with the laser beam blocked to external radiation, were also recorded.

TABLE 2. PRELAUNCH BACKGROUND TEST ON 21 MARCH 1982^{a b}

<u>5800Å</u>	<u>10Å BW</u>	<u>5800Å</u>	<u>44Å BW</u>
<u>PM VOLTAGE</u>	<u># COUNTS</u>	<u>PM VOLTAGE</u>	<u># COUNTS</u>
1500	1-2	1500	2
1600	2	1600	1
1700	2	1700	3
1800	1	1800	10
1900	2	1900	16
2000	5	2000	30
2100	11	2100	65
2200	18	2200	--
2300	30	2300	--
2400	45	2400	--
2500	--	2500	--
2600	--	2600	--
2700	--	2700	--

^a General Sky Lighting - Bright Sun

^b Telescope System Looking Toward Pad 39A Lightning Mast

TABLE 3. SUMMARY OF PRELAUNCH LIDAR TESTS

	<u>Date</u>	<u>Time</u>	<u>Sample Intervals</u>	<u>Delay</u>	<u>Channel #</u>
Pad B	21 March	11:10 - 11:31 EST	20ns	140	212
Pad A	21 March	11:31 - 11:45 EST	20ns	178	219
Met Tower	21 March	11:45 - 12:14 EST	20ns	48	217
Pad A	21 March	12:14 - 12:45 EST	20ns	178	219
Met Tower	22 March	06:00 - 06:15 EST	20ns	50	199
Pad B	22 March	10:59:50 - 11:00:38 EST	50ns	60	39

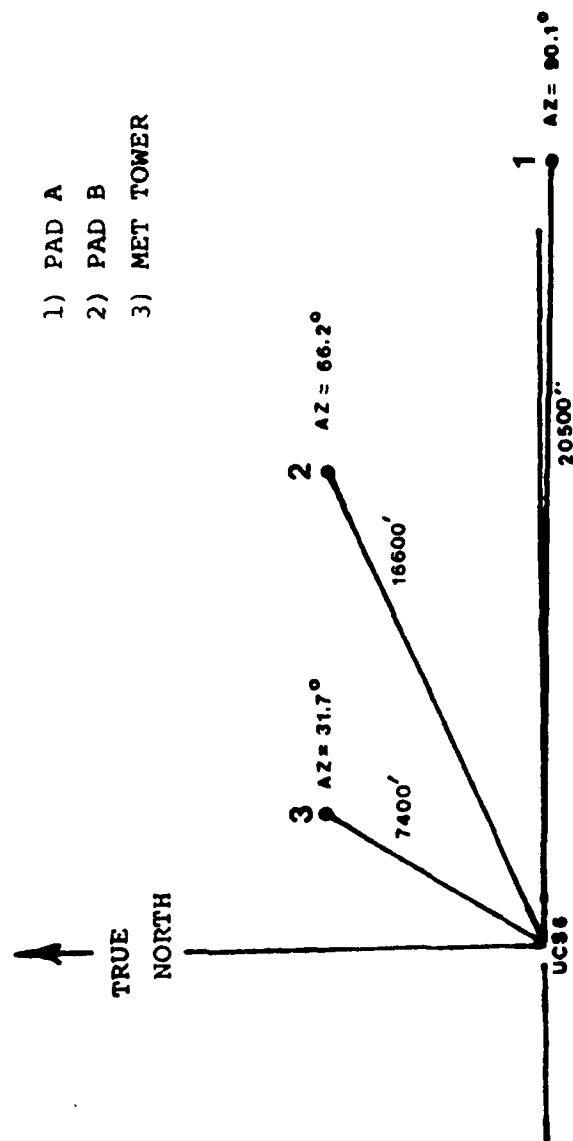


Figure 26. Range and True Azimuth from UCS-6

Examples of hard target data obtained by the lidar during STS-3 prelaunch tests to establish lidar range calibration are shown in Figures 27, 28, and 29. The lidar data are plotted as amplitude versus digitizer channel number. Here are shown typical strong signal returns from the 150-meter meteorological tower, Pad A, and Pad B. Signal-to-noise ratios of returns have all been calculated to be greater than 20:1.

Using these prelaunch calibration returns, an inherent system delay of 678 nanoseconds was documented. Lidar-measured ranges to the three targets and their corresponding map-measured distances are found to be:

	<u>Lidar</u>	<u>Measured</u>
Meteorological Tower	7419 feet	7400 feet
Pad B	16,562 feet	16,600 feet
Pad A	20,429 feet	20,500 feet

All ranging has shown data to be within the accuracy of a lidar utilizing a pulse of 300 ns, corresponding to a range window of ± 75 feet.

C. LASER CALIBRATION AND PERFORMANCE ASSESSMENT

Preparatory to the lidar measurement effort in support of the STS-3 launch, extensive quality assurance calibration and performance assessments were carried out on the laser subsystem. These tests were conducted as part of both the prelaunch and postlaunch lidar procedures. As discussed in Section B, initial alignment and transmitter wavelength adjustments were performed within the lidar van. Additional tests were done to measure laser output power and beam quality.

Prelaunch analysis of system performance at sampling rates resembling those to be used during STS launches determined that real-time adjustment of laser operating parameters is necessary to maintain constant output power and beam quality. Working in close collaboration with the laser manufacturer, a real-time adjustment procedure was developed. Comparison of prelaunch and postlaunch measurements of lidar output power and beam quality showed no change in the laser system performance.

D. ANTICIPATED GROUND CLOUD SIGNAL RETURN

Assuming the lightning mast atop Pad 39B is 10 feet in diameter, a signal-to-noise ratio of the lidar return from the far field (16,600 feet) can be calculated. The laser radiation

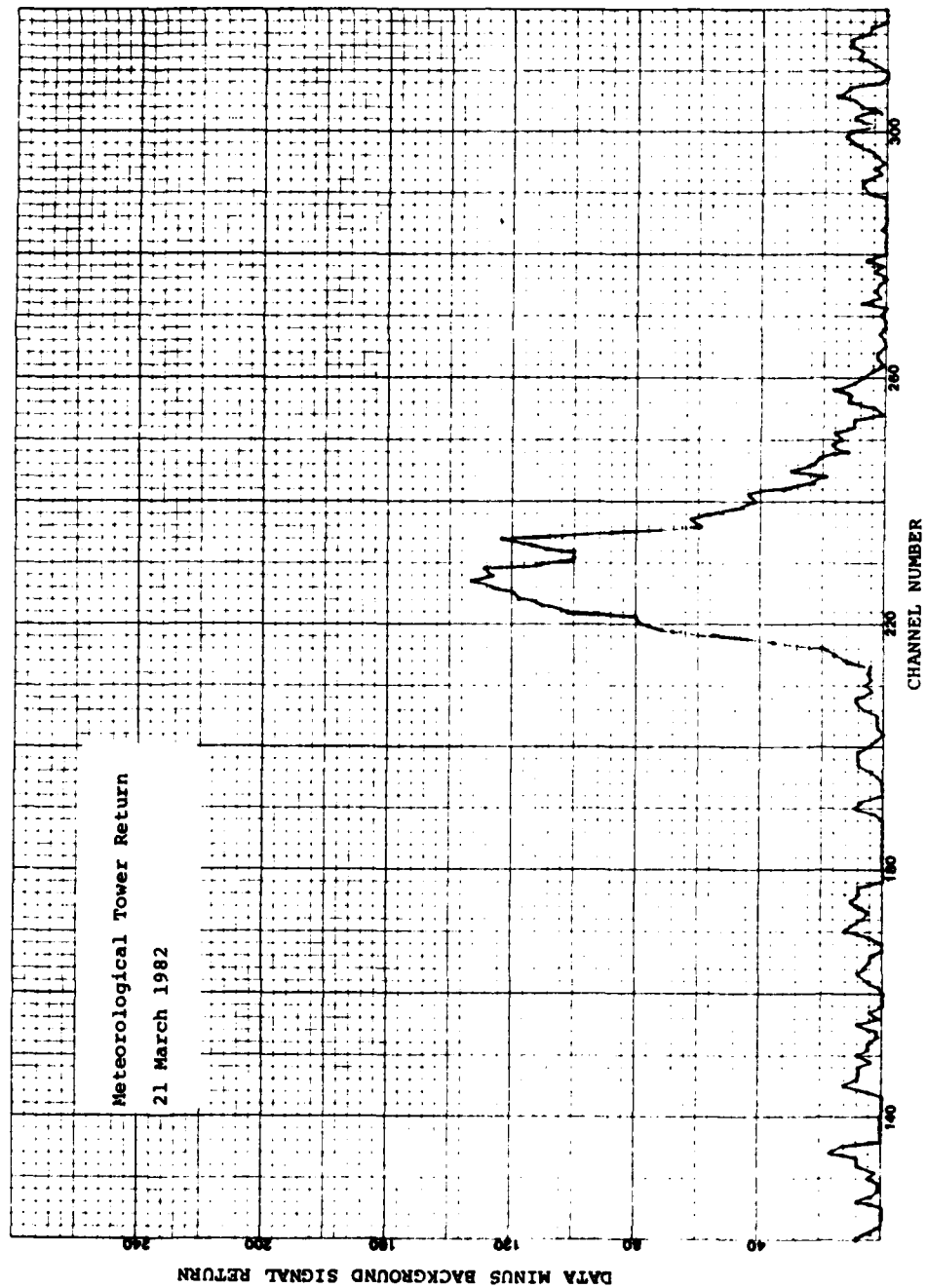


Figure 27. Meteorological Tower Return, 21 March 1982

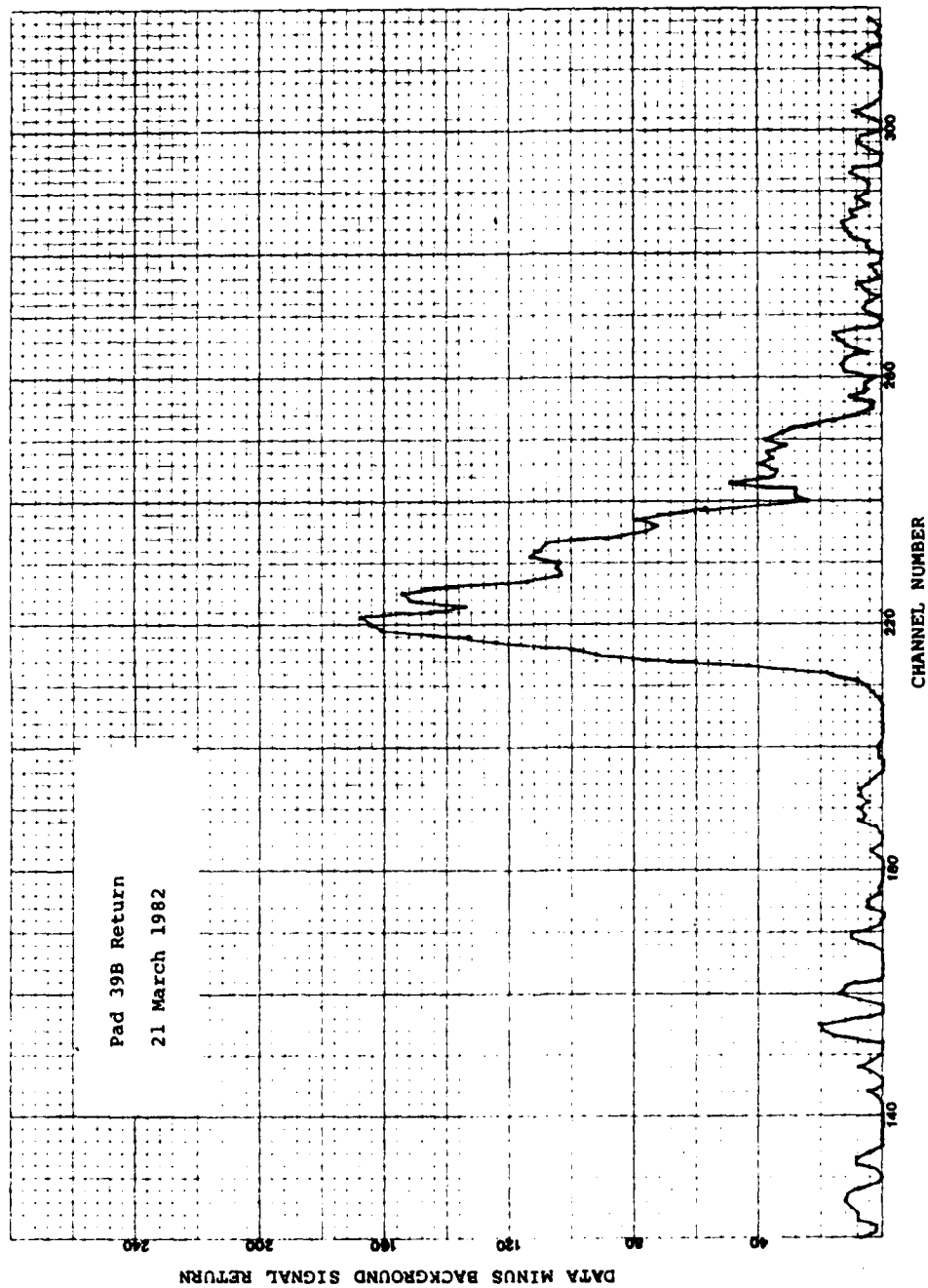


Figure 28. PAD 39B Return, 21 March 1982

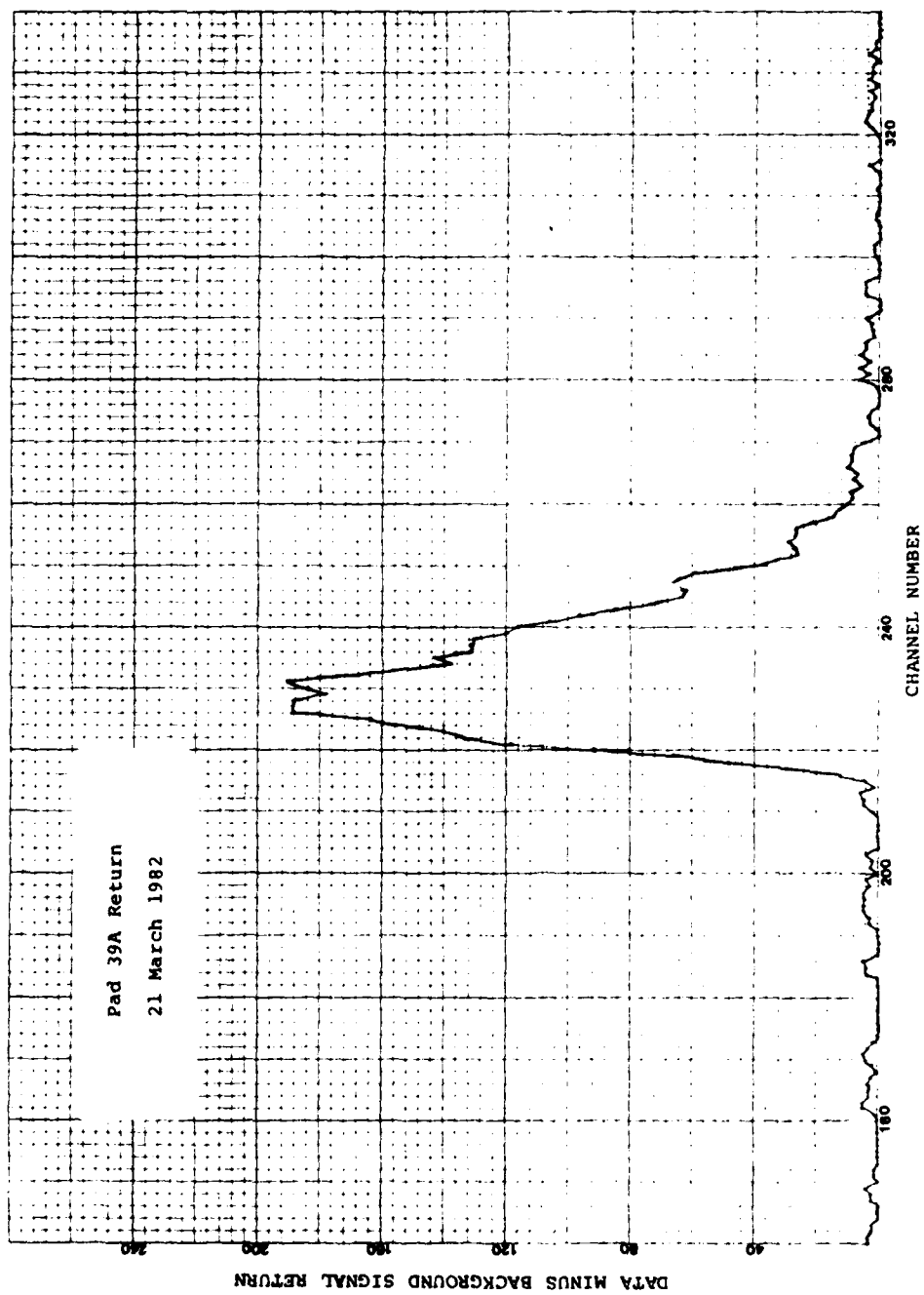


Figure 29. PAD 39A Return, 21 March 1982

pattern is 25 feet in diameter at this range. Evaluation of the lidar returns obtained during prelaunch tests yield a signal-to-noise ratio for the mast of 30:1.

The return signal expected from the mast can be estimated from the equation:

$$I_L = P_o \cdot R \cdot \Psi \cdot \cos \theta \cdot \frac{A}{R^2} \exp \left[-2 \int_0^r \sigma(r') dr' \right]$$

where P_o is the laser output power, R is the reflectivity of the mast, Ψ is the overlap function of the beam and mast areas, θ is the angle of scattering, A the telescope area, R the range to target, and the exponential function is the atmospheric attenuation.*

The scattering from the first range element in the cloud is:

$$I_M = P_o \beta \left(\frac{c\tau}{2} \right) \frac{A}{R^2} \exp \left[-2 \int_0^r \sigma(r') dr' \right]$$

where β is the volume scattering coefficient of the cloud and $c\tau/2$ is the length of each laser pulse (the speed of light times the laser pulse duration over two). The ratio of the two returns would then be:

$$I_M/I_L = \beta(c\tau/2)/R \cdot \Psi \cdot \cos \theta$$

* This equation assumes that the surface of the mast is a Lambertian reflector.

Pal and Carswell** have shown that β 's typical of cumulus clouds range from values of 2 to 20km^{-1} at a wavelength of 6943\AA . At 5800\AA these values must be increased by about 25 percent. The laser pulse duration is 350ns, the reflectivity of the white mast 95 percent, the overlap function 0.5, the $\cos \theta = 0.99$. From this the value of I_M/I_L ranges from values of 0.4 to 4, depending on the cloud density. Based on these considerations, the signal-to-noise ratio of the scattering from the ground cloud should range from 12:1 to 25:1 for clouds at the range of Pad 39B.

E. PRELAUNCH AND POSTLAUNCH TESTING

The objectives of the prelaunch tests are to (1) verify optical system alignment after mobile lidar over the road transport, (2) maximize (peak) system sensitivity, (3) verify range calibration, (4) establish a reference point for the data reduction geometry of all lidar acquired launch data, (5) initiate site-specific computer parameters, (6) establish ambient background levels, (7) test signal-to-noise ratios, and (8) provide a quality assurance data base. Postlaunch tests (1) verify system performance and (2) provide additional quality assurance data.

In addition to standard alignment and testing procedures and as a result of the STS-2 booster exhaust testing experience, modifications were introduced that would enhance data quality and measurement probability. Modifications included the telescope baffle as discussed in Section III C, and prelaunch scanning changes. No scanning of the Pad A area was performed until a preset time had elapsed, preventing exposure of the sensitive receiver optics to the booster exhaust flame. Working closely with the manufacturer, real-time laser adjustment procedures were initiated that enhanced laser subsystem operation.

All prelaunch and postlaunch tests verified system integrity and were documented as part of standard quality assurance procedures.

**S.R. Pal and A J. Carswell, "Multiple Scattering in Atmospheric Clouds: Lidar Observations," Applied Optics, vol 15, No. 8, August 1976.

SECTION V

CONCLUSIONS AND RECOMMENDATIONS

A. GENERAL SUMMARY

This STS-3 lidar ground cloud measurement feasibility study shows that current lidar particulate mapping technology is well matched to typical launch operations in terms of scanning coverage, tracking, spatial resolution, and data dynamic range. Coupled with the legalized status of lidar particulate measurements, the capability provides a validated documentation trail of cloud transport, dispersion, and deposition locations. At the minimum, it is recommended that particle mode lidar, which required no further research development, be routinely used in rapid scan scenario during all launch operations to archive exhaust cloud behavior. Hardware, software, and procedural recommendations to legally qualify the instrument and enhance data acquisition rates and processing for routine particulate measurements service are discussed later in this section.

It is also noted that strong potential exists, with additional development and field testing, to obtain remote measurements of other important parameters to ground cloud study and modeling. These include particulate sizing and distribution, discrimination of liquid and vapor state water and HCl vapor concentration cross sections.

Evaluation of each of the lidar remote sensing modes can be largely and economically supported with the existing CGC mobile lidar test bed design through modest, phased-in modification. Ancillary electronics, computers, software and scanner are common to all modes. The feasibility of these techniques for STS application should be further studied on a parameter priority basis and the additional capabilities should be incrementally added and tested, using the existing test bed design. The increasing frequency of planned STS launches will provide evaluation data base acquisition opportunities as the capabilities are developed. The data base acquired using the mobile test bed will determine feasibility. This can be used where applicable, for the specification and development of parameter-optimized, dedicated, and permanently installed or mobile instruments.

Lidar participation and field experience during the STS-2 and STS-3 launches have identified a number of procedural and equipment limitations. The program and system improvements described in the following paragraphs are designed to increase data acquisition quantity, quality and efficiency, improve data analysis techniques, increase detection sensitivity, and prepare for future addition of multiparameter measurement capability.

B. PRINCIPAL INVESTIGATOR LEVEL OF EFFORT

The systematic development of multiparameter measurement lidar instrumentation and techniques for shuttle applications require the program planning, supervision, and analytical experience of a laser remote sensing specialist to determine objectives, maintain program continuity, and provide a point of contact with Government technical coordinators.

C. SOFTWARE DEVELOPMENT AND DATA PROCESSING LEVEL OF EFFORT

Data products produced by lidar monitoring operations are used (1) by physical and environmental science study groups, (2) by the cloud modeling community, (3) to document cloud transport and fallout regions, and (4) by principal investigators and instrument developers to improve the technology and add additional capability for shuttle applications.

A typical 20-30 minute tracking and scanning mission can produce 29×10^6 individual spatially and temporally resolved volumetric measurements with dynamic range spanning clear air through optically opaque air. Examination and analysis of such large arrays of data can be difficult and labor intensive to users. Incorporation of numerous data processing and presentation techniques is needed to customize the organization of data products to individual user needs assuring maximum utility and efficiency. User groups will help determine processing objectives and require periodic lidar data processor support.

A software development and data reduction level of effort budget averaging 6 man-months of Senior Analyst, Programmer, and CPU support is recommended.

D. ADDITION OF LOG AMPLIFIER

Lidar-acquired ground cloud data span the dynamic range from clear air at the plume perimeter to total optical opacity in the first several minutes of dissipation of the cloud main body. Good concentration resolution (high sensitivity) at the 0-30 percent opacity region is needed to detect, discriminate, and document fallout. The existing digitizer linear amplifier has a dynamic range of 1 part in 256 (for practical purposes, 5-8 levels of gray). Operating at maximum sensitivity to maximize the detection of fallout causes data saturation in the dense cloud formation. Conversely, operating at a reduced digitizer sensitivity scale factor to reduce or eliminate saturation sacrifices fallout detection. It can be said that data is being thrown away. More "levels of gray" are needed at the data acquisition level.

It is recommended that a 5:1 or 10:1 log amplifier subsystem be added to the system digitizer. This requires the acquisition, installation, testing, and calibration of the amplifier, minor modification to the digitizer, and modification to the processing software. A table of calibration constants and operational procedure changes is required and should be implemented prior to log amplifier use in the field.

E. INCREASED DATA ACQUISITION RATE

The field monitoring cost-to-data-acquired benefit ratio can be greatly improved by firing the laser at a higher repetition rate. During the STS-3 field measurements, the optimum laser fire rate was below 3 pps. Two factors in the existing configuration control the optimum firing rate and, therefore, the maximum accumulation of data during a mission.

The dye laser system deviates very substantially downward from its power output specification as the firing rate is increased beyond 3 pps. An investigation has determined that the flow of dye through the flashlamp at properly maintained temperatures is inadequate.

The dye and cooling water circulator pumps and plumbing should be modified to substantially increase laser fire repetition rate at maintained power levels.

The greater volumes of data per unit time which must be processed and recorded by the computer while it is controlling the balance of the subsystems require greater CPU capacity. It is recommended the the software be modified to reduce operating CPU overhead and incorporate additional core memory to the computer.

F. LIDAR LEGAL QUALIFICATION

The lidar community recognizes the need for a universally applied lidar calibration standard which quantitatively establishes background and plume cross section sensitivity/intensity (opacity). In the absence of such a standard, discrimination of a plume against varying backgrounds has been more or less arbitrarily selected by the lidar operating organization. Defining consistent plume dimensions over long term measurements can be particularly sensitive to arbitrary background assumptions.

Over the last decade the EPA National Enforcement Investigation Center (NEIC) has invested substantially to develop, test, and document standards employing lidar techniques for the nonsubjective, quantitative determination of particulate plume intensities. The method was reported in the Federal Register of 28 October 1981 and is now a legal alternative

(Method 1) to Reference Method 9 of the Clean Air Act. This provides a standard that can be used by all lidars to obtain the same data results and a validated, traceable calibration procedure which assures admissible evidence.

Lidar data products may be used to defend the Government against suits arising from environmental effects caused by large solid booster operations. It seems prudent to meet the new standards, if only to provide uniform accuracy, data consistency, and better quality assurance. The comprehensive and exacting mechanics of fully compliant lidar equipment features, calibration techniques, and data processing are reported in The Use of Lidar For Emissions Source Opacity Determination, (EPA-300/1-79-002R). Extensive tests have shown the method to be consistent and accurate to within 1 percent over the opacity range to 80 percent.

Consistently accurate plume dimensions can be obtained under varying atmospheric particulate loadings with a uniformly and locally calibrated lidar instrument and lidar-measured background and opacity values.

Calibration will require an optical generator which can be procedurally programmed to accurately simulate targets of known size, density and range. The system should also be fitted with a logarithmic channel. Minor changes in the optics and beam divergence are also required along with the fabrication of four mesh screen targets of EPA certified opacity value.

The standard is very exacting in the method to be used for initial data processing. This will require easily implemented changes to the current data acquisition procedure and nontrivial modification of the system software which will also require expansion of the core memory and an additional real-time display.

G. IMPROVED CLOUD TRACKING AND DATA ACQUISITION EFFICIENCY

Tracking of the ground cloud is a semiautomated, operator-aided procedure. The quality and data efficiency of lidar cloud measurements depend greatly upon the ability of the lidar operator to make effective decisions in real time and use the scanning resources to maximum advantage and efficiency.

The method used to track the exhaust cloud, for example, could use considerable revision and system modification. During the tracking of the STS-2 and STS-3 clouds, several changes in TV camera position and TV monitor grid reference were required. The real-time interactions with the system by the operator resulted in a loss of measurement time.

A number of TV pointing and graphic display techniques are recommended to provide the operator with improved real-time knowledge to assess the effectiveness of scanning scenarios and make rapid, appropriate adjustments.

1. Track Ball Pointed Acquisition Video Camera

A lidar system has a very narrow field of view specified to complement laser beam divergence and reject excess ambient background light. Scanning of the ground cloud with nominal dimensions of 4000 feet by 4000 feet requires a wider field (capable of 360° sky coverage) support subsystem which can aid the test conductor in the real-time lidar pointing and optimization of scanning. A basic system utilizing a TV camera and lidar operator's monitor was implemented to support STS-2 and STS-3 measurements. A 28° field-of-view video camera is mounted on a surveyor's transit tripod with high-resolution graduated azimuth and elevation scales. Azimuth and elevation readings are relayed to the test conductor over a voice link to be manually entered in the lidar computer. The method is highly labor-intensive, but proved to be an excellent concept which can be easily automated, providing greater data acquisition efficiency, and reducing the field crew requirement by one person.

The implementation of this recommendation requires the acquisition and modification of a motorized "Pan and Tilt" camera mount which can be controlled by a remote track ball located at the test conductor station inside the van. The camera mount will be additionally fitted with azimuth and elevation encoders which will be interfaced to the acquisition and control computer eliminating the external camera crew, voice link, and manual entry of reference coordinates by the test conductor.

2. Composite Video "Current" Telescope Point Display

In the present system the operator selects and initiates one of several predetermined, best-fit scan patterns. During execution of the automated scan pattern, it is difficult and labor intensive to correlate "current" lidar pointing with a specific point in the cloud formation. A video composite technique is recommended which will superimpose scan patterns over TV-displayed cloud formation. A broken line format would display the overall scan pattern in execution while a solid line format would display portions completed.

3. Range Height Indicator

The composite video monitor will provide correlated real-time display in two dimensions i.e., azimuth and elevation. The third dimension, range, can be more effectively displayed through

incorporation of an RHI (Range Height Indicator) display. A lidar-modified version of this traditional radar display technique will screen, display, and retain elevation versus range or azimuth versus range for each scan segment under execution. Z-axis modulation is proportional to the range resolved volumetric cloud measurement detected by the lidar. Incorporation of an RHI display video tape recording capability will enable immediate postmission playback and rapid assessment of lidar performance during the mission. Used in combination with other recorded data, the capability will more effectively support "quick-look" debriefing and user group analysis.

4. Telescope Boresighted Video Display and Recording System

The rooftop-mounted lidar telescope is nominally pointed by the operator from a remote location inside the environmentally controlled van. In the existing system, an externally mounted, semifixed line-of-sight, wide-angle TV camera feeds an operator's display for tracking and scanning decisions. The display does not follow the telescope. The recommended video camera and display system, coaxially aligned with the lidar telescope and equipped with remote control zoom, will provide a valuable real-time aid to the lidar test conductor, substantially reduce future data reduction costs and serve as permanent, easily interpreted, visual records of scanner coverage.

H. RADAR AIRCRAFT INTRUSION ALERT

During shuttle launch operations an aircraft is deployed to fly through the ground cloud to collect emissions samples. A laser safety review prior to STS-2 and STS-3 determined that under certain meteorological conditions the aircraft's flight pattern may intrude into the laser scanning pattern at laser to aircraft ranges which are below minimum eye-safe distances. Two procedures were used during the STS-2 and STS-3 launches to assure eye-safe lidar operation.

1. An observer was posted at the lidar site with a laser "kill" switch during all lasing periods (prelaunch calibrations and launch operation). The "kill" switch could be used to immediately override and deactivate the laser fire circuit in the event of aircraft intrusion into the eye safety zone.

2. Aircraft and laser operations were coordinated through launch control on a mutually exclusive basis.

The addition of a small, commercially available radar scanner, equipped with operator selectable intrusion zone alarms, would improve safety and increase the volume of lidar-acquired data. A Decca model 090 scanning radar, used in conjunction with a Radar Devices, Inc., Model MK 111 "Radar Watch," can monitor an

operator-defined azimuth and range sector and would, therefore, automatically provide an alarm and deactivate the laser fire circuit. The MK 111 also has the capability for early warning detection, i.e., the operator can define a secondary monitor zone (alert zone) greater in size than the primary monitor zone (eye safety zone).

I. LIDAR MOBILITY

Maximum lidar cross sections are obtained when the lidar is positioned normal to the plume path. During STS-3 there was a light wind from the West-Southwest, moving the exhaust cloud out to sea, and away from UCS-6. Measurement time, therefore, exceeded 30 minutes. During the launch of STS-2 a relatively strong wind from the North caused the exhaust cloud to move toward the South, orthogonally traversing the field of view of the lidar located at UCS-6. Even under the high wind velocity no difficulty was experienced in tracking the cloud with the lidar and 8 minutes and 45 seconds of measurement time were experienced before the unit was deactivated due to radiation restrictions. However, for the previous launch date for STS-2 on November 4th, 1981, the wind from the East would have blown the exhaust cloud directly towards UCS-6. It was estimated that, had the launch occurred on November 4th, a maximum of 3 minutes of measurement time would have been available prior to arrival of the cloud overhead which would necessitate shutdown due to acidic fallout.

Since the lidar equipment is fully self-contained including onboard power in a van, its mobility can be used on relatively short notice to acquire data under the most favorable viewing conditions by establishing several sites for lidar deployment to be selected on the basis of predicted meteorological conditions. At least two sites, a primary and an alternate, are recommended. Complete setup procedures and alignment requirements would be established for each site to permit selection of the actual site to be made as close to launch as T-12 hours. Using UCS-6 as the site for coverage of a N/S wind direction and a site South of launch complex 39 for coverage of an E/W wind direction would assure nominal orthogonal viewing conditions and substantially increase data quantity under E/W wind conditions.

J. DIRECT CALCULATION OF CLOUD ATTENUATION AND BACKSCATTER COEFFICIENTS

An ability to determine profiles of attenuation and backscatter coefficients in a heterogeneous atmosphere directly from lidar measurements is a primary goal of any lidar measurement data processing system. Traditional lidar community processing methods to solve the single scattering lidar equation have produced inconsistent results because of the inherent instabilities in the solution.

The reasons for the instabilities were recently examined by Klett (Reference 5) who derived a different and more appropriate solution form for the single-scattering lidar equation.

Using the Klett technique, raw data, adjusted for background levels, can be processed directly to locate a plume or cloud in the field of lidar data and to define its extent and mass distribution. The important feature here is that the vast amount of data does not require extensive preprocessing prior to the application of the Klett algorithm.

The lidar acquires several hundred thousand range-resolved volumetric measurements which include spatial regions of plume content and regions of clear air. Any data reduction technique which can be applied directly to the raw data base for a given plume or cloud cross section to locate the plume or cloud would greatly improve on the time and cost required to obtain cross-section parameters. In addition, since the actual cross-section data may be bracketed in the vast field of measurements by the first data reduction step, subsequent data processing steps to obtain plume/cloud dimension, centroid and particle size distribution may be performed on a reduced volume of measurement data.

The Klett algorithm should be fully evaluated and applied to some existing lidar data; the results then compared to the results as determined by the lidar community standard techniques currently employed. If the Klett algorithm to process raw lidar measurements performs as expected, the technique should be incorporated into the data reduction processing system.

K. SEED CHANGES

The authorized Safe Eye Exposure Distance (SEED) forms the basis for lidar operational restrictions and, therefore, all field activities. During the STS-3 lidar onsite operations, safety restrictions were found to reduce the efficiency and quantity of prelaunch calibration, as well as the potential lidar coverage during launch. In particular, quantitative signal-to-noise performance requires plentiful hard target data from targets of known area under a variety of ambient lighting conditions. Hardware modifications can be implemented which would result in a substantially shorter SEED without sacrifice of personnel safety.

As background, an error is noted in the Operation Instruction document KPB-01-2001, Lidar Operations for STS Exhaust Cloud Measurement. The text on page four states that 0.1-joule peak power is assumed for purposes of SEED calculation resulting in a 19,000-foot SEED. Inspection of the calculation shows that a peak power of 0.3 joule is required to produce a 19,000-foot SEED. As part of this reporting effort, cognizant

KSC personnel were contacted and it has been verified that 0.3 joule was used in the calculation. The calculation is reproduced below substituting 0.1 joule leading to a SEED of 10,990 feet.

The SEED calculations currently established by KSC-MD assume a radiated-pulsed laser energy of 0.3 joule. The assumed value is a safely conservative interpretation of the laser manufacturer's advertised claims of 0.25 joule for a model DL1400 which is not equipped with prisms for tunability. The manufacturer estimates additional prism losses of 10 percent. The 0.3-joule figure also neglects the significant losses introduced by each element in the lidar system optical train. The lidar transmitter surfaces are aluminum coated with a heavy overcoat of silicon monoxide. The reflectivity of these mirrors is 96 percent in the visible. The turning mirror in the laser is a broad band dielectric mirror of 99-percent reflectance. The uncoated beam expander lenses cause 5-percent loss per surface of 90.3 percent transmission per element. The product of these losses is:

$$T_T = 0.99 \times (.903)^2 \times (0.96)^3$$

$$T_T = 0.99 \times 0.815 \times 0.885$$

$$T_T = 0.71$$

Therefore, the lidar optics external to the laser cavity contribute an additional attenuation of output power of 29 percent. Significant scattering losses at each surface further reduce externally radiated output power. Since the actual energy transmitted into the atmosphere constitutes the eye safety hazard, the SEED should be recalculated using the actual transmitted energy, as directly measured with proper instrumentation outside the lidar van. This results in an actual radiated power of 0.1 joule.

Substituting the more realistic output energy in the calculations, the SEED becomes 11,000 feet, i.e.,

$$5 \times 10^{-7} = \frac{1.27(0.1)}{[1.5 + r(1.5 \times 10^3)]^2}$$

$$r = 3.3499 \times 10^5 \text{ cm}$$

$$r = 10,990 \text{ feet}$$

The SEED can be further reduced by eliminating the OPTIONAL "beam expander" (divergence reducer) and substituting aⁿ steering element. The laser would then be operating at the manufacturer's "raw" beam divergence of 3 milliradians (or

3×10^{-3} radians). Incorporating this change into the calculation, SEED becomes 5500 feet, i.e.,

$$5 \times 10^{-7} \text{ J/cm}^2 = \frac{1.27(0.1\text{J})}{[1.5\text{cm} + r(\text{cm})(3.0 \times 10^3)]^2}$$

$$r = 1.6749 \times 10^5 \text{ cm}$$

$$r = 5495 \text{ feet}$$

Reduction in SEED to 5500 feet eliminates the eye hazard from all elevated structures surrounding UCS-6, including the VAB, which could then also be considered as a target for comprehensive calibration tests. Reduction will also simplify coordination with cloud sampling aircraft and eliminate the T+20 operating restriction for observations over the space shuttle orbiter landing facility.

Appendix A
CGC MOBILE LIDAR SYSTEM DESCRIPTION

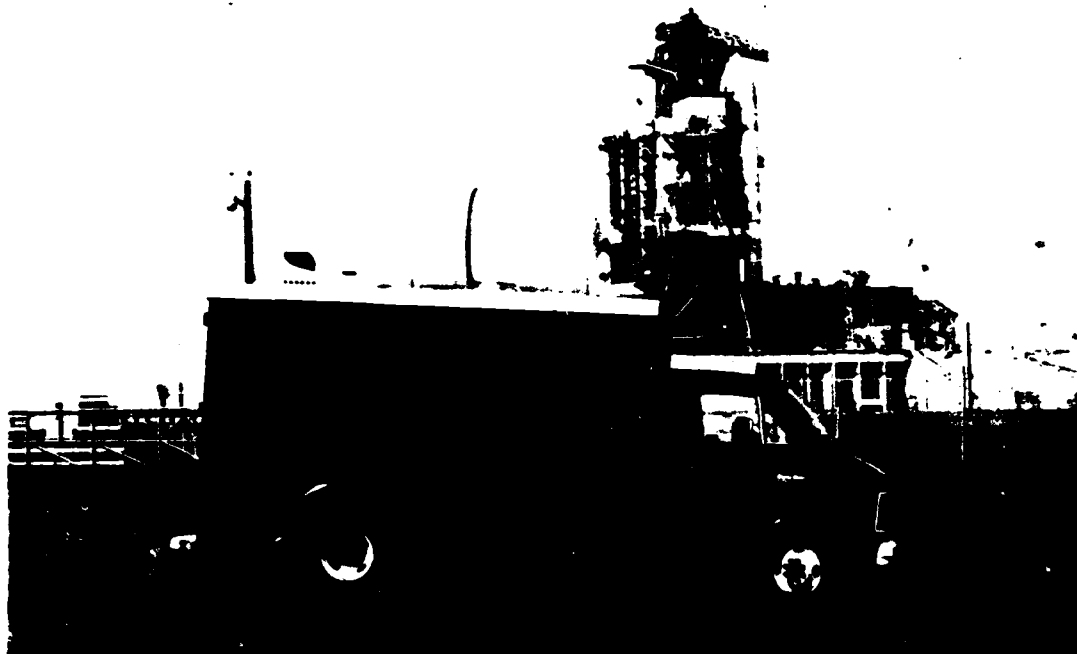


Figure A-1. CGC Mobile Lidar

APPENDIX A

CGC MOBILE LIDAR SYSTEM DESCRIPTION

A. SYSTEM CAPABILITIES

The current CGC Mobile Lidar Test Bed (Figure A-1) combines performance and operational features developed through participation in research and development and field measurement programs carried out over a period of 7 years. The lidar can be software-selected to operate in Rayleigh, Mie or Raman backscatter modes and is used to acquire data which includes Mie particulate cross sections and Raman measurements of atmospheric temperature, water vapor, N_2 , O_2 , CO_2 , CH_4 , and other species of interest. The design incorporates all features necessary to substitute alternative lasers as transmitters and is currently equipped with both a tunable dye laser and a pulsed N_2 laser. The basic design anticipates modest modification for operation as a Differential Absorption Lidar (DIAL).

Major capabilities and features incorporated in the design include:

- Weatherproofed 12 inch coaxial scanning telescope
- Rapid (.8 sec/degree) computer-automated horizontal ($\pm 170^\circ$) and vertical (horizon-to-horizon) scanning

- Dual laser transmitter configuration
- Computer tunable dye laser
- Automated filter selection
- Temperature-controlled filter housing
- Adjustable field stops
- 2048 computer adjustable range resolution data gates (480 are recorded)
- Digitizer resolution to 1 part in 256
- Real-time oscillographic signal display
- CRT displayed operator checklist prompting
- High-speed real-time line print of selected measurement data
- Complete data and housekeeping parameters recording on dual industry-compatible magnetic tape recorders
- Existing real-time and post-real-time software support
- Existing manuals, procedures and documentation

The functional configuration of the lidar fielded in support of the STS-3 Booster Exhaust Study Test (BEST) can be visualized in Figure A2 while a block diagram of the major subsystem is shown in Figure A4.

B. HARDWARE SUMMARY

In the cutaway drawing (Figure A2) it can be seen that the unique custom designed telescope transmitter configuration atop the van provides rapid azimuth and elevation scanning without moving or rotating the vehicle. The laser output is coaxial within a 12-inch weatherproof Newtonian telescope (Figure A3) that is totally scannable in both azimuth and elevation under computer program control. The receiver optical train completely housed within the telescope cowling is equipped with a six-station, high-speed computer-controlled filter wheel assembly which can be fitted with appropriately specified filters. The filter wheel housing is temperature-controlled to maintain filter center frequency integrity. The van is equipped with rapid deployment, six-ton capacity remote-controlled leveling jacks to level the telescope. Residual errors in true level are measured in two planes by inclinometers mounted and aligned within the telescope housing itself.

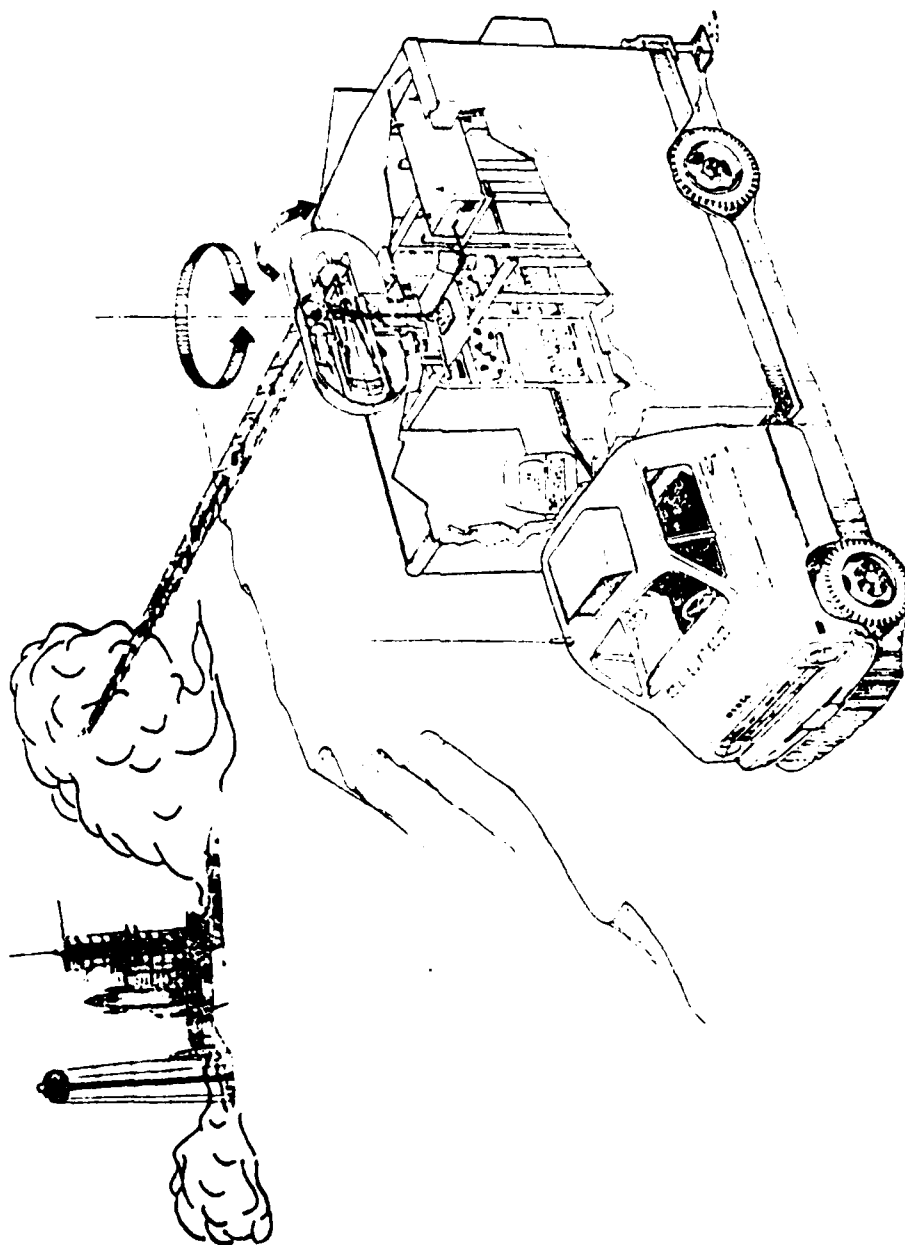


Figure A-2. Cutaway Drawing of CGC Mobile Field Lidar

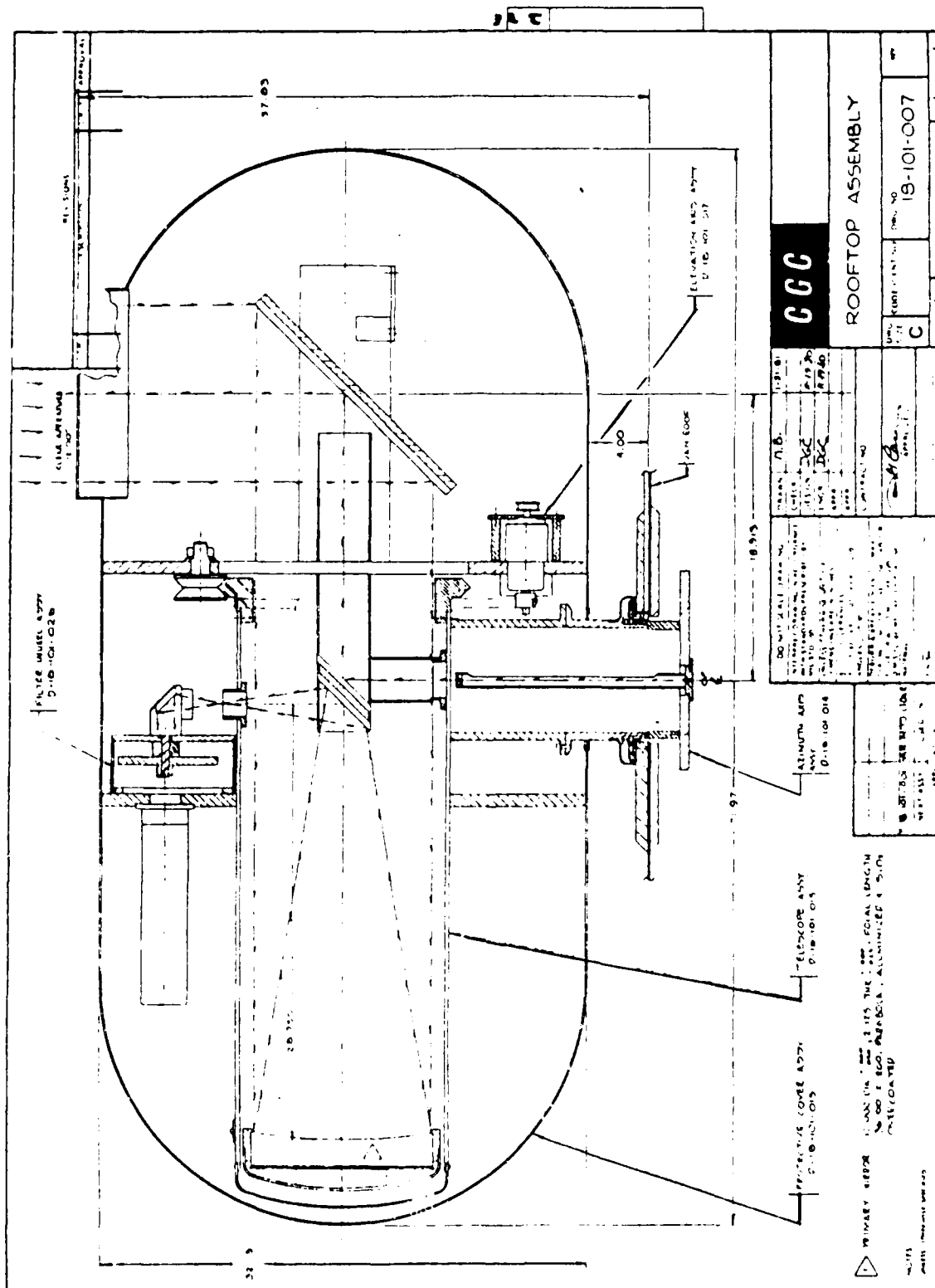


Figure A-3. Mobile Lidar Van-Mounted Telescope Configuration

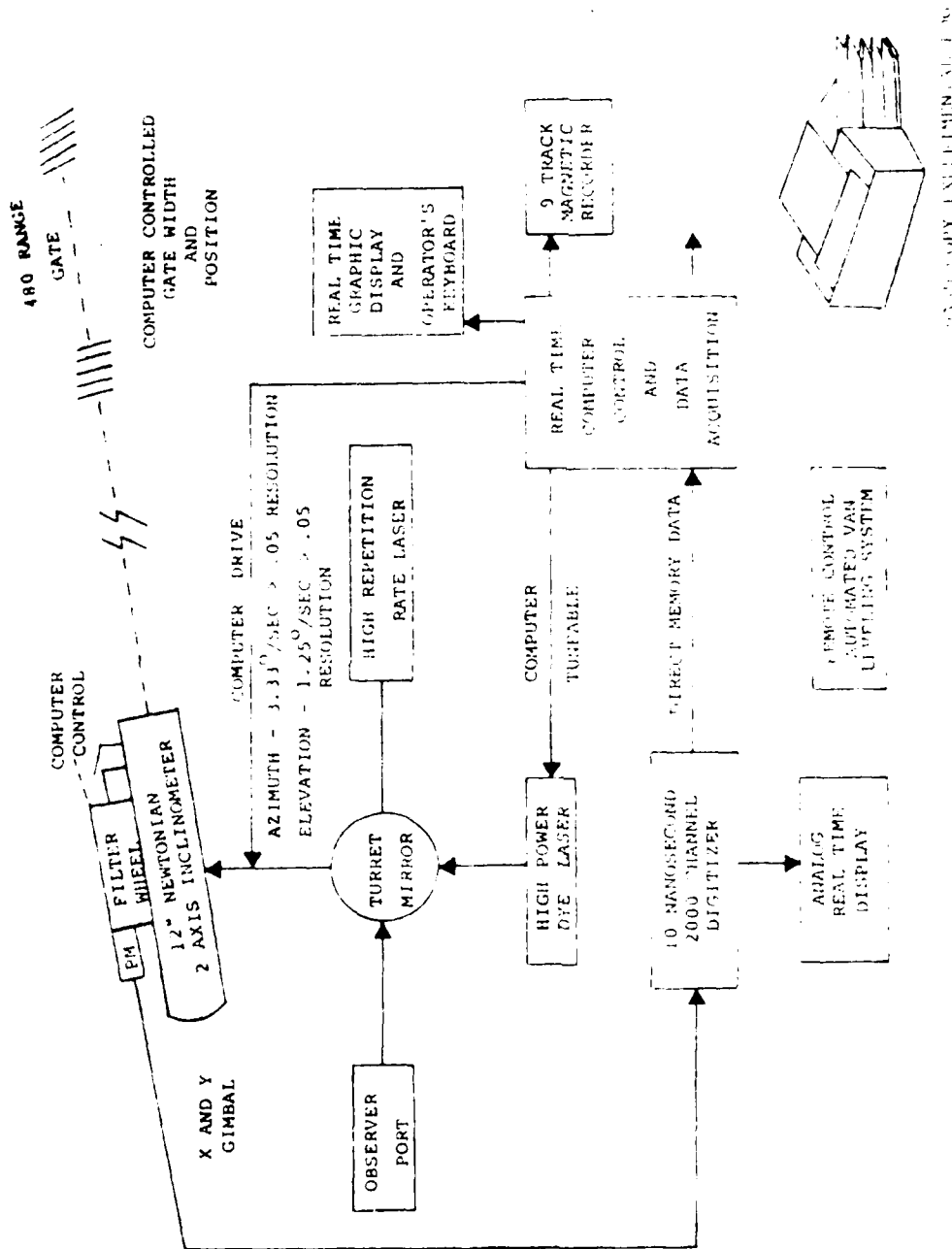


Figure A-4. Existing CGC Mobile Lidar System

The primary transmitter used for particulate measurement is a Phase-R tunable flashlamp-pumped dye laser which produces nominal 300-nanosecond pulses with 0.1 joule per pulse at a pulse repetition rate of 8Hz.

Referring to Figure A4, light backscattered from the measurement volume is collected by the telescope, filtered as appropriate to the application and detected by an RCA photomultiplier (PM) tube in RFI housing. PM-detected data are digitized by a 2048-channel computer-controlled Biomation transient digitizer and input to a Data General computer by direct memory access where it is formatted for raw recording on Digi-Data 9-track industry-compatible magnetic tapes. Processed data for real-time monitoring and data acquisition log are simultaneously produced in hard copy on a Centronics high-speed line printer.

The operator is provided with a fully software-supported real-time CRT/Keyboard/Display which is primarily used as an operator's console to preset and reset the operational parameters of each measurement scenario and to monitor operations. All the operational parameters specified by the operator through the console are recorded in the header record of each magnetic tape data block. The operator is also provided with a real-time analog display which monitors the measurement volume signal on a laser shot-to-laser shot basis.

C. SOFTWARE SUMMARY

The computer subsystem provides the primary functions of:

- a. automatic system operation
- b. data acquisition and recording
- c. operator/system interaction

The resident real-time software has two phases of operation, a measurement phase and a scenario definition phase. Functions a and b are performed during the measurement phase, while function c is performed during both the measurement phase and the scenario definition phase.

During the scenario definition phase the operator specifies the various system parameters which, as a group, define the operational scenario. At this point the operator may activate the automatic measurement phase from the console. The system then begins automatic execution of the specified scenario and continues until the scenario has completed or the operator requests termination.

During the measurement phase the acquired data is recorded on a printer and/or magnetic tape. The real-time printout

provides a tabulation of selected scenario identification data. Recording of the measurement data on magnetic tape facilitates post-real-time processing of the data for in-depth analysis.

The operator's console is an alphanumeric display with keyboard, used by the operator to define and control the system operation. The system parameters required as part of the scenario definition are prompted to the operator in a manner similar to a checklist, requiring only an operator response to accept or modify the value of each parameter displayed. This relieves the operator of maintaining a list of the system parameters. Figure A5 is a sample of a parameter list as implemented in the present CGC lidar.

As an additional quality assurance procedure, the field operator maintains a detailed log of the schedule of events of each sampling period. Items such as meteorological conditions, in-field communications with NASA personnel, target data and system notes are placed in the log.

D. REAL-TIME PROCESSING

The raw data are acquired by the CPU in the form of digitized Mie-scattered light intensity versus range (time of flight) for each laser shot. The raw data arriving at the computer are "tagged" with the filter wheel hole number, angles of azimuth and elevation and all additional information needed to describe the conditions under which data were acquired. Microseconds before each laser pulse, a background (without laser) reading is taken of the incoming light.

The real-time processing of the data consists of averaging a number of laser pulses (normally four) at each line of sight. Of the 480 range gates that are recorded on magnetic tape, the operator can choose 24 and display them on the printer. With the range set to view the leading or trailing edge of the plume, the operator has a real-time display of the plume's position. Any change in wind direction or size of plume is immediately observed by the lidar operator, who can then initiate plans to optimize the sampling scenario, if needed.

E. TYPICAL POST-REAL-TIME PROCESSING

Post-real-time processing is carried out using a software library that permits processing of raw field data into outputs used by modelers and other environmental scientists. The flow chart for processing of particulate plume measurement is shown in Figure A6.

```

COMMAND = 10  DISPLAY/MODIFY PARAMETERS
PARAMETER # = 1      DATE = 811112
PARAMETER # = 4      SITE ID = 6
PARAMETER # = 135     VAN AZIMUTH = 90
PARAMETER # = 121     SCAN # = 5
PARAMETER # = 157     MAGNETIC TAPE UNIT # = 4
PARAMETER # = 136     MAGNETIC TAPE # = 110
PARAMETER # = 122     MAGNETIC TAPE PHYSICAL RECORD = 56
PARAMETER # = 124     PM VOLTAGE = 2200
PARAMETER # = 134     SCANNING MODE = 0
PARAMETER # = 56      RANGE ADJUSTMENT = 0
PARAMETER # = 18      DYE LASER PULSE RATE = 1000
PARAMETER # = 19      MANUAL TRIGGER CONTROL = 0
PARAMETER # = 7       LINE PRINTER VS TELETYPE SWITCH = 0
PARAMETER # = 8       BACKGROUND SWITCH FOR REALTIME PRINT = 0
PARAMETER # = 9       FIRST CHANNEL FOR REALTIME PRINT = 1
PARAMETER # = 10      # OF CHANNELS FOR REALTIME PRINT = 4
PARAMETER # = 12      ALTERNATE STEPPING MOTOR SPECIFICATION SWITCH = 0
PARAMETER # = 140     BEAM EXPANSION FACTOR = 22
PARAMETER # = 117     MINIMUM ELEVATION FIRING POSITION = 10000
PARAMETER # = 112     MANUAL ELEVATION DELTA = 50
PARAMETER # = 116     MANUAL LASER TUNER DELTA = 100
PARAMETER # = 133     MANUAL AZIMUTH DELTA = 25
PARAMETER # = 119     ELEVATION STEPPING MOTOR RATIO = 373000
PARAMETER # = 74      LASER TUNER STEPPING MOTOR RATIO = 100000
PARAMETER # = 120     AZIMUTH STEPPING MOTOR RATIO = 187500
PARAMETER # = 101     CURRENT ELEVATION POSITION = 20000
PARAMETER # = 102     CURRENT LASER TUNER POSITION = 4000
PARAMETER # = 103     CURRENT FILTER WHEEL POSITION = 3
PARAMETER # = 104     CURRENT AZIMUTH POSITION = 10000

```

```

COMMAND = 14  DISPLAY/MODIFY PARAMETERS
PARAMETER # = 184     TV REFERENCE = 51.31
PARAMETER # = 185     SCENARIO 4 AUTO SEQUENCE SWITCH = 0
PARAMETER # = 164     CHANNEL A, INPUT VOLTAGE RANGE (S4) = 0
PARAMETER # = 166     TRIGGER DELAY (S4) = 0
PARAMETER # = 167     SAMPLE INTERVAL (S4) = 3
PARAMETER # = 168     # OF CYCLES (S4) = 32767
PARAMETER # = 169     SCENARIO RECYCLE TIME (S4) = 0
PARAMETER # = 180     SCALE FACTOR (S4) = 10
PARAMETER # = 181     SCANNING PATTERN INDEX (S4) = 4.1

```

Figure A-5. Parameter List

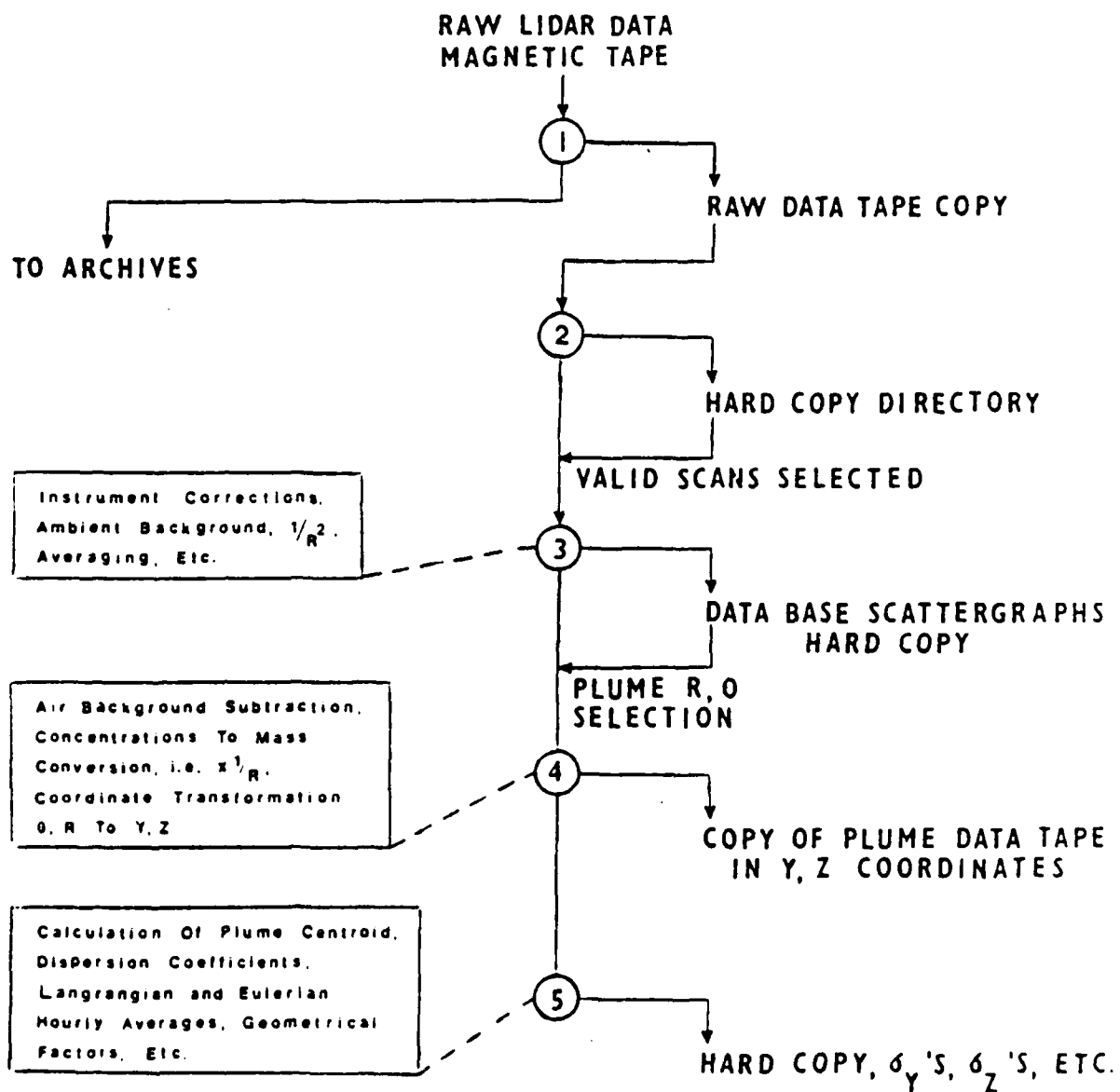


Figure A-6. Typical Lidar Data Processing Flow Chart For Particulate Plume Measurement.

A lidar two-dimensional cross section of a plume is obtained by recording 480 range resolved lidar scattering data points along lines of sight of the scanned vertical plane. The third dimension of the plume is obtained by rotation in azimuth of the vertical elevation scan plane.

Typcial data product is a computer-generated two-dimensional cross section in scattergraph format. Such a scattergraph is shown in Figure A7 which displays scattering intensity as a function of range and elevation angle. Lidar data can also be used to generate a series of plotted plume cross sections as shown in Figure A8.

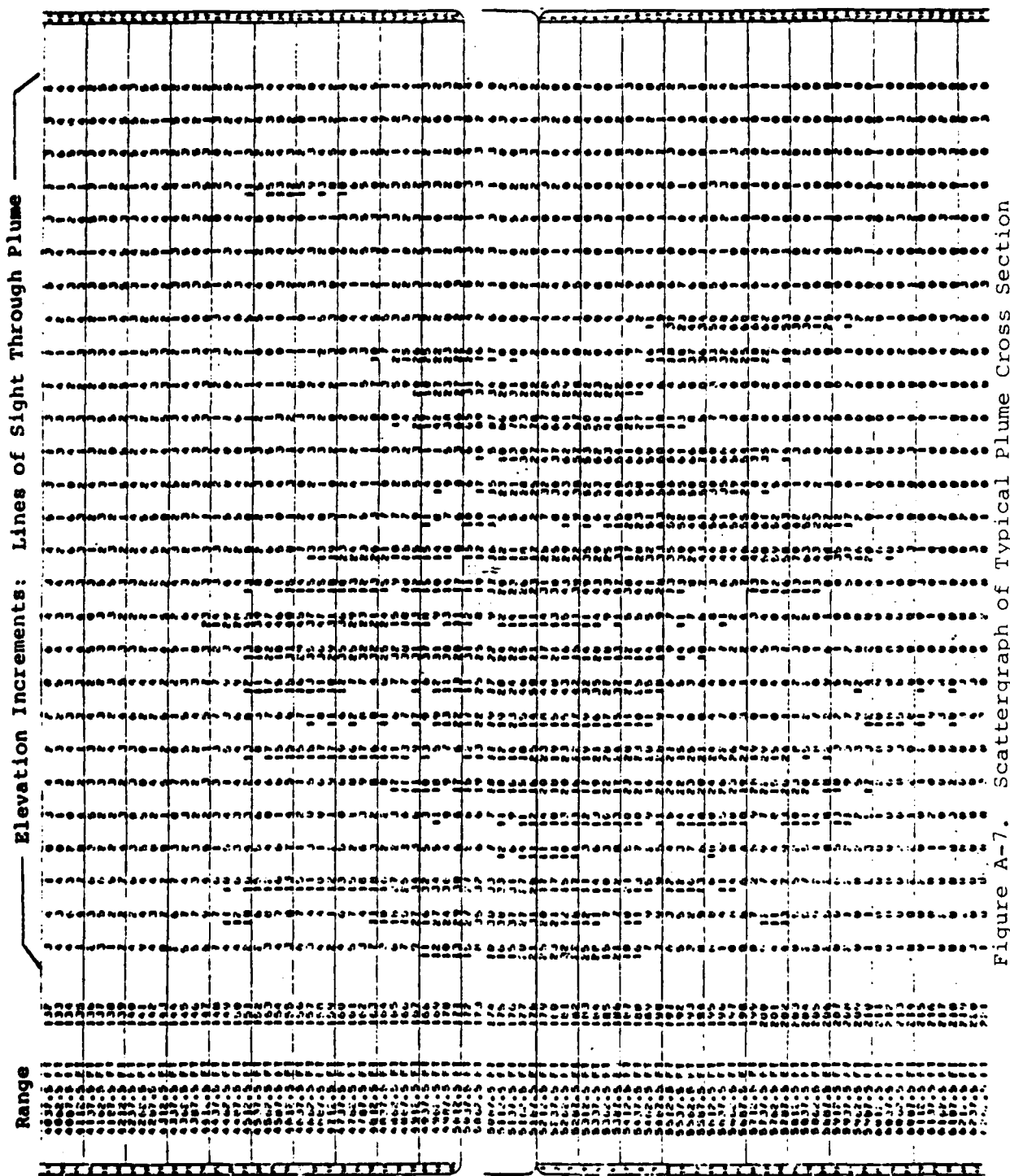


Figure A-7. Scattergraph of Typical Plume Cross Section

PUBLIC SERVICE CO. PLUME STUDIES

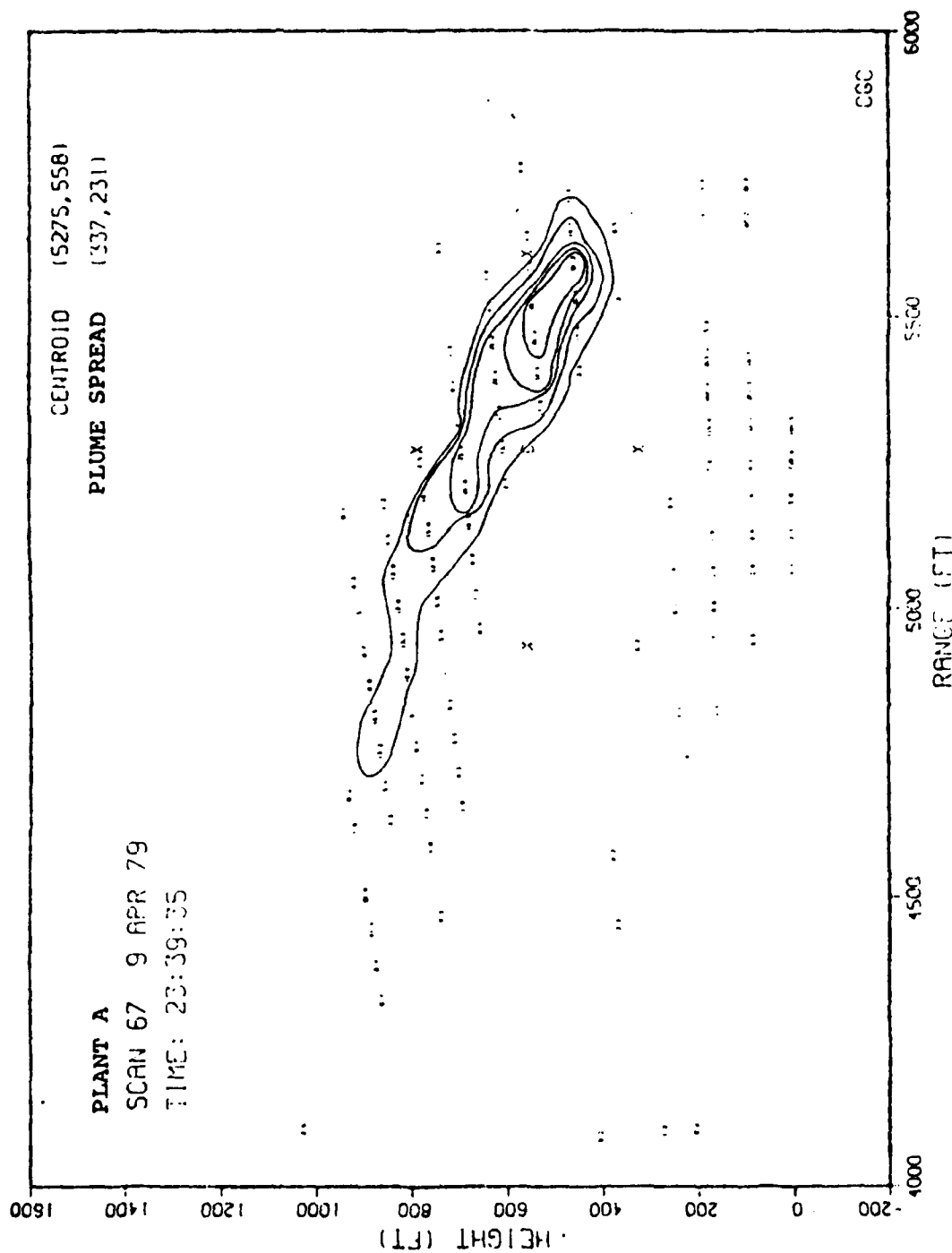


Figure A-8. Plume Scan #67, 23:39:35, 9 April 1979

Appendix B

STS-3 Exhaust Cloud Cross-Section Scattergraphs

Appendix B

STS-3 EXHAUST CLOUD CROSS-SECTION SCATTERGRAPHS

The scattergraph format for presentation of lidar data was developed to permit evaluation of large volumes of raw data in order to locate the lidar measurements acquired. Consequently, very little processing of the data is done beyond background subtraction, which is done to enhance the visualization of the scattergraph. It should be noted that the perspective of the data field of a scattergraph is slightly distorted since the range tabulated is slant range and the line of sight should actually diverge with increasing range. These distortions; however, do not inhibit the ability to locate the lidar measurements in the field of view. Once located and bracketed in the range and azimuth or elevation, more advanced data reduction techniques could be applied to this much reduced volume of data.

Figures B1 - B16 consist of scattergraphs which show STS-3 exhaust cloud lidar cross sections viewed as slant range versus azimuth or elevation. Range, azimuth and elevation values are all relative to UCS-6, the location of the CGC lidar during STS-3 launch. Table B1 provides a listing of the numbers contained in the scattergraphs, as well as other concomitant information. The numbers contained in the scattergraphs represent the relative backscattered intensity (arbitrary units) measured by the lidar. These numbers were generated by taking the data signal return of each channel and LOS incorporated in the scattergraph and subtracting from it an adjusted average background value. The adjusted average background values utilized in the scattergraphs are shown in the last column of Table B1. These values were determined by calculating an average background value based upon the background values measured for each channel and LOS, and multiplying that average value by 1.4. The adjustment factor of 1.4 was chosen on the basis of several preliminary scattergraph productions which illustrated that value provided the most appreciable enhancement of exhaust cloud returns.

Finally, those instances which result in data, minus average adjusted background values less than or equal to zero, are represented by "dots" in the scattergraphs.

TABLE B-1. LIST OF SCATTERGRAPHS

<u>Figure #</u>	<u>Scan #</u>	<u>Segment</u>	<u>Time</u>	<u>Adjusted Average Background</u>
B1	137	E2	11:00:51 - 11:01:04	15
B2	138	F1	11:01:30 - 11:01:43	11
B3	138	F3	11:01:55 - 11:02:08	13
B4	138	F4	11:02:25 - 11:02:35	12
B5	139	F1	11:02:41 - 11:02:53	10
B6	139	F3	11:03:16 - 11:03:27	13
B7	140	F1	11:03:46 - 11:03:58	12
B8	140	F2	11:04:00 - 11:04:11	13
B9	140	F3	11:04:12 - 11:04:23	16
B10	141	F1	11:04:42 - 11:04:53	12
B11	141	F3	11:05:08 - 11:05:19	17
B12	142	F1	11:05:46 - 11:05:57	11
B13	142	F3	11:06:16 - 11:06:28	18
B14	143	F1	11:06:44 - 11:06:55	13
B15	144	F1	11:08:03 - 11:08:14	13
B16	145	F3	11:09:48 - 11:10:00	15

Figure B-3. Scan #138-F3, 11:01:55 - 11:02:08

AD-A130 515

LIDAR (LIGHT DETECTION AND RANGING) REMOTE MEASUREMENTS
OF STS-3 GROUND C. (U) COMPUTER GENETICS CORP WAKEFIELD
MASS B CAPUTO ET AL. APR 83 AFESC/ESL-TR-82-52

2/2

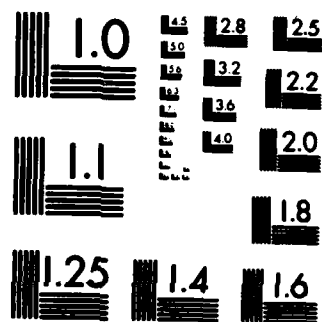
UNCLASSIFIED

NAS10-10299

F/G 17/8

NL





MICROCOPY RESOLUTION TEST CHART
NATIONAL BUREAU OF STANDARDS-1963-A

Figure B-5. Scan #139-F1, 11:02:41 - 11:02:53

SLANT	2.0	2.1	2.2	2.3	2.4	2.5	2.6	2.7	2.8	2.9	3.0	3.1	3.2	3.3	3.4	3.5	3.6	3.7	3.8	3.9	4.0	4.1	4.2	4.3
DEPTH	04.0	04.1	04.2	04.3	04.4	04.5	04.6	04.7	04.8	04.9	04.0	04.1	04.2	04.3	04.4	04.5	04.6	04.7	04.8	04.9	04.0	04.1	04.2	04.3
00001	161	2																						
00002	162																							
00003	163																							
00004	164																							
00005	165																							
00006	166																							
00007	167																							
00008	168																							
00009	169																							
00010	170																							
00011	171																							
00012	172																							
00013	173																							
00014	174																							
00015	175																							
00016	176																							
00017	177																							
00018	178																							
00019	179																							
00020	180																							
00021	181																							
00022	182																							
00023	183																							
00024	184																							
00025	185																							
00026	186																							
00027	187																							
00028	188																							
00029	189																							
00030	190																							
00031	191																							
00032	192																							
00033	193																							
00034	194																							
00035	195																							
00036	196																							
00037	197																							
00038	198																							
00039	199																							
00040	200																							
00041	201																							
00042	202																							
00043	203																							
00044	204																							
00045	205																							
00046	206																							
00047	207																							
00048	208																							
00049	209																							
00050	210																							
00051	211																							
00052	212																							
00053	213																							
00054	214																							
00055	215																							
00056	216																							
00057	217																							
00058	218																							
00059	219																							
00060	220																							
00061	221																							
00062	222																							
00063	223																							
00064	224																							
00065	225																							
00066	226																							
00067	227																							
00068	228																							
00069	229																							
00070	230																							
00071	231																							
00072	232																							
00073	233																							
00074	234																							
00075	235																							
00076	236																							
00077	237																							
00078	238																							
00079	239																							
00080	240																							
00081	241																							
00082	242																							
00083	243																							
00084	244																							
00085	245																							
00086	246																							
00087	247																							
00088	248																							
00089	249																							
00090	250																							

Figure B-8. Scan #140-F2, 11:04:00 - 11:04:11

Figure B-15. Scan #144-F1, 11:08:03 - 11:08:14

REFERENCES

1. Federal Register, Rules and Regulations, Vol 46, No. 208, Pg 53144, October 28, 1981.
2. Evaluation of a Multiwavelength LIDAR Backscatter Technique for Remote Measurement of Particle Size of Smokestack Emissions, Computer Genetics Corporation-P205-81, July 1981.
3. DF Lidar Measurements of Hydrogen Chloride in the Plume of Incineration Ships, Institute UR Physik - Federal Republic of Germany.
4. Raman Lidar Measurement of Atmospheric Water Vapor Profiles During the May-June 1977 USNS Hayes Atlantic/Mediterranean Cruise, D. Leonard and B. Caputo, Computer Genetics Corp., Pgs 228-238.
5. J.D. Klett, Applied Optics, Vol 20, No. 2 (1981)

DATE
FILMED
- 8